



## MPHIL

### Microstructure and Chemical Composition of Colletes halophilus Nest Cell Linings

Belisle, Rebecca

*Award date:*  
2012

*Awarding institution:*  
University of Bath

[Link to publication](#)

## Alternative formats

If you require this document in an alternative format, please contact:  
[openaccess@bath.ac.uk](mailto:openaccess@bath.ac.uk)

Copyright of this thesis rests with the author. Access is subject to the above licence, if given. If no licence is specified above, original content in this thesis is licensed under the terms of the Creative Commons Attribution-NonCommercial 4.0 International (CC BY-NC-ND 4.0) Licence (<https://creativecommons.org/licenses/by-nc-nd/4.0/>). Any third-party copyright material present remains the property of its respective owner(s) and is licensed under its existing terms.

### Take down policy

If you consider content within Bath's Research Portal to be in breach of UK law, please contact: [openaccess@bath.ac.uk](mailto:openaccess@bath.ac.uk) with the details. Your claim will be investigated and, where appropriate, the item will be removed from public view as soon as possible.

# **Microstructure and Chemical Composition of *Colletes halophilus* Nest Cell Linings**

**Rebecca Anne Belisle**

A thesis submitted for the degree of Master of Philosophy

University of Bath

Department of Mechanical Engineering

**September 2011**

## **COPYRIGHT**

Attention is drawn to the fact that copyright of this thesis rests with the author. A copy of this thesis has been supplied on condition that anyone who consults it is understood to recognise that its copyright rests with the author and that they must not copy it or use material from it except as permitted by law or with the consent of the author.

This thesis may be made available for consultation within the University Library and may be photocopied or lent to other libraries for the purposes of consultation.

## **I. Table of Contents**

<i>I. Table of Contents</i>	<i>i</i>
<i>II. List of Figures</i>	<i>iv</i>
<i>III. Acknowledgements</i>	<i>vi</i>
<i>IV. Abstract</i>	<i>vii</i>
<i>V. Glossary of Terms and Abbreviations</i>	<i>viii</i>
<b>Chapter 1: Introduction</b>	<b>1</b>
<b>Chapter 2: Research Background</b>	<b>3</b>
2.1 Chapter Overview	3
2.2 Bee Diversity	3
2.3 Colletes	5
2.3.1 Familial Overview	6
2.3.2 Anatomy	7
2.3.3 Colletes Development	9
2.3.4 Nest Construction	10
2.4 Nest Cell Linings	13
2.4.1 Nest Cell Lining Origin	14
2.4.2 Known Microstructure	15
2.4.3 Known Chemical Composition	15
2.4.4 Additional Material Properties	18
2.5 Related Materials	18
2.5.1 Silk	19
2.5.2 Polyester	22
2.6 Goals for Thesis	24
<b>Chapter 3: Methods of Characterization</b>	<b>26</b>
3.1 Chapter Overview	26
3.2 Microstructure	26
3.2.1 Scanning Electron Microscopy	26
3.2.2 Transmission Electron Microscopy	27
3.2.3 Confocal Microscopy	29
3.3 Chemical Composition	30
3.3.1 Combustion Analysis	30
3.3.2 X-Ray Diffraction	31
3.3.3 Amino Acid Analysis	32
3.3.4 Fourier Transform Infrared & Raman Spectroscopy	32
3.3.5 Gas Chromatography – Mass Spectroscopy	33
3.3.6 Time of Flight	33
3.4 Material Properties	34
3.4.1 Thermogravimetric Analysis	34
3.4.2 Differential Scanning Calorimetry	34
3.4.3 Mechanical Testing	35
3.5 Chapter Summary	36

<b>Chapter 4: Review of Previous Research</b>	<b>37</b>
4.1. <i>Chapter Overview</i>	37
4.2. <i>Introduction</i>	37
4.3. <i>Materials and Methods</i>	37
4.3.1.    Combustion Analysis	37
4.3.2.    Amino Acid Analysis	38
4.3.3.    Confocal Microscopy	38
4.3.4.    Gas Chromatography – Mass Spectroscopy	38
4.4. <i>Relevant Results</i>	39
4.4.1.    Combustion Analysis	39
4.4.2.    Amino Acid Analysis	39
4.4.3.    Confocal Microscopy	40
4.4.4.    Gas Chromatography – Mass Spectroscopy	41
4.5. <i>Conclusions</i>	42
<b>Chapter 5: Materials and Methods</b>	<b>43</b>
5.1. <i>Chapter Overview</i>	43
5.2. <i>Nest Cell Lining Acquisition</i>	43
5.3. <i>Microstructure</i>	44
5.3.1.    Scanning Electron Microscopy	44
5.3.2.    Transmission Electron Microscopy	44
5.3.3.    Confocal Microscopy	45
5.4. <i>Chemical Composition</i>	46
5.4.1.    X-Ray Diffraction	46
5.4.2.    Amino Acid Analysis	47
5.4.3.    Fourier Transform Infrared & Raman Spectroscopy	47
5.4.4.    Time of Flight	47
5.5. <i>Material Properties</i>	48
5.5.1.    Thermogravimetric Analysis	48
5.5.2.    Differential Scanning Calorimetry	49
5.5.3.    Mechanical Testing	50
5.6. <i>Chapter Summary</i>	51
<b>Chapter 6: Microstructure of <i>Colletes halophilus</i> Nest Cell Lining</b>	<b>52</b>
6.1. <i>Chapter Overview</i>	52
6.2. <i>Scanning Electron Microscopy</i>	52
6.3. <i>Transmission Electron Microscopy</i>	62
6.4. <i>Confocal Microscopy</i>	68
6.5. <i>Chapter Summary</i>	71
<b>Chapter 7: Chemical Composition of <i>Colletes halophilus</i> Nest Cell Lining</b>	<b>72</b>
7.1. <i>Chapter Overview</i>	72
7.2. <i>X-Ray Diffraction</i>	72
7.3. <i>Amino Acid Analysis</i>	76
7.4. <i>Fourier Transform Infrared &amp; Raman Spectroscopy</i>	79
7.5. <i>Time of Flight</i>	83
7.6. <i>Chapter Summary</i>	88



<b>Chapter 8: Material Properties of <i>Colletes halophilus</i> Nest Cell Lining</b>	<b>90</b>
8.1. <i>Chapter Overview</i>	90
8.2. <i>Thermogravimetric Analysis</i>	90
8.3. <i>Differential Scanning Calorimetry</i>	92
8.4. <i>Mechanical Testing</i>	98
8.5. <i>Chapter Summary</i>	102
<b>Chapter 9: Final Discussion and Conclusions</b>	<b>103</b>
9.1. <i>Chapter Overview</i>	103
9.2. <i>Resolution of Discrepancies in Chemical Composition</i>	103
9.3. <i>Resolution of Discrepancies in Nest Cell Construction</i>	104
9.4. <i>Relation of Chemical Composition to Microstructure</i>	105
9.5. <i>Potential of Nest Cell Lining Material</i>	106
9.6. <i>Comparing <i>Colletes halophilus</i> to <i>Colletes inaequalis</i></i>	107
<b>Chapter 10: Future Directions</b>	<b>108</b>
10.1. <i>Chapter Overview</i>	108
10.2. <i>Resolution of Discrepancies in Chemical Composition</i>	108
10.3. <i>Resolution of Discrepancies in Nest Cell Construction</i>	109
10.4. <i>Relation of Chemical Composition to Microstructure</i>	110
10.5. <i>Potential of Nest Cell Lining Material</i>	111
<b>References</b>	<b>112</b>
<b>Personal Bibliography</b>	<b>118</b>
<b>Appendix A: Krypton™ Protein Stain Instructions</b>	<b>119</b>
<b>Appendix B: Journal of Materials Science Publication</b>	<b>122</b>
<b>Appendix C: Article Submitted to the Journal of Materials Science</b>	<b>126</b>

## II. List of Figures

Figure 1: Accepted evolutionary relationship between bee families (adapted from C. Michener, <i>Bees of the World</i> ) [6].	4
Figure 2: An example of <i>Colletes halophilus</i>	5
Figure 3: SEM micrograph of the glossa of <i>Colletes inaequalis</i> (unpublished work, Olin College).	7
Figure 4: Schematic showing the position of the glands of female <i>Colletes</i> bee (adapted from S.W.T. Batra, 1980) [14].	8
Figure 5: Nesting aggregation of <i>Colletes halophilus</i> in East Tilbury, UK	10
Figure 6: Diagram of <i>Colletes</i> nest (adapted from S.W.T. Batra, 1980) [14].	11
Figure 7: Diagram of <i>Colletes</i> nest cell lining.	11
Figure 8: <i>Colletes halophilus</i> nest cell linings, one cleaned and one as excavated.	12
Figure 9: Reaction of Dufour's gland secretions to form <i>Colletes</i> nest cell lining as suggested by Hefetz et al [22].	14
Figure 10: Generic polyester molecule	23
Figure 11: Diagram of scanning electron microscope	26
Figure 12: Diagram of transmission electron microscope	28
Figure 13: Diagram of a confocal microscope	29
Figure 14: Diagram of combustion analyser	31
Figure 15: Confocal image of <i>Colletes inaequalis</i> nest cell lining	41
Figure 16: Schematic of nest cell lining samples for Instron testing	50
Figure 17: Tensile testing setup for nest cell samples.	51
Figure 18: SEM image of external surface of nest cell lining.	52
Figure 19: SEM image of internal surface of nest cell lining	53
Figure 20: SEM image showing detail of a transverse section of nest cell lining.	54
Figure 21: SEM image of a transverse section of an embedded nest cell. The external and internal surfaces and fibre location are identified.	55
Figure 22: SEM image of a transverse section of an embedded nest cell. Fibres are identified.	55
Figure 23: SEM image of tensile fractured nest cell lining. Sample from nest cell cap.	56
Figure 24: SEM image of freeze fractured nest cell lining. Sample from nest cell cap.	57
Figure 25: SEM image of freeze fractured nest cell lining. Sample from nest cell body.	57
Figure 26: SEM image of large nest cell lining fibre, approximately 8µm in diameter.	58
Figure 27: SEM image of small nest cell lining fibre, approximately 1µm in diameter.	59

Figure 28: TEM micrograph of a transverse section of nest cell lining exposed to osmium tetroxide. Fibre structure revealed.....	62
Figure 29: TEM micrograph of a transverse section of nest cell lining exposed to osmium tetroxide. Layered structure revealed. ....	63
Figure 30: TEM micrograph of a transverse section of nest cell lining exposed to ruthenium tetroxide. Fibre revealed. ....	64
Figure 31: TEM micrograph of a transverse section of nest cell lining exposed to ruthenium tetroxide. Layered structured revealed. ....	65
Figure 32: Confocal image of stained nest cell lining with the black and white field image included. ....	68
Figure 33: Confocal image of stained nest cell lining, the black and white field image excluded. ....	69
Figure 34: X-Ray diffraction pattern of powderised nest cell lining. ....	72
Figure 35: X-ray diffraction pattern of nest cell lining showing peaks between 15° and 40° 2-Theta. ....	73
Figure 36: X-ray diffraction pattern of nest cell lining showing peaks between 20° and 30° 2-Theta. ....	74
Figure 37: IR spectra of transverse sections through <i>Colletes halophilus</i> nest cell linings with significant peaks identified. Spectra (a) and (b) are from the same nest cell lining while (c) represents a different embedded sample.....	80
Figure 38: Raman spectrum for <i>Colletes halophilus</i> nest cell lining. ....	81
Figure 39: Spectrum for ESI-TOF analysis of <i>Colletes halophilus</i> nest cell linings. Polymeric pattern highlighted. ....	84
Figure 40: Spectrum for MALDI-TOF analysis of <i>Colletes halophilus</i> nest cell linings. ....	86
Figure 41: Decomposition of <i>Colletes</i> nest cell lining achieved through TGA. Varying decomposition stages distinguished. ....	90
Figure 42: DSC spectrum for a PLA sample with heating rate of 5°C /min. Glass transition temperature ( $T_g$ ) and melting temperature ( $T_m$ ) identified. ....	93
Figure 43: DSC spectrum for a <i>Bombyx mori</i> silk cocoon with heating rate of 5°C/min. Endothermic peaks identified.....	93
Figure 44: DSC spectrum for a <i>Colletes halophilus</i> nest cell lining with a heating rate of 10°C/min. ....	95
Figure 45: DSC spectrum for a <i>Colletes halophilus</i> nest cell lining with a heating rate of 2°C/min. ....	95
Figure 46: <i>Colletes halophilus</i> nest cell lining heated to 200°C on a hot stage microscope at 200X.....	97
Figure 47: Tensile stress versus strain in three different <i>Colletes halophilus</i> nest cell linings. ....	99

### **III. Acknowledgements**

My sincerest gratitude is expressed to Dr. Irene Turner and Dr. Martin Ansell for their support and guidance from the time of my application to the University of Bath to the completion of my MPhil. I would not have been able to come to the UK never mind complete this project without their help. I am deeply grateful for our many discussions, both formal and not.

I'd also like to extend my thanks to all the technicians and staff who helped to make this project possible. In particular I'd like to thank Ursula Potter and the rest of the Microscopy and Analysis Suite for their continued interest and support of my project. My thanks also go out to the many members of the University of Bath and University of Bristol Chemistry Departments who helped to make this study a success.

Special acknowledgments go to the US-UK Fulbright commission, who have not only funded my work but have served as a support group during my time here, as well as Dr. Debbie Chachra and Dr. Chris Morse of Franklin W. Olin College of Engineering who have remained friends and collaborators during my time here.

Finally, I would like to express my gratitude to my friends and family. Thanks to my parents and sister for supporting my academic endeavours whether close to or far from home. Thanks to my dear Jona for crossing the Atlantic to share in this amazing experience with me. And thanks to those who welcomed me onto this small island and helped me make it home: Robin Long, Tim Holsgrove and Helen Liang.

#### IV. Abstract

Bees of the genus *Colletes* have the unique ability to create what has been described as a cellophane-like nest cell lining material for the protection of their developing brood. Chemically, this material has been described as a linear polyester and has been noted for being naturally derived, robust and strongly resistant to chemical degradation as well as biodegradable. Despite these interesting properties little is known about the structure, chemistry or physical properties of the *Colletes* nest cell lining. This study investigates the nest cell linings of *Colletes halophilus* to addresses the discrepancies in the published literature on nest cell lining chemistry and structure. Using a variety of microscopical, analytical chemistry, mechanical and thermal characterization techniques a more complete model of the nest cell lining material is revealed. As opposed to simply being composed of a linear polyester as previously thought, the *Colletes halophilus* nest cell linings are shown to be biocomposite structures constructed from silk fibres laid down as a scaffolding for the application of a copolymer matrix composed of multiple ester containing compounds. Notably a composite structure has been revealed using SEM, TEM and confocal microscopy, and a more complex chemical composition revealed through FTIR and TOF techniques. Additionally, the *Colletes halophilus* nest cells show mechanical and thermal properties characteristic of a largely amorphous, thermoset polymer. These results advance the current understanding of the anatomy and behaviour of the *Colletes* bees as well as providing new information on the morphology and chemistry of the nest cell lining material. The overall outcome of this study is a clearer understanding of the structure and composition of the nest cell lining itself as well its potential as biopolymer. Advances in the understanding of the structure and composition of this naturally derived composite may serve as a model for non-petroleum derived polymers in the future.

## V. Glossary of Terms and Abbreviations

- **AAA:** Amino Acid Analysis
- **Ampullate glands:** Glands within spiders responsible for the creation of web scaffolding (minor ampullate) and dragline silk (major ampullate).
- **Analyte:** Chemical being quantified through an analytical technique
- **Annulae/Annulate:** A row of hairs on the *Colletes* tongue all connected at their base/Relating to these rows of hairs
- **Arthropoda:** A group of organisms including all insects, crustaceans and arachnids, characterized by having an exoskeleton, a segmented body and hinged legs.
- **Apoidea:** The superfamily containing all families of bee
- **Apoids:** Member of the superfamily Apoidea; Bees
- **Bilobed:** Containing two-lobes; refers to the structure of *Colletes* tongues
- **Chemosystematics:** Taxonomic classification based on secretions produced by an organism
- **Colletid:** Relating to *Colletes*
- **DMTA:** Dynamic Mechanical Thermal Analysis
- **DSC:** Differential Scanning Calorimetry
- **Dufour's gland:** Basic gland in the abdomen of *Colletes* bees; source of nest cell lining polymer
- **ESI-TOF:** Electrospray Ionization – Time of Flight
- **Family:** The third lowest taxonomic ranking; e.g. Colletidae is a family in Hymenoptera
- **FTIR:** Fourier Transform Infrared Spectroscopy
- **GC-MS:** Gas Chromatography – Mass Spectroscopy
- **Genus:** The second lowest taxonomic ranking; e.g. *Colletes* is a genus in Colletidae
- **Glossa/Glossal:** The tongue of a bee/relating to the tongue
- **Hymenoptera:** The order containing bees, ants and wasps
- **Interspecific:** Between species
- **Intron:** A segment of DNA which does not code for a protein

- **Lactone:** A cyclic ester containing molecule
- **MALDI-TOF:** Matrix-Assisted Laser Desorption/Ionization – Time of Flight
- **Monophyly:** A group of organisms all descended from their closest common ancestor.
- **Order:** The fourth lowest taxonomic ranking; e.g. Hymenoptera is the order containing all bees, wasps and ants
- **Parsimony:** In reference to evolution, the evolution pathway having the least complexity
- **PET:** Polyethylene terephthalate
- **Phylum:** The fourth highest taxonomic ranking; e.g. all insects are members of the phylum Arthropoda.
- **PLA:** Polylactic acid
- **Propolis:** A resin-like material produced by honey bees in hive construction
- **Provisioned:** Containing food, in the case of *Colletes* containing nectar and pollen
- **Residue:** In reference to amino acids, the chemical side group that varies between amino acids
- **SEM:** Scanning Electron Microscopy
- **Social:** In reference to bees, those species which live in hierarchical colonies containing a single fertile female
- **Solitary:** In reference to bees, those species where each female is fertile and creates its own nests
- **Sphecid:** Referring to ground nesting wasps thought to be the closest ancestors to bees
- **Superfamily:** Not a main taxonomic classification but a level of zoological classification between a family and an order; e.g. Apoidea is a superfamily containing all the families of bees
- **TEM:** Transmission Electron Microscopy
- **TGA:** Thermogravimetric Analysis
- **Thermoplastic:** Polymer which is capable of melting and recrystallization.
- **Thermoset:** Polymer which once solidified cannot melt and instead degrades with increasing temperature
- **XRD:** X-Ray Diffraction

- **C:** Carbon
- **CO<sub>2</sub>:** Carbon dioxide
- **H:** Hydrogen
- **H<sub>2</sub>O:** Water
- **HCl:** Hydrochloric acid
- **O:** Oxygen
- **M:** Molarity
- **N:** Nitrogen
- **NO:** Nitrogen monoxide
- **NO<sub>2</sub>:** Nitrogen dioxide
- **NaOH:** Sodium hydroxide
- **S:** Sulphur
- **$\sigma$ :** Engineering stress
- **$e$ :** Engineering strain
- **$F$ :** Force
- **$A$ :** Cross-sectional Area
- **$L$ :** Measured length
- **$L_0$ :** Starting length
- **$T_g$ :** Glass transition temperature
- **$T_m$ :** Melting temperature



## Chapter 1: Introduction

Bees in the genus *Colletes* are often referred to as the “polyester bees” due to their unique ability to produce a material that has been described as a linear polyester. For the *Colletes* bees, this polymer constitutes a main portion of their nest, serving as a waterproof and antifungal barrier between their developing brood and the external environmental conditions. However, the current understanding of the chemistry of this material and noted properties makes it unique in the biological world and thus the subject of this investigation.

*Colletes* bees represent one of the many genera of solitary bees. Unlike social bees, such as the common honey bee, each solitary female is responsible for the procurement of pollen to feed herself and her brood, as well as the construction of her own nest. The nests of *Colletes* bees consist of a series of tunnels dug into the earth with a nest cell at the end of each tunnel into which an egg is deposited. The material that constitutes the walls of this nest cell, referred to as the nest cell lining, has been previously shown to be a robust polyester material composed of secretions from the *Colletes* Dufour’s glands. This material is derived from natural sources, is robust during use and is biodegradable. Such characteristics would be desirable in creating a more environmental engineering plastic, as traditional plastics are petroleum based and resistant to biodegradation.

Nests of bees have long been of interest to entomologists for taxonomic purposes. However, more recently material scientists and biologists have turned to these nesting materials for inspiration for novel materials for use in engineering applications. Such has been the case for the study of honey bee silk, which has shown to have promise for engineering applications due to its biocompatibility and high material toughness. Hence the focus of this study – characterizing the microstructure and chemical composition of the nest cell linings of *Colletes halophilus* (a particular species of *Colletes*) in the hope of inspiring novel biologically derived and biodegradable polymers. Though preliminary investigations of the chemistry of *Colletes* nest cell linings have been conducted by other research groups, the results are conflicting and fail to characterize the whole of the nest cell lining. In order to develop materials inspired by this robust

natural polymer, a more complete understanding of its characteristics and performance are needed. This study aims to fill this need and serve as a stepping stone for the creation of more environmentally responsible polymers by examining the following:

- The microstructure of the *Colletes halophilus* nest cell linings.
- The chemical composition of the *Colletes halophilus* nest cell linings.
- The relationship between microstructure and chemical composition in the *Colletes halophilus* nest cell linings.
- The mechanical and thermal properties of the *Colletes halophilus* nest cell linings.

## **Structure of Thesis**

This thesis is structured into nine chapters. Chapter 1 has presented a brief introduction to this research and the goals of this study. Chapter 2 presents a review of the relevant background to this work, discussing the entomological background of the *Colletes halophilus* species as well as the current understanding of its nest cell lining material and related polymers. The materials and methods employed are presented in Chapters 3 and 5, with the theory behind the various characterization techniques presented in Chapter 3 and a detailed account of the execution of these techniques presented in Chapter 5. This material has been split over two chapters due to the wide diversity of techniques employed in this investigation. Results and their implications are presented in Chapters 4, 6, 7 and 8, with results grouped into chapters relating to the experimental technique for ease of understanding. Chapter 4 discusses work carried out by the author prior to coming to the University of Bath on *Colletes inaequalis*. This previously unpublished work has been included for comparison with the work carried out on *Colletes halophilus*. Chapter 6 discusses results relevant to the microstructure of the nest cell lining. Results relating to the chemical makeup of the nest cell lining are presented in Chapter 7. Remaining results relating to the material performance of the nest cell lining are presented in Chapter 8. Chapter 9 summarizes the conclusions of the study and connects the various results presented. Finally, Chapter 10 discusses the opportunities for future work arising from this study.

## Chapter 2: Research Background

### 2.1 Chapter Overview

In this chapter the relevant background literature on the nest cell lining of *Colletes halophilus* is discussed. Appropriate information on the materials and entomological background of this research is presented below.

### 2.2 Bee Diversity

The order of Hymenoptera consists of 100,000 species of insects characterized by their possession of two pairs of membranous wings. Within this order, which also contains all species of wasps and ants, is the superfamily Apoidea: the bees [1]. What distinguishes the 20,000 or more species of bees from the rest of Hymenoptera is their unique use of pollen as a food source [2]. While wasps and ants are carnivorous, bees have evolved alongside flowering plants and these organisms now depend on each other for survival [1].

For most of history, bees have been thought to have been derived from sphecid ground-nesting wasps, with the apoids of Colletidae being the base ancestor [2]. This evolution was supported by the similarities in glossal and thorax morphologies between wasps and bees as well as their ground nesting habits [3]. This was later supported through chemosystematic studies by Cane showing Colletidae as the basal ancestor [4]. Recently, this evolutionary pathway has come under question [1, 5, 6]. Using genetic information, improved parsimony in the development of bees has been found by placing Melittidae as the initial ancestor [7]. This finding is supported by the prevalence of Melittidae species in the early fossil record of bees and suggests an African origin for the development of modern bee species [7].

Of the 20,000 species, the bees can be ordered into eleven different families. These families are distinguished by a number of factors including anatomy, foraging habits,

nesting and sociality [1]. A diagram of the bee families and their evolved relationships to each other can be seen in Figure 1.

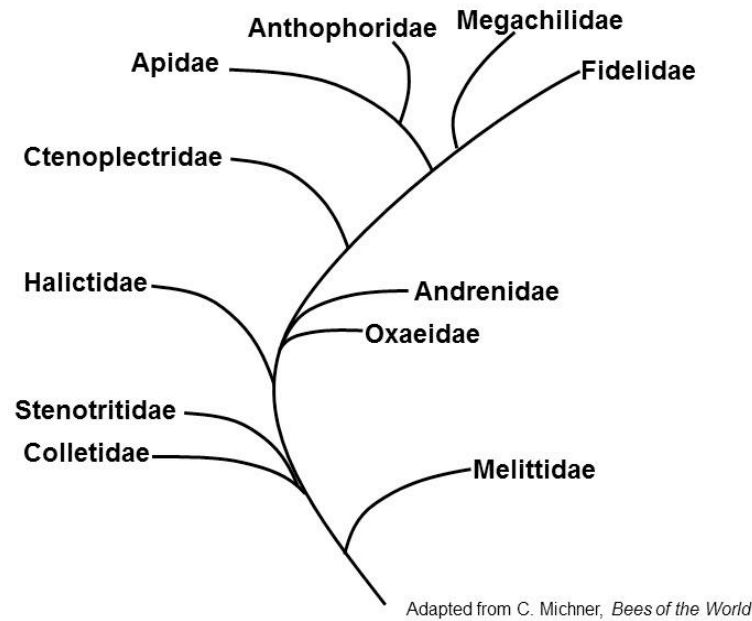


**Figure 1: Accepted evolutionary relationship between bee families (adapted from C. Michener, *Bees of the World*) [6].**

Initial morphological studies of apoids made by Kirby noted two distinct types of bees based on glossal morphology [8]. The existence of long-tongued and short-tongued bees was noted, and this anatomical difference is still used for taxonomic and evolutionary classification with the seven least evolved families being short-tongued and the more advanced being long-tongued [9]. Additional anatomical features which separate bee species include features used for pollen and nectar transportation [2].

Nesting habitat and nest construction also distinguish the families of Apoidea. Varying nesting habitats exist, ranging from isolated tunnels in the ground in the case of mining bees such as Melittidae, to nests constructed out of wax and propolis cells such as those constructed by members of Apidae [2]. Within nesting, how nests are provisioned and young fed varies widely across families. Many species create a solid food ball consisting mostly of nectar and pollen for their brood. However all species of Colletidae provide provisions that are more liquid due to their lower pollen content [2]. Additionally, some species leave food for their young that will support them throughout

their development, as is the case with *Colletes* species, and this is discussed in greater detail in section 2.3.4. Other species such as *Apis mellifera* (the western honey bee) feed their young continuously throughout their development [2].

Apoids are also distinguished by sociality. The vast majority of bee species are solitary with only one out of the eleven families, Apidae, being social [1]. Social bees, like the common honey-bee, have non-reproductive females who work collectively to construct and defend the nest. These are absent in solitary bees and each female is responsible for the construction of her own nest and the development of her brood [1]. Of particular interest to this study is the group of short-tongued, ground-nesting, solitary bees: Colletidae.

### 2.3. Colletes

*Colletes* is a genus of ground-nesting solitary bees of the family Colletidae and the subfamily Colletinae. Species of *Colletes* are found across the world except in Australia. In this study much of the focus is on *Colletes halophilus*, a species which feeds on *Aster tripolium* (sea aster) and is found across continental Europe and on the eastern coast of the United Kingdom [10]. An image of *Colletes halophilus* can be seen in Figure 2.



**Figure 2:** An example of *Colletes halophilus*

### 2.3.1. Familial Overview

Colletidae is a family of bees consisting of six subfamilies (Colletinae, Paracolletinae, Euryglossinae, Hylaeinae, Xeromelissinae, and Scapterinae), 54 genera and over 2400 species [11]. This family represents what were long thought to be the most primitive of bee species [2]. Though this has been recently challenged with genetic information [7], putting the family Melittidae at the base instead, the Colletidae have many morphological and behavioural similarities to sphecoid wasps making them appear quite primitive.

The bees of Colletidae are very diverse, ranging widely in appearance and behaviour. For instance, while bees of Colletinae have external structures made of hair to carry pollen, those of Hylaeinae ingest pollen in order to transport it [11]. Despite these morphological differences, there is strong genetic evidence for the unification of the family. A unique intron, a section of DNA which is removed during RNA splicing of the expressed gene, has been discovered in the genes of Colletid species that appears to not be present in any other bee or member of the order of Hymenoptera, making a strong case for the monophyly of the family [12].

All species of Colletidae are solitary, meaning each female is responsible for the construction of her own nest and the protection and survival of her brood. Colletidae have long been noted for the secretions that they make as part of their nest creation to protect their brood. Both the nesting structures and the nest cell linings vary across species, but Colletidae can be broadly divided into two distinct nesting groups: those which nest exclusively in soil (the vast majority of Colletinae and all of Scapterinae) and those which nest in a diversity of materials including soft wood, plant stems and soil (Euryglossinae, Hylaeinae, and Xeromelissinae) [3]. The particular genus which is the subject of this study is *Colletes*, a soil-nesting bee of the subfamily Colletinae.

### 2.3.2. Anatomy

Bees of the subfamily Colletinae range in size from 7mm to 16mm in length [12]. These bees can be described in terms of the following anatomical components: glossa, scopa, main body, wings, abdominal glands, thoracic glands, and mandibular glands. The most significant of these, to nest construction, are the glossa and thoracic, mandibular and abdominal glands which are discussed in further detail below.

#### Glossa

The glossa is the tongue of the *Colletes* bee and is significant in nest cell lining construction. Glossal morphology of Colletidae was first noted as being unique in 1802 [8] and is one of the traits that until recently linked Colletidae to the spechoid wasps [13]. Colletidae are one of four families of short-tongued bees with *Colletes* being distinct for having a broad glossa [9]. An SEM image of the glossa can be seen in Figure 3.

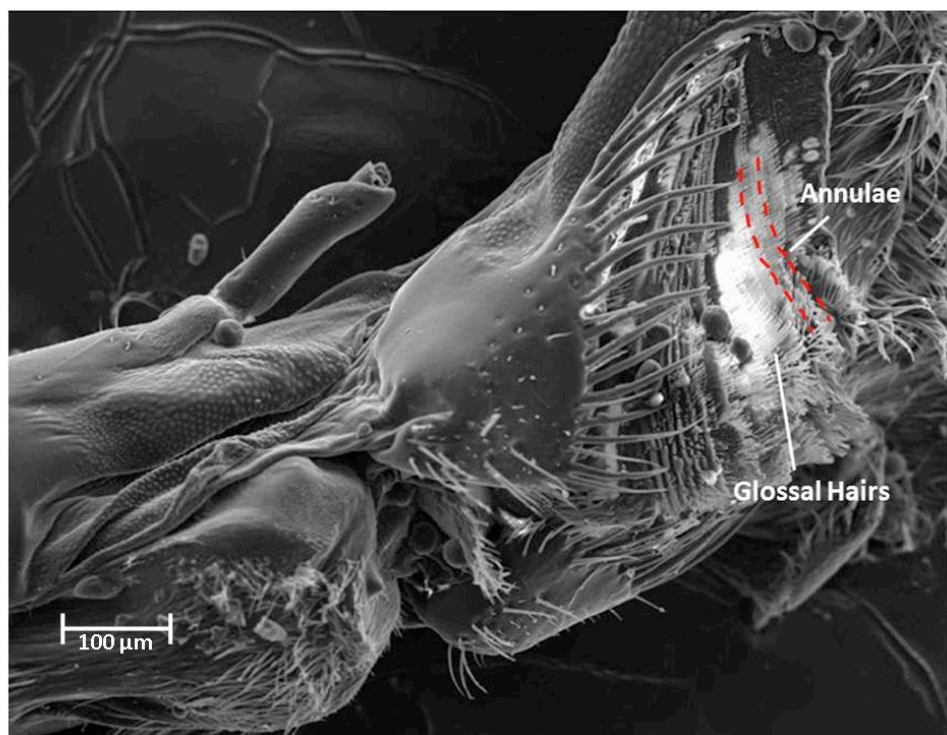
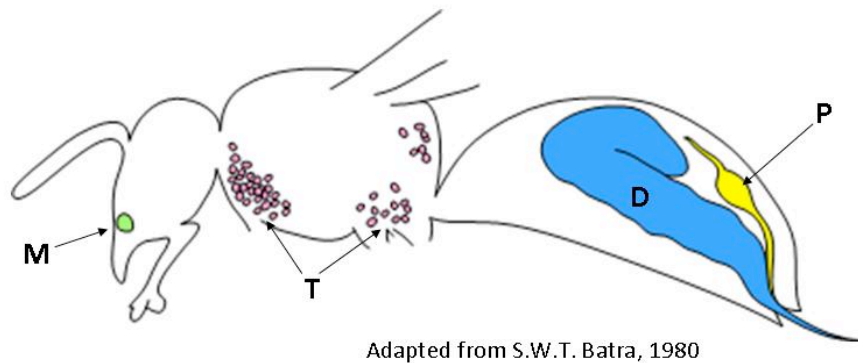


Figure 3: SEM micrograph of the glossa of *Colletes inaequalis* (unpublished work, Olin College).

The glossa of *Colletes* is bilobed and densely covered with glossal hairs. These hairs are organized into rows called glossal annulae, with all the hairs in an annulae being basally connected. *Colletes* are distinctly annulate amongst the Colletidae [9].

## Glands

*Colletes* bees have four different glands, the positions of which can be seen in Figure 4. These glands include: the mandibular glands (M), the thoracic salivary glands (T), the Dufour's glands (D), and the poison gland (P).



**Figure 4: Schematic showing the position of the glands of female *Colletes* bee (adapted from S.W.T. Batra, 1980) [14].**

### *Mandibular Glands*

The mandibular glands contain volatile secretions, such as citral and linalool in *Colletes* species, which appear to serve a dual purpose for the bees. For instance, these particularly floral compounds released by females may indicate their presence to males thus encouraging copulation [15]. Additionally, these secretions may serve as a disinfectant when colletid females first begin nest cell lining construction [16].



### *Thoracic Glands*

The thoracic salivary glands have been linked to silk production in various bees, though never confirmed in *Colletes*. For instance, bees of the genus *Hyleaus* have more developed salivary glands than *Colletes* and it is believed that these glands are the source of the *Hylaeus* bees' silken nest cell lining [14, 17].

### *Abdominal Glands*

Bees are commonly known to have two different glands located in their abdomen. These glands were first identified by Dufour in 1841 [18] and were entitled the basic and acid gland. The basic gland, now commonly referred to as the Dufour's gland, is the one principally responsible for the *Colletes* nest cell lining (this will be discussed in greater detail in 1.2.3). The acid gland, sometimes called the poison gland [14], is responsible for the venom released during stinging [19].

The relative size of these glands varies between species. In species which produce a cellophane-like nest cell lining, such as *Colletes* bees, the Dufour's gland is much bigger than the acid gland. In *Colletes* bees this large U-shape gland occupies the majority of the space in the abdomen. In bees which produce a different type of lining, or no lining at all, the size of the gland is much reduced, as is the case with bees of the genus *Hylaeus* which produce a silken lining [14]. Similarly, bees which have lost their ability to sting have a reduced acid gland, or no gland at all, as is the case with some Andrenidae species [19]. In *Colletes* bees the acid gland is distinctly smaller than the Dufour's gland, consisting of two thin ducts joining to form a reservoir which can be emptied if the bee were to sting [14].

### **2.3.3. *Colletes* Development**

*Colletes* bees, like many insects, go through a multi-staged development process. The developmental stages are: egg, larva, prepupa, pupa and adult. In *Colletes* species this

maturation process will take place entirely in the protected environment that is the underground nest cell (discussed in 2.3.4) [14].

*Colletes* species are seasonal in their development, meaning that only one new generation of bees will develop every year. In Northern Europe and North America this seasonality means that *Colletes* bees are generally active between late-spring and summer and spend the winter protected in their nests. Depending on the species type and soil temperature *Colletes* bees will be active at different times of the year and will overwinter in varying stages of development [1]. For example, *Colletes validus* emerges from its nest early and is active in nest construction and provisioning from the beginning of April to the end of May. The laid eggs will then continue to develop and become adults by September, the resulting *Colletes validus* overwintering in the adult stage [14]. *Colletes halophilus* however is active much later, from the middle of August until the middle of October and thus has less time for development before the winter [20]. As a result, *Colletes halophilus* overwinters in its inactive prepupae developmental stage [1].

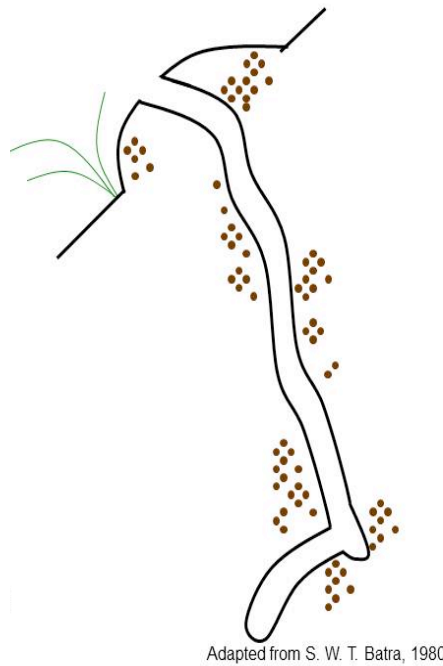
#### **2.3.4. Nest Construction**

Although species of Colletidae nest in a variety of environments, *Colletes* species typically nest in sandy soil with little interspecific variation in nest construction [21]. Though solitary in behaviour, some *Colletes* bees, such as *Colletes halophilus*, have been seen to nest in aggregations [20]. An aggregation, from where the nest cell linings used in this study were excavated, can be seen in Figure 5.



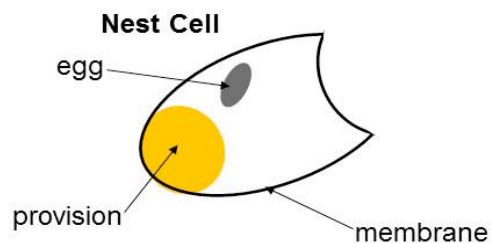
**Figure 5: Nesting aggregation of *Colletes halophilus* in East Tilbury, UK**

Within these aggregations each circular opening represents an individual female's nest. These nests consist of a central burrow typically 7-15cm in depth, off of which multiple tunnels radiate for a distance of 3-11cm in length [21]. At the end of each of these radial tunnels the female will create a nest cell lined with a polymer material. An illustration of a *Colletes* nest can be seen in Figure 6.



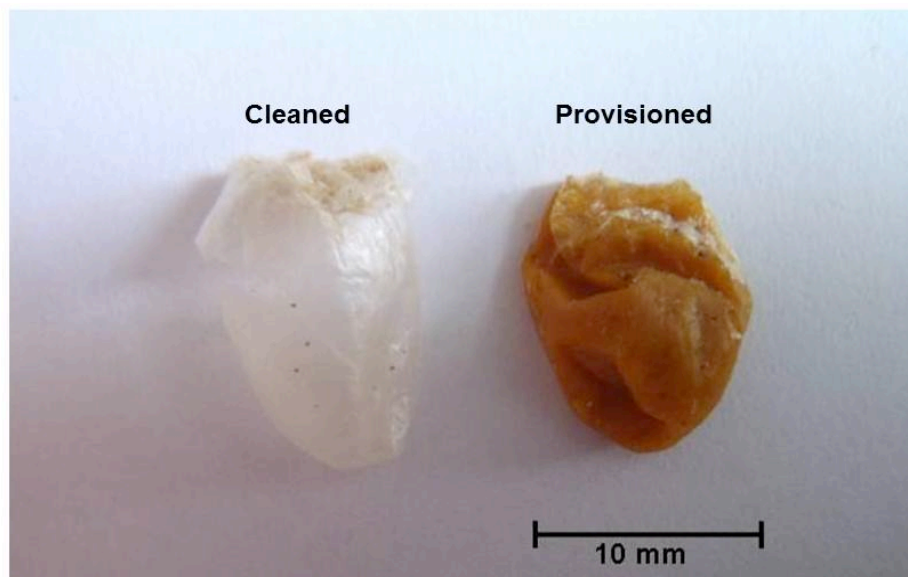
**Figure 6: Diagram of *Colletes* nest (adapted from S.W.T. Batra, 1980) [14].**

Figure 6 represents a typical *Colletes* nest with a highlighted central burrow. A lateral branch can be seen off this central burrow; a nest cell would be constructed at the end of this branch. A diagram of a nest cell can be seen in Figure 7.



**Figure 7: Diagram of *Colletes* nest cell lining.**

For the *Colletes* bee, the nest cell serves as a protective environment in which its brood can develop. The nest cells are approximately 5-17mm in length and 7-9mm in diameter. They are constructed with a polymer membrane approximately 20µm to 30µm in thickness for the main body of the nest cell and approximately 50 µm in thickness for the cap of the nest cell. This membrane serves as an antifungal and waterproof barrier. Within this membrane the *Colletes* female will store liquid provisions of pollen and nectar and lay a single egg. The liquid provisions will serve to feed the colletid as it matures from an egg through the larval stages and into adulthood [14]. A provisioned nest cell and a cleaned nest cell, both excavated from the aggregation in East Tilbury, can be seen in Figure 8. Both nest cells are oriented with the nest cell cap up.



**Figure 8:** *Colletes halophilus* nest cell linings, one cleaned and one as excavated.

Once a burrow has been dug, female *Colletes* begin the process of creating the nest cell. As mentioned, what makes *Colletes* unique is their production of nest cell lining material which is used to protect the egg during its development through the larval stages into maturity. The actual process by which this nest cell is constructed is somewhat unclear, with two main hypotheses presented here.

The first hypothesis is based on observations made by Batra [13] who noted that after having dug a nest cell cavity, the female began construction by licking the outlet of her abdomen. The female then spreads this secretion along the earthen wall of the nest cell

cavity. In doing this, the material solidifies. The female repeats this process, folding her body in half to lick the outlet of her abdomen and spreading these secretions with her bilobed tongue, until the nest cell cavity is fully coated with polymer. Batra conjectured that the process is one whereby the female licks the contents of the Dufour's gland, ingesting them and through this ingestion process mixes the Dufour's secretions with some polymerizing enzyme such that when the mixture is licked on the dirt walls it solidifies [14]. The presence of such a polymerizing enzyme is supported by the fact that, if extracted from a female Colletid Dufour's gland, secretions do not self-polymerize [22]. No such polymerizing enzyme has yet been identified.

The second hypothesis is based on observations made by Torchio et al [21] on the nesting behaviour of *Colletes*. Instead of ingesting their Dufour's gland secretions, Torchio et al observed *Colletes* females applying two separate secretions in order to create the nest cell lining. They noted the females began by depositing a secretion from the tip of her abdomen, most probably from the Dufour's gland, on to the dirt surface. The female then approaches the droplets with her glossa and spreads them while extruding an additional salivary secretion. It is proposed that the interaction of these two secretions causes the nest cell lining material to polymerize during the brushing process [21].

After laying down this initial layer, the *Colletes* females are seen to apply additional layers of polymer akin to Batra's description, by licking the tip of their abdomen and mixing this with salivary secretions in their mouth before licking onto the cell walls. Another important observational difference is that Torchio et al noted the production of strands of salivary secretion used to create a lattice work upon which the cap of the nest cell was later created [21]. The current study will shed additional light onto the nest cell construction and the observations made by both Batra [14] and Torchio et al [21].

## **2.4. Nest Cell Linings**

The nest cell lining material is functionally used to protect the *Colletes* brood throughout their development, serving as an environmental barrier preventing flooding, moulding or desiccation of the nest cell [3, 15, 16].

### 2.4.1. Nest Cell Lining Origin

The source of *Colletidae* nest cell lining material has long been considered, with the Dufour's gland being a likely candidate [18]. This was supported by observations of nest cell construction (as described in 2.3.4) and has since been confirmed chemically with several studies showing the same products present in the Dufour's gland as in the nest cell lining [10, 19, 22, 23]. May [23] was the first to test this hypothesis, comparing the oily Dufour's gland secretions of *Augochlora pura* (a bee of the family Halictidae) with the waxy nest cell lining it produced. Using Thin-layer Chromatography and IR spectroscopy the author noted that the wax could be an oxidation product of the secretion [23]. Albans et al. [10] and Hefetz et al. [22] expanded this work to *Colletes*, confirming the Dufour's gland origin using Gas Chromatography – Mass Spectroscopy.

In their study, Hefetz et al. attempted to describe the chemical process by which the Dufour's gland secretions become the solid nest cell lining material. A diagram of the likely chemical reaction is shown in Figure 9.

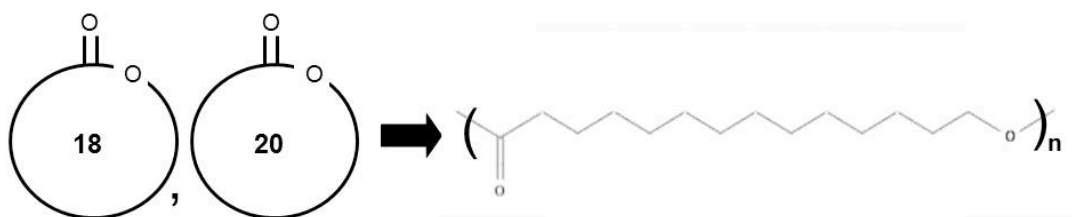


**Figure 9: Reaction of Dufour's gland secretions to form *Colletes* nest cell lining as suggested by Hefetz et al [22].**

The Dufour's gland contains a variety of molecules, including 18-Carbon and 20-Carbon macrocyclic lactones. These lactones are polymerized in a ring-opening polymerization reaction. The chain length of the resulting polymer is unknown though its chemical stability (described in section 1.4.3) suggests it is of high molecular weight. The catalyst for this ring-opening polymerization reaction is also unknown. As mentioned, the Dufour's gland secretions do not self-polymerize when exposed to the atmosphere. It is believed that polymerizing enzymes for this reaction exist in the salivary glands, though their existence has not been confirmed experimentally.

### 2.4.2. Known Microstructure

The nest cell lining material of *Colletes* has often been described as cellophane like, being a clear-solid polymer film. Though observations on the construction of this material have been made, little work has been carried out to investigate the microstructure of the *Colletes* nest cell. None have addressed the species *Colletes halophilus* that will be the focus of the current study.

Using Scanning Electron Microscopy (SEM) the nest cell linings of several Colletidae species have been examined with varying findings. Within *Colletes*, *Colletes succinctus* was examined. The nest cell lining was seen to be smooth and continuous. The only variation noted was when pollen became embedded into the polymer surface [10]. These images stand out in sharp contrast to SEM images of the nest cell lining of *Hylaeus cressoni*, a species of the same subfamily Colletidae known for its silken nest cell lining, showing a fibrous exterior [24]. Striations on the surface of nest cell linings constructed by *Chilicola araucana*, members of Colletidae, have also been observed and attributed to being an artefact of nest cell construction [25].

### 2.4.3. Known Chemical Composition

The current understanding of the chemistry of *Colletes* nest cell lining is that it is a polymer system, composed primarily of polyester material with smaller amounts of a proteinaceous, most likely silk, component. The investigation which supports this understanding is presented here.

### Solubility

The nest cell linings of *Colletes* bees have proved difficult to analyse due their chemical resistance. This is supported by a forced hydrolysis using propionic acid and 6M HCl being needed to hydrolyse nest cell lining samples [10]. Jakobi attempted to quantify this resistance and relative solubility of a variety of bee nest cells including *Colletes* [26]. The findings show *Colletes* nest cells to be increasingly soluble in cyclic solvents

including dioxan, pyridine and toluene, and resistant to non-cyclic solvents including chloroform, ethyl alcohol and methyl butanol [26].

## Combustion Analysis

A preliminary understanding of the elemental makeup of this polymer has been established using combustion analysis. The elemental makeup of a variety of *Colletes* species can be seen in Table 1 [10].

**Table 1 Combustion Analysis of *Colletes* Nest Cell Linings from Albans et al. [10]**

<b>Element</b>	<b><i>C.c.c.</i> (%)</b>	<b><i>C.s.</i> (%)</b>	<b><i>C.h.</i> (%)</b>	<b><i>C.d.</i> (%)</b>
<b>Carbon</b>	49-52	60-65	65-69	65-68
<b>Hydrogen</b>	5-9	9-10	9-11	9-11
<b>Nitrogen</b>	3-4	3-5	2-4	2-4
<b>Oxygen</b>	35-43	19-20	16-24	17-24

*C.c.c.* = *Colletes cunicularius cunicularius*; *C.s.* = *Colletes succinctus*; *C.h.* = *Colletes halophilus*; *C.d.* = *Colletes daviesanus*  
from Albans et al. [10]

Of particular interest in these results is the elevated nitrogen content. Though lower than entirely silk materials, it is higher than would be expected for a purely polyester material with some nitrogen containing debris on the nest cell lining. This suggests that the material may contain a proteinaceous as well as a lipid component [10].

## Amino Acid Analysis

To further analyse the nitrogen component found in the combustion analysis results, an amino acid assay was completed for several *Colletes* species by Albans et al. [10]. This data is presented in Table 2.0



**Table 2 Amino Acid Assay of *Colletes* Nest Cell Lining from Albans et al. [10]**

<b>Amino Acid</b>	<b><i>C.c.c.</i> (%)</b>	<b><i>C.s.</i> (%)</b>	<b><i>C.h.</i> (%)</b>	<b><i>C.d.</i> (%)</b>
<b>Lysine</b>	3.8	7.0	3.8	3.9
<b>Histidine</b>	2.6	1.5	2.3	2.1
<b>Aginine</b>	0.0	1.3	0.0	0.0
<b>Aspartic Acid</b>	2.9	5.2	1.2	5.6
<b>Threonine</b>	0.3	1.0	0.6	1.2
<b>Serine</b>	1.3	3.8	2.3	2.9
<b>Glutamic Acid (I)</b>	62.0	44.6	71.8	65.3
<b>Proline</b>	0.0	0.0	0.0	0.0
<b>Glycine</b>	4.7	5.3	2.8	4.8
<b>Alanine (II)</b>	14.7	15.0	12.1	10.7
<b>Valine</b>	2.1	4.8	0.0	4.2
<b>Methionine</b>	0.0	1.0	0.0	0.0
<b>Isoleucine</b>	1.6	2.4	0.7	0.4
<b>Leucine</b>	2.4	3.4	0.7	1.2
<b>Tyrosine</b>	0.0	1.4	0.0	0.0
<b>Phenylalanine</b>	0.0	1.4	0.0	0.0

*C.c.c.* = *Colletes cunicularius cunicularius*; *C.s.* = *Colletes succinctus*; *C.h.* = *Colletes halophilus*; *C.d.* = *Colletes daviesanus*  
from Albans et al. [10]

These results were compared to pollen samples to ensure the nitrogen content was not a residue of pollen debris. The results show elevated levels of glutamic acid, serine and alanine suggesting that the proteinaceous element in the nest cell lining could be a silk [10]. Members of Hymenoptera have independently evolved the ability to produce silk numerous times so it would be reasonable for *Colletes* to have this ability [27]. How this silk component could be produced has not been identified.

## Gas Chromatography – Mass Spectroscopy (GC-MS)

To better understand the chemical makeup of the non-proteinaceous nest cell lining component GC-MS was performed on Dufour's gland secretions and on hydrolysed nest cell linings [10, 22]. The results show the presence of a variety of macrocyclic lactones, mostly 18-octadecanolide and 20-eiconosolide (rings with 18 and 20 carbons respectively), within the Dufour's glands of *Colletes* bees as well as the fragmentation pattern of ester containing molecules, such as methyl 18-hydroxyoctadecanoate, within the nest cell lining. These results suggest that nest cell lining is constructed from polymerized lactones found in the Dufour's gland of *Colletes* bees. The resulting material was identified as a linear polyester [22]. The mechanism of polymerization is yet unknown as well as the chain length of the present linear polyesters. However, the chemical robustness of the material suggests it is of high molecular weight.

### 2.4.4. Additional Material Properties

Little has been done to characterize additional material properties of the nest cell lining which relate to its performance. Observations which have been made of the nest cell lining are of the transparency of the material as well as it being successfully biodegradable within a five year time span [28]. These characteristics are relevant when considering the broader potential of the nest cell lining material.

## 2.5. Related Materials

To understand the nest cell lining material it is useful to have a basic understanding of related materials. The background on related materials, including polyester and silk, is presented here.

### **2.5.1. Silk**

Due to the presence of nitrogen and high levels of glycine and alanine in the nest cell lining material, it has been suggested that this cellophane like material contains a silk [10]. The location of the silk in the nest cell material, or the source of its production, has not been confirmed, though the abundance of silk production in nature (particularly in Hymenoptera) makes it a reasonable suggestion that it is a component in the nest cell lining.

### **General Properties**

Silk can loosely be defined as a well oriented chain of amino acids which differ from other proteinaceous fibres in that they exist external to the organism's body. They acquire their unique orientation by having a specific chemical makeup as well as undergoing an intensive extrusion process which forms the liquid silk dope into fibres generally through shear forces [29].

Chemically, silks are mainly formed from the amino acids glycine, alanine and serine – the small amino acids. These smaller amino acids, without bulky side chains, allow for tighter packing of the protein chain and result in areas of high crystallinity [29]. Under Fourier Transform Infrared Spectroscopy (FTIR) analysis silks demonstrate the peaks characteristic of amide I (sharp peak between  $1680\text{cm}^{-1}$  and  $1630\text{cm}^{-1}$ ), amide II (sharp peak between  $1570\text{cm}^{-1}$  and  $1515\text{cm}^{-1}$ ) and amide III (sharp peak between  $1270\text{cm}^{-1}$  to  $1235\text{cm}^{-1}$ ) bonding with some variation in peaks due to varying residue composition and crystallinity [30-33].

Silks have long been of interest commercially and scientifically due their unique properties, ranging from aesthetic beauty to mechanical strength. They have also been seen to be viable in temperature ranges up  $220^{\circ}\text{C}$  allowing their use in a range of environments [34-36]. Though different silks have chemical similarities their performance and structure ranges widely. To illustrate this, three of the most common silks are described in the following sections.

## Occurrences of Silk in Nature

Though recent attempts have been made to synthesise it, silk is a naturally occurring material produced exclusively within the phylum Arthropoda [37]. Many species of insect and spider are capable of silk production however the properties and production of these silks vary widely. Various arthropods produce silk at different stages of development (adult, larval or throughout life) and from different glands (often labial glands or Malpoghian tubules). The produced silks also range widely in terms of use, chemistry and structure [27, 37]. The production and properties of some notable silks are presented below.

### *Silk Moth (Bombyx mori) Silk*

The most common commercially available silk is that of *Bombyx mori*, usually referred to as the silk moth. The silk from these insects is widely farmed and used in textile production.

In *Bombyx mori*, silk is a by-product of the metamorphosis process. It is produced by the larval form of the insect to make a cocoon in which it will mature [38]. The extruded silk is composed of a proteinaceous core known as fibroin surrounded by an amorphous sericin [29].

The protein structure of silkworm fibroin can be characterized as parallel  $\beta$ -sheets. The abundance of small-chain residue amino acids (glycine, alanine and serine) and the parallel  $\beta$ -sheet structure allow for regions of high crystallinity where pleated sheets can pack tightly upon each other. These crystalline regions are broken up with amorphous areas, providing space for long-chain residue amino acids. This structure allows for fibre stiffness through the crystalline regions and molecular deflection through the amorphous regions [39]. This results in a material with a tensile strength of 600MPa and an extensibility of 18% [29].

### *Spider silk*

Spiders are capable of producing a wide range of silks using a variety of silk ducts and spinnerets. For example, *Nephila clavipes*, more commonly known as the golden-orb weaving spider, has five to seven silk glands and is capable of varying the stickiness and strength of its silk depending on the material's purpose [40]. The most interesting of these materials scientifically is generally considered to be dragline silk, the silk which serves as a tether between the spider and the web protecting it should it fall or encounter other dangers [41]. Dragline silk has the unique properties of high toughness, high strength to weight ratio and biological compatibility that would make it potentially useful in a variety of engineering fields [39].

In spiders, silk production is carried out by mature insects principally using secretions from the major ampullate gland. These secretions are passed through a series of spinnerets which serve to orient the fibres. It is through the use of these different spinnerets that spiders are capable of creating a range of silks with varying performances [40]. In dragline silk in particular, the resulting material is extremely robust and resistant to chemical degradation [40].

Like *Bombyx mori*, the structure of spider silk is composed of  $\beta$ -sheets arranged into highly crystalline regions broken up by amorphous segments. However, in the case of dragline silk there exist more long-chain residue amino acids (argine in particular) resulting in more extensive amorphous regions. It has been suggested that this ratio of amorphous to crystalline ratio effects the silk performance resulting in spider dragline silk having improved mechanical performance relative to silkworms [40]. In dragline silk these material properties are a tensile strength of 1420MPa and an extensibility of 21% [29].

### *Honeybee silk*

Though spider and silkworm silk have long been considered the most promising of silk materials, honeybee silk has been increasingly investigated as an alternative material

since it lends itself to production by recombinant-DNA techniques. In honeybees the adult bees create wax comb in which they raise their brood. Within this comb mature larva will produce a silken cap to reinforce the comb cell walls and protect them during their hibernation as pupae [42].

Unlike the other silks discussed, the fibroin of honeybee silk is predominately made up of four non-repetitive fibrous proteins arranged as  $\alpha$ -helices. These helices have a coiled-coil structure, meaning that the four proteins are entwined in an arrangement unique to some species of Hymenoptera [43]. This unique coiled-coil structure provides honeybee silk with increased extensibility and toughness over silkworm silk and better adaptability to transgenic production than spider silk. Honeybee silk has a tensile strength of 400MPa and a high extensibility of 204% due to its coiled-coil structure. Additionally, its four non-repetitive proteins sequences are more effectively and reliably expressed by bacteria with recombinant DNA than the repetitive protein sequences of spider silk, making it more promising for study using recombinant DNA techniques [44].

### **2.5.2. Polyester**

The nest cell lining of *Colletes* bees has been described as a high molecular weight polyester, supported by GC-MS findings [45]. A general discussion of polyesters and their rare occurrences in nature are presented here.

#### **General properties**

The term polyester refers to a wide range of polymers with a variety of properties. What links all polyesters chemically is their carbon backbone and repetition of an ester group. Beyond this, the amount and complexity of side groups vary widely. For example, two common commercial polyester products are polyethylene terephthalate (PET), a thermoplastic commonly used in plastic bottles, and thermoset polyesters used as boat exteriors [46]. An example of a simple polyester can be seen in Figure 10 where the ester group is clearly visible and the R-groups vary depending on the polymer.

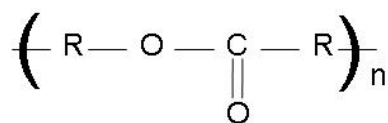


**Figure 10: Generic polyester molecule**

Polyesters are generally formed through condensation reactions where the by-product is a small molecule, typically water or methanol. This is carried out commercially to create most forms of synthetic polyester with naturally occurring polyesters being extremely rare [46].

As previously mentioned, polyester is a relatively generic term for a class of polymers with a wide range of properties. Some polymer characteristics that affect material properties include chain chemistry, chain length and crystallinity. For example, the more crystalline a polymer and the longer its chain length, the higher the molecular bonding within a sample and the higher its melting temperature will be. Chain length and crystallinity are the differences between methane, a colourless liquid with a melting temperature of  $-182^{\circ}\text{C}$ , and paraffin wax, an opaque solid with a melting temperature of approximately  $50^{\circ}\text{C}$  – the monomers of these two substances are chemically identical. Additionally, chain chemistry greatly affects material performance. For instance PET, a polyester composed of an aryl ester group, has a melting point of  $260^{\circ}\text{C}$  and a decomposition temperature of over  $340^{\circ}\text{C}$  while polylactide (PLA), a biologically derived polyester composed of an methyl branched ester, has a significantly lower melting point at  $175^{\circ}\text{C}$  but a similar decomposition temperature of  $335^{\circ}\text{C}$  [47, 48]. As well as varying thermal properties, mechanical performance varies in polyesters with properties such as tensile strength ranging from 40MPa to 70MPa [49]. Little information is known about the crystallinity or chain length of the polymers present with in the *Colletes* nest cell lining.

## Occurrences in nature

Beyond the nest cell linings produced by *Colletes* bees, the only other known natural occurring long-chain polyesters are produced by bacteria. Polyhydroxybutyrate (PHB) is a polyester produced by over 100 species of bacteria to be used as an energy source in the event of starvation [50]. Due to its uniqueness, PHB has been investigated as a potential source for the production of biodegradable polyesters for commercial use [51].

Though long-chain polyesters are rare in nature, wax esters are very common and serve a similar biological purpose. Like other waxes, wax esters have relatively low melting and decomposition temperatures [52]. Both polyesters and wax esters are used for waterproofing as well as to control humidity and water-loss. Wax esters are used by many arthropods and plants for this purpose. For example cutin, the waxy material on the surface of plants, is a wax ester used to moderate evaporation [53]. In the case of *Colletes* bees the polyester nest cell lining helps to control water content in their food provisions as well as allowing them to nest in areas subject to flooding [2].

Another relevant naturally occurring wax ester, similar in function to the *Colletes* nest cell linings, is beeswax. Many species of bee, including members of the genera *Bombus* (bumblebees) and *Apis* (honeybees), produce beeswax to construct their hives for food storage and brood rearing. Though not entirely composed of ester containing compounds, the majority of beeswax is made up of monoesters and diesters resulting in a pliable material with a melting point between 35°C and 70°C and a decomposition temperature between 120°C and 200°C depending upon the bee species [54, 55]. The appearance of beeswax stands in sharp contrast to the cellophane like lining of *Colletes*, however their chemical building blocks appear to be quite similar.

## 2.6. Goals for Thesis

Although the nests of bees, including those of *Colletes*, have long been of interest to entomologists this is the first investigation looking at the nest cell lining of *Colletes halophilus* from an engineering materials perspective. Studies have suggested that these nest cell linings are composed of a robust polyester made from the secretions of the



Dufour's glands of *Colletes* bees. However, many characteristics of this material remain contested, with varying reports of chemical composition and physical construction. The aim of this study is to resolve some of these contradictions in the literature by enhancing the understanding of the chemistry and formation of the nest cell lining material.

The result of this work will be an improved understanding of the *Colletes halophilus* nest cell lining material and greater knowledge of the genus as a whole. Additionally, this study will serve as a stepping stone to the creation of polymers inspired by this robust natural material. With increased focus on alternatives to traditional petroleum based plastics, a biologically derived and biodegradable polyester material such as the nest cell lining could have a valuable environmental impact. To accomplish this, the study will attempt to do the following:

1. Resolve discrepancies in chemical data by creating a complete picture of nest cell lining chemistry.
2. Resolve discrepancies in observed nest cell construction.
3. Explore the microstructure of the nest cell lining and how this relates to chemical composition.
4. Characterize material properties of nest cell lining material to assess the potential of the material in engineering applications and the potential environmental benefit.

## Chapter 3: Methods of Characterization

### 3.1. Chapter Overview

In this chapter the various methods of characterization used in the current study are presented. The functions of the various instruments utilized as well as the aim of these studies are outlined here. Details of testing protocol and materials used are discussed in Chapter 5.

### 3.2. Microstructure

The microstructure of the nest cell lining samples was explored using a variety of microscopy techniques. The background to these techniques is presented here.

#### 3.2.1. Scanning Electron Microscopy

Scanning Electron Microscopy (SEM) was the imaging technique used to analyse much of the microstructure and surface topography of the nest cell lining, viewing features on the micron scale. A schematic of a scanning electron microscope can be seen in Figure 11.

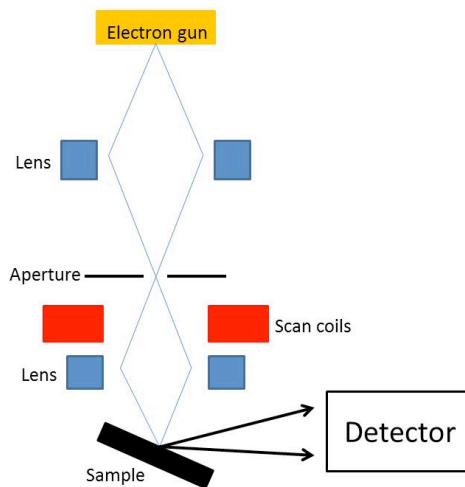


Figure 11: Diagram of scanning electron microscope

In brief, an SEM works by firing electrons at a conductive surface and monitoring the position of these electrons. Before a sample can be analysed using the SEM it must first be made conductive if it is not naturally so. This typically involves applying a conductive layer using either a gold sputter coating or carbon evaporation process.

Once the sample is prepared it can be loaded under vacuum into the SEM and imaged. The first step in this process is the emission of electrons from the electron gun, typically a tungsten-filament cathode heated to release an electron beam. From the electron gun, electrons pass down the column of the microscope through a number of magnetic condenser lenses which serve to focus the beam. Next, the condensed beam is passed through the scan coils which spread the beam such that it can scan the surface of the specimen. The beam then interacts with the specimen, experiencing an elastic collision and redirecting the electrons. These scattered secondary electrons are then picked up by a detector, which constructs an image of the surface topography based on the scattering. The resulting image is a 3D representation of the specimen with an optimal resolution down to the nanometre scale.

### **3.2.2. Transmission Electron Microscopy**

Transmission Electron Microscopy (TEM) was used to analyse the more detailed molecular structure of the nest cell lining, looking at features on the nanometre scale. A schematic of a transmission electron microscope can be seen in Figure 12.

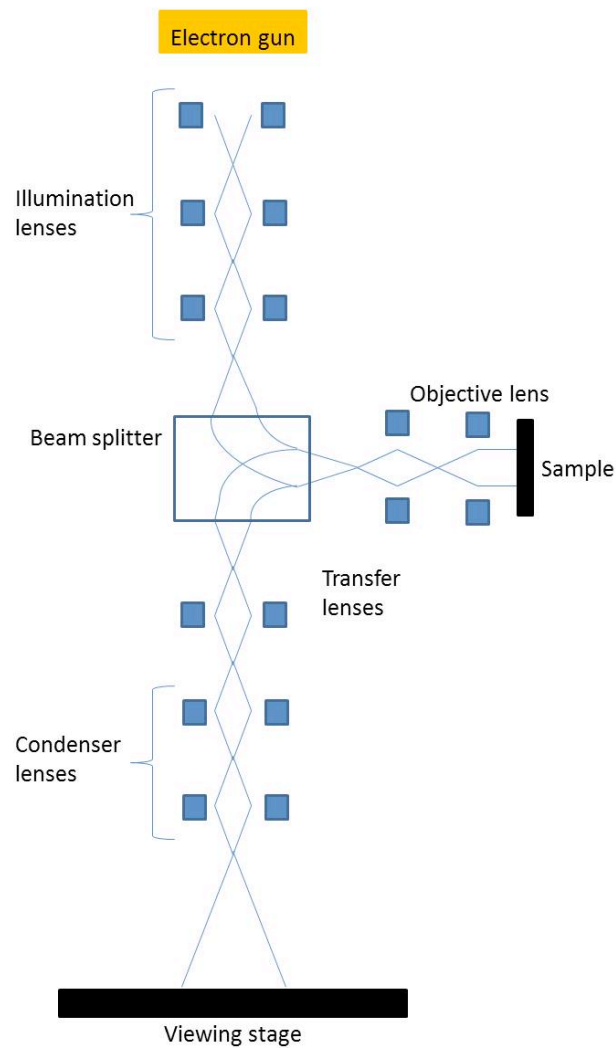


**Figure 12: Diagram of transmission electron microscope**

A TEM works under vacuum much in the same way as the SEM; electrons are fired at a conductive surface and their position monitored. However it uses transmission of the electron beam through the surface of an ultra-thin specimen to achieve higher resolution. Before samples can be put into the TEM they must first be sectioned, and often stained, to enhance imaging. In order for the electron beam to effectively pass through a sample, the specimen must be less than 100nm thick. Specimens are thus sectioned on a microtome to the desired thickness and placed on grids to support them in the TEM. Non-conductive samples are next stained to achieve contrast in the TEM, one of the most common stains for biological materials being osmium tetroxide.

Once the samples are prepared they can be loaded into the TEM. As in SEM, a filament, often made of tungsten, is heated to emit electrons from the electron gun. This electron beam passes through a series of condenser lenses and the aperture which serve to focus and restrict the beam. The beam then passes through the specimen, causing a disruption in the electrons before continuing through a variety of lenses that serve to refocus and project the final image. The resulting image is a black and white projection showing the varying crystalline phases and molecular structure within a material.

### 3.2.3. Confocal Microscopy

Confocal microscopy was performed to better visualize the microstructure of the nest cell lining material by assessing its fluorescence. A diagram of a confocal microscope is presented in Figure 13

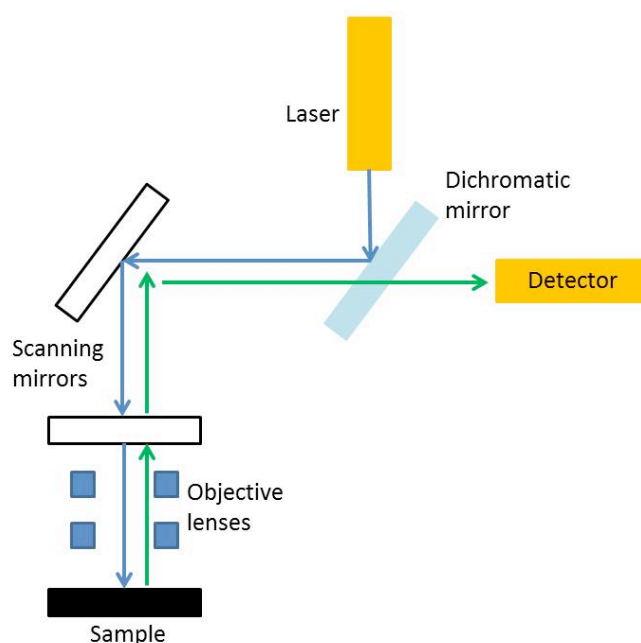


**Figure 13: Diagram of a confocal microscope**

A confocal microscope is a fluorescence microscope that can achieve a very narrow focal plane, allowing for high definition through the profile of a sample and the construction of 3D images of a sample. Since it is a fluorescence microscope, samples for confocal microscopy are often stained with a fluorescent dye before visualization.

Common stains include 4', 6-diamidino-2-phenylindole (DAPI) for staining DNA and krypton red for staining protein. Some materials, such as the nest cell lining material, autofluoresce so they do not require staining in order to be seen under the confocal microscope.

Confocal microscopy begins with the selection of an excitation laser. Most confocal microscopes are fitted with a variety of lasers that produce different wavelengths of light. These different wavelengths will excite different fluorescent dyes and lasers have to be chosen accordingly. Once selected and activated, the laser will emit a beam of light that is restricted through an aperture. This beam hits a dichromatic mirror which is selected to reflect the laser but allow other wavelengths of light to pass through. The beam then hits the sample which will excite the fluorescent dye causing an emission wave length of light to be reflected. This light is able to pass through the dichromatic mirror and through an additional aperture before hitting the detector. The resulting image represents a thin slice through the material but can be digitally combined with additional slices to reconstruct a full 3D image. Though lower magnification than the techniques previously discussed, with a resolution alike that of an optical light microscope versus that of SEM or TEM, confocal microscopy has the added benefit of fine focusing through the material thickness.

### **3.3. Chemical Composition**

The chemical makeup of the nest cell lining samples was explored using a variety of characterization techniques. The background to these techniques is presented here.

#### **3.3.1. Combustion Analysis**

Combustion analysis was performed on the nest cells to determine their basic elemental content. In brief, combustion analysis works by burning a hydrocarbon sample, collecting the resulting products and using those products to determine the elemental composition of the hydrocarbon. A diagram of a combustion analyser can be seen in Figure 14.

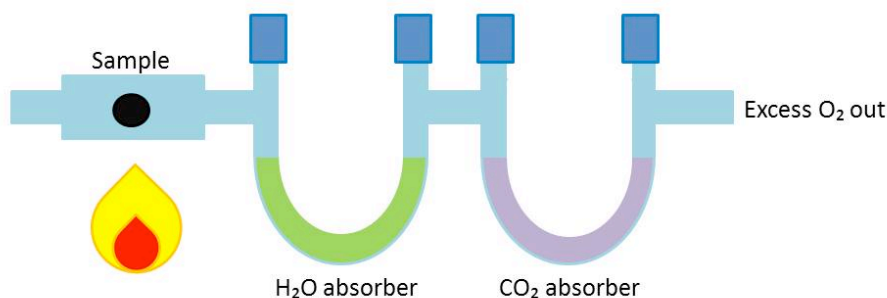


**Figure 14: Diagram of combustion analyser**

To perform combustion analysis a sample must first be burned in the presence of oxygen. In combusting, the hydrocarbon material reacts with the oxygen forming a variety of combustion gases, such as H<sub>2</sub>O, CO<sub>2</sub>, NO<sub>2</sub> and NO. These combustion gases then travel through the analyser where they can be selectively absorbed by a variety of solvents. These solvents are then analysed to determine the amount of gases they absorbed. The quantity of each particular element present can be derived from the relative amounts of the combustion gases. It should be noted that only carbon, nitrogen, oxygen, sulphur and hydrogen can be detected using this process.

### **3.3.2. X-Ray Diffraction**

Powder X-Ray Diffraction (XRD) was used to analyse the crystal structure and composition of the nest cell lining material. In powder XRD, a sample is first pulverized, if it is not already in powder form, the intention being that the distribution of crystal orientations will then be random and all crystal orientations will be represented equally.

Once in powder form, the sample is loaded into the machine and x-rays are directed into the sample. The x-rays interact with groups of atoms that are organised in such a way as to represent specific crystallographic orientations within the structure. The resultant elastic collisions and scattering from the sample are collected and analysed by a detector. The output is a diffractometer trace which contains peaks which are indicative

of the phases present and features of crystal structure such as inter-planar spacings. The XRD diffractometer plots scattering angle,  $2\theta$ , against relative intensity.

### **3.3.3. Amino Acid Analysis**

Since the combustion analysis indicated a significant presence of nitrogen, an Amino Acid Analysis (AAA) was carried out to see if this corresponded to a proteinaceous nest cell component. AAA begins with a hydrolysed sample, the hydrolysis normally being performed in strong acid. This sample then goes through a liquid chromatography system which separates the various amino acids. Once separated, the amino acid analytes can be fed into a detector where the relative amounts present are quantified.

### **3.3.4. Fourier Transform Infrared & Raman Spectroscopy**

Fourier Transform Infrared Spectroscopy (FTIR) was used to analyse the nature of the chemical bonds which make up the nest cell lining material. FTIR works by recording the absorption of different wavelengths of light by a sample, and then correlating those absorbed wavelengths with characteristic bond absorptions.

FTIR begins by shining a beam of light through a treated mirror which reflects selected wavelengths onto a sample. This process is repeated, changing the angle of the mirror and thereby changing which wavelengths are omitted. The absorption data is compiled and by means of a Fourier transform, converted into a full absorption spectrum which can be interpreted. Since chemical bonds have characteristic absorptions, for example C=O characteristically absorbs light at  $1750\text{cm}^{-1}$ , molecular structure can be deduced from this spectrum.

Raman spectroscopy was carried out to complement information from FTIR. Similar to IR spectroscopy, Raman spectroscopy measures the vibrations of bonds within a sample. However, while IR spectroscopy measures these frequencies directly using infrared light, Raman spectroscopy compares the shift in wavelength of a laser light source before and after interacting with a sample. These changes in wavelength, called



the Raman shift, can be attributed to excitation or decay within a sample. Though less commonly used for organic materials, Raman spectroscopy offers complementary information to FTIR as symmetric bonds, which are not visible in FTIR, can be detected with Raman spectroscopy.

### **3.3.5. Gas Chromatography – Mass Spectroscopy**

Gas Chromatography – Mass Spectroscopy (GC-MS) was used to determine the molecular makeup of the nest cell lining material. GC-MS begins with a hydrolysed sample in solution, often methanol or methylene-chloride. This sample is then passed through the GC to separate constituent molecules by their relative affinities to a mobile phase. Once separated, these molecules can be analysed using MS.

Mass spectroscopy has three main components: the ion source, the mass analyser, and the detector. Samples must first be ionized. This can be achieved in a variety of ways, but can most simply be carried out by passing the sample through a beam of electrons. Once ionized, the sample moves into a magnetic field which is able to separate molecules by their relative masses which are then picked up and recorded by a detector. It should be noted that in the ionization process many of the molecules become unstable causing them to fragment into smaller ions, so the output of the detector is generally a fragmentation pattern of the desired molecule.

### **3.3.6. Time of Flight**

To further determine the molecular makeup of the nest cell lining material two Time of Flight (TOF) techniques were used – Electrospray Ionization (ESI) and Matrix-Assisted Laser Desorption/Ionization (MALDI). The benefit of these techniques is their wide range of detection. While GC-MS is only suitable for smaller molecules, ESI-TOF and MALDI-TOF are commonly used for polymers since these techniques can ionize and detect molecules with molecular weights of over 10,000amu. Both techniques begin with a sample in solution. With ESI, a high voltage is applied to a liquid sample thereby turning the dissolved sample into an aerosol, causing a loss in solvent and ionization of

the remaining molecules in the process. With MALDI, the molecules to be examined are incorporated onto a crystalline matrix at which an ionizing laser is fired. The matrix serves both to protect the molecules from the ionizing laser and transfer charge to the molecules.

These techniques both use the same time of flight technique. Once ionized, the sample is fired across an oppositely charged plate. Ions of different molecular weight within the sample will travel different distances along the plate in proportion to their weight. Molecules can then be identified by their relative molecular weights.

### **3.4. Material Properties**

To better understand the nest cell lining material, its thermal properties and mechanical properties were characterized. Descriptions of the techniques used for characterization are presented here.

#### **3.4.1. Thermogravimetric Analysis**

Thermogravimetric Analysis (TGA) was completed to determine the relative decomposition temperatures for the various components within the nest cell material. TGA works by heating up a sample of material while it is on a balance to continually measure its mass. This allows for changes in mass to be noted, providing information such as water absorption and decomposition temperature. The normal temperature range over which this is carried out is from room temperature to an excess of 1000°C

#### **3.4.2. Differential Scanning Calorimetry**

Differential Scanning Calorimetry (DSC) was carried out to determine the characteristic phase changes, such as glass transition, melting point and recrystallization temperatures in the material. DSC functions by monitoring the amount of energy needed to increase the temperature in a sample. A prepared sample, normally placed into an aluminium

pan, is heated alongside an empty pan. The amount of energy required to heat the pans at the same rate is then measured. The sample will require more or less energy to be heated at a constant rate if it is undergoing a phase transition, more if an endothermic reaction and less if exothermic. Thus, by monitoring heat flux different types of phase transitions can be identified. These experiments can be carried out from temperatures below 0°C to detect glass transition temperatures and up to higher temperatures on the order of hundreds of degrees Celsius to witness melting or material decomposition.

### 3.4.3. Mechanical Testing

An Instron testing machine was used to measure the tensile strength and approximate elastic modulus of the nest cell lining material. An Instron is a standard mechanical testing machine that can apply a controlled load to a sample and measure the resulting stress and strain. The engineering stress is calculated from the force on the sample, measured by the load cell on the machine, divided by the specimen's cross-sectional area. This relationship is described by Equation 1 where  $\sigma$  is engineering stress,  $F$  is the measured force and  $A$  is the cross-sectional area.

$$\sigma = \frac{F}{A} \quad (1)$$

The engineering strain is calculated by comparing the length of the sample before and during deformation. This relationship is described in Equation 2 where  $e$  is the engineering strain,  $L$  is the measured length of the specimen and  $L_0$  is the original length of the specimen. The amount of deformation under tensile loading is preferably measured using an extensometer, but due to the size and delicacy of the sample, the position of the crosshead was used a less accurate alternative.

$$e = \frac{L - L_0}{L_0} \quad (2)$$

In the case of the nest cell lining material, the sample was loaded in tension and the output recorded. The small size of the specimens constrains the loading rate and load

cell that can be used. With the outputs of stress and strain calculated, other material properties can be concluded. Of particular interest to this study were fracture stress, the stress at which the material fails, and Young's modulus, which relates to the stiffness of the material. Young's modulus, or the modulus of elasticity, is defined as tensile stress divided by tensile strain for the linear-elastic portion of a stress-strain curve.

### **3.5. Chapter Summary**

A wide variety of analytical techniques were employed for this investigation. Before implementation of these techniques, an understanding of the background to these methodologies was necessary. The breadth of techniques, including those for chemical analysis, microscopy and material characterization, was used to achieve a comprehensive understanding of this material. The detailed implementation and results from these investigations and how they relate to entomological knowledge will be presented in the following chapters.

## **Chapter 4: Review of Previous Research**

### **4.1. Chapter Overview**

Before coming to the University of Bath, the author completed research on the nest cell linings of *Colletes inaequalis* (a species of bee closely related to *Colletes halophilus*) at Franklin W. Olin College of Engineering with Dr. Debbie Chachra and Dr. Christopher Morse. A review of the unpublished results relevant to this study is presented here.

### **4.2. Introduction**

*Colletes inaequalis* is a solitary bee native to the north-eastern portion of the United States. Like other members of *Colletes*, *Colletes inaequalis* females construct their nests by digging burrows into sandy soil and creating a nest cell at the end of each burrow. The aim of this project was to investigate the chemistry and microstructure of the *Colletes inaequalis* nest cell. To do this a variety of analytical chemistry and microscopy techniques were used.

### **4.3. Materials and Methods**

For this study *Colletes inaequalis* nest cells were excavated from a site in Acton, MA. These nest cell linings were then cleaned with deionised water before being stored at 4°C until use.

#### **4.3.1. Combustion Analysis**

Combustion analysis was carried out to determine the elemental makeup of the *Colletes inaequalis* nest cell lining. Cleaned nest cell linings were sent to Atlantic Microlab, Inc. in Norcross, Georgia to undergo combustion analysis. Two sets of nest cell linings were analysed for carbon, hydrogen, nitrogen, oxygen and sulphur at their laboratory.

#### **4.3.2. Amino Acid Analysis**

To further assess the chemical makeup of this material AAA was performed. To conduct the AAA, cleaned nest linings were sent to the University of California Davis Proteomics Core Facility. At this facility samples were hydrolysed using 6M HCl at 110°C for 24 hours. Hydrolysed samples were then analysed using a Hitachi L-8800 amino acid analyser.

#### **4.3.3. Confocal Microscopy**

Cleaned nest cell linings were analysed using confocal microscopy to better understand their structure, particularly across the thickness of the material. Samples were mounted onto glass slides and treated with Nile Red in vegetable oil just before imaging. The Nile Red did not interact with the nest cell lining, but rather surrounded the material making the surface of the material more visible.

Imaging was carried out using a Leica confocal microscope with a 63X oil-immersion objective. A Helium-Neon 543 laser was used to excite the Nile Red and a UV laser for the excitation of the nest cell lining material.

#### **4.3.4. Gas Chromatography – Mass Spectroscopy**

In an attempt to recreate the work done by Hefetz et al [22], GC-MS was used to investigate the *Colletes inaequalis* nest cell linings. Nest cell lining material was hydrolyzed in a solution of equal parts 6M hydrochloric acid and propionic acid for 24 hours at 110°C. Once completely hydrolyzed, samples were neutralized with 3M NaOH before solvent removal under vacuum. Methylene chloride and methanol, solvents suitable for GC-MS, were then attempted as solvents for the nest cell lining samples. Very little of the nest cell lining material successfully dissolved into solution, most material immediately precipitated out of solution as white particulate. The partially dissolved solution was sent to the GC-MS facility at Wellesley College in Wellesley, MA for analysis.

## 4.4. Relevant Results

### 4.4.1. Combustion Analysis

The results of the chemical makeup of *Colletes inaequalis* nest cells obtained through combustion analysis can be seen in Table 3.

**Table 3: Combustion analysis results of *Colletes inaequalis* nest cell linings**

Element	Run 1 (wt %)	Run 2 (wt %)
Carbon	59.22	59.06
Hydrogen	9.60	9.46
Nitrogen	1.54	1.55
Oxygen	15.76	15.61
Sulphur	0.0	0.0

Table 3 lists some of the elemental components of the nest cell lining. It should be noted that in both runs the total wt% of the elements listed is approximately 86wt%. The remaining 14wt% is composed of elements not detected using this technique, most likely silica from debris on the surface of the nest cell lining. The most notable finding from this study is the appreciable nitrogen content present in the nest cell linings. If the nest cell linings were composed entirely of a polyester, as previously suggested [22], no such nitrogen presence should be detected. This suggests there is an additionally nitrogenous component in the material – potentially protein.

### 4.4.2. Amino Acid Analysis

The nitrogen containing component of the nest cell lining was further investigated using AAA. The results of this investigation are presented in Table 4.

**Table 4: Amino Acid Content of *Colletes inaequalis* nest cell lining**

<b>Amino Acid</b>	<b><i>Colletes inaequalis</i> (%)</b>
<b>Lysine</b>	5.05
<b>Histidine</b>	3.03
<b>Aginine</b>	0.79
<b>Aspartic Acid/Asparagine</b>	2.55
<b>Threonine</b>	1.24
<b>Serine</b>	18.59
<b>Glutamic Acid/Glutamine</b>	34.87
<b>Proline</b>	0.0
<b>Glycine</b>	4.64
<b>Alanine</b>	17.30
<b>Valine</b>	4.77
<b>Methionine</b>	1.28
<b>Isoleucine</b>	2.05
<b>Leucine</b>	2.76
<b>Tyrosine</b>	0.46
<b>Phenylalanine</b>	0.60

The AAA results presented in Table 4 show elevated levels of small residue amino acids, particularly alanine and serine. This, combined with the high level of glutamic acid, suggests that the measured protein could be attributed to the presence of silk [27, 37].

#### **4.4.3. Confocal Microscopy**

The nest cell lining material was seen to autofluoresce green with excitation from the UV laser. This allowed for effective imaging of the *Colletes inaequalis* nest cell lining, a sample of which can be seen in Figure 15.



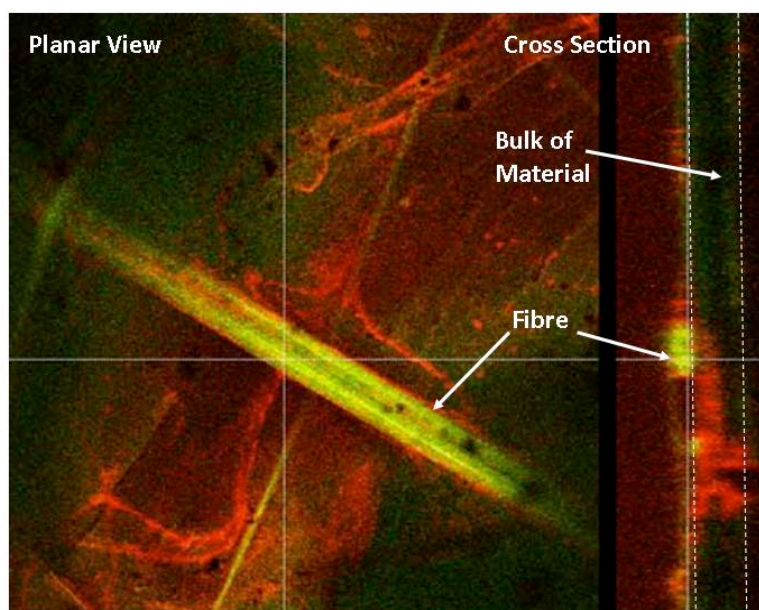


**Figure 15: Confocal image of *Colletes inaequalis* nest cell lining**

In Figure 15 the nest cell lining material is visible in green and the Nile Red stain surrounding the material in red. It is clear from this that fibre like structures exist and that they are present exclusively on one surface of the nest cell lining. This suggests that the nest cell lining of *Colletes inaequalis* is made up of two main structural components and there is preferentiality in fibre placement.

#### **4.4.4. Gas Chromatography – Mass Spectroscopy**

Despite the successful hydrolysis of the nest cell lining material, no success was achieved in recreating the results of Hefetz et al [22]. Samples were not soluble in either methanol or methylene chloride at a sufficient concentration for detection by GC-MS. Resulting spectra from GC-MS showed the presence of environmental contamination but nothing reflecting the contents of the nest cell lining. This suggests that some component of the nest cell lining is more chemically resistant than previously thought.

## 4.5. Conclusions

From these investigations it can be concluded that the nest cell linings of *Colletes inaequalis* appear to be a composite structure, comprising fibre-like structures on a surface of the nest cell lining and a polymer matrix. The data also suggests that the nest cell lining contains a proteinaceous component that could be silk. These results will be considered alongside those for *Colletes halophilus* to ascertain if the detected features are unique to a particular *Colletes* species or suggest an across genus trend.

## **Chapter 5: Materials and Methods**

### **5.1. Chapter Overview**

In this chapter the detailed materials and methods used to investigate the nest cell lining of *Colletes halophilus* are detailed.

### **5.2. Nest Cell Lining Acquisition**

Before investigation of the nest cell lining material could begin, material had to be acquired from *Colletes halophilus* nesting sites. Nests were excavated from the Coalhouse Fort grounds in East Tilbury. A spade was used for the excavation, with care taken to ensure limited disturbance to the *Colletes halophilus* habitat. Once collected nest cells were transported back to the University of Bath in sealed glass vials for cleaning and storage.

Before analysis could be carried out nest cells were categorized into one of three groups, provisioned, dirt-filled or empty, and then cleaned. Categorization provided an indication of the age of the nest cell lining. Provisioned nest cell linings, those filled or partially filled with pollen and nectar provisions, were produced in the same season as when they were collected. Dirt-filled nest cell linings, those filled with dirt instead of provisions, are known to be at least a season old. Empty nest cell linings are unknown in age.

Once categorized, nest cell lining samples were cleaned in deionised (DI) water to remove dirt, pollen and debris. Cleaned nest cell linings were then stored at 4°C until use.

### **5.3. Microstructure**

The microstructure of the nest cell lining samples was explored using a variety of microscopy techniques. The methods and materials used in these techniques are described here.

#### **5.3.1. Scanning Electron Microscopy**

A number of nest cell lining samples with varying orientation were investigated using Scanning Electron Microscopy (SEM). Both the internal and external planar surfaces of the nest cell lining were examined using this method. Transverse sections of the nest cell lining were also examined. These sections included tensile fracture surfaces of both the main nest cell body and the nest cell cap, freeze fractured surfaces of both the body and cap, and embedded transverse sections of both the nest and cap (embedding method discussed in section 5.3.2).

Since all nest cell lining samples were polymeric and non-conductive in nature, samples were sputter coated with gold at a pressure of approximately 5mbar for 3 minutes using a Sputter Coater S150B produced by Edwards before imaging. A JEOL 6480LV scanning electron microscope with an accelerating voltage of 10kV was used for imaging.

#### **5.3.2. Transmission Electron Microscopy**

Both the nest cell body and nest cell cap were examined using Transmission Electron Microscopy (TEM). To support nest cell lining pieces, and to cut them to an appropriate thickness, samples were first embedded in resin. Two materials were used for embedding, an acrylic based low viscosity resin known as LR White and an epoxy based TAAB LV resin.

Nest cell lining samples were immersed in liquid resin and left to rotate overnight to facilitate absorption of resin into the material. Samples were then placed under vacuum

to remove trapped air within the resin. When air bubbles were no longer visible, the epoxy embedded samples were transferred to moulds and the acrylic samples to gelatine capsules. All samples were left at 60°C for 24 hours to harden.

Once solid, the embedded samples were shaped and smoothed on a Reichart Jung Ultracut E ultra-microtome using glass knives made using a LKB Bromma 7800 Knife Cutter. Once sufficiently smooth, a Micro Star diamond knife was used to cut 100nm thick sections of material which were mounted on grids suitable for TEM. Both coated 200 mesh nickel and uncoated 300 mesh nickel grids were used.

When mounted, samples were exposed to either osmium tetroxide or ruthenium tetroxide vapour to improve sample contrast for TEM. These two different chemicals were used for contrast enhancement for their different reactivities. While osmium tetroxide is commonly used for biological materials and oxidizes alkenes, ruthenium tetroxide is more reactive and will oxidize most hydrocarbons [56-58]. Samples with different exposures to these reagents will image differently under TEM. After staining, samples were examined using a Jeol 1200 TEM.

### **5.3.3. Confocal Microscopy**

Nest cell lining samples were examined using confocal microscopy to further characterize the microstructure of the nest cell and examine the proteinaceous component of the material. Nest cell lining samples were stained with Krypton™ Protein Stain – a fluorescent stain produced by Thermo Scientific, Inc. which is selective for protein. Staining protocol was taken from the manufacturer's instructions for gel staining [59]. The standard procedure was followed using sufficient fixing, staining and destaining solution to cover the surface of the nest cell lining samples. Samples were left in staining solution overnight to ensure permeation into the nest cell lining.

Once stained samples were immediately imaged using a LSM 510META Zeiss confocal microscope under a 40X oil-immersion objective. A Helium-Neon (HeNe) 543 laser

was used for excitation of the Krypton™ Protein Stain with an emission filter for wavelengths greater than 580nm.

## **5.4. Chemical Composition**

The chemical makeup of the nest cell lining samples was explored using a variety of characterization techniques. The methods and materials employed for analysis are presented here.

### **5.4.1. X-Ray Diffraction**

To prepare the nest cell lining samples for X-Ray Diffraction (XRD) it was necessary to first pulverize the nest cell. To do this, the sample was cooled in liquid nitrogen before being ground using a mortar and pestle. Once ground it was dried in a desiccator for 24 hours and only removed just prior to testing to prevent excessive water reabsorption. The sample was inserted into glass capillary tubes which in turn were placed in a Bruker D8 powder diffractometer. In initial tests, data was collected from 5° to 50° 2- $\theta$  with a step size of 0.025° and 2 second sample time. Scan angle and step size were decreased in subsequent investigations in an attempt to yield more detailed results. Additional tests were performed from 15° to 40° 2- $\theta$  with a step size of 0.016° and from 20° to 30° 2- $\theta$  with a step size of 0.016°.

Once collected, powder diffraction data of the nest cell lining was compared to materials' diffraction pattern standards found in the PDF2 database produced by the International Centre for Diffraction Data (ICDD). It should be noted that the PDF2 database has been developed for the analysis of inorganic materials so is not ideal for the analysis of the nest cell lining material, which is believed to be an organic polymer. However, this was the database available at the time of completing this study.

#### **5.4.2. Amino Acid Analysis**

To perform the Amino Acid Analysis (AAA), cleaned nest linings were sent to the University of California Davis Proteomics Core Facility. At the facility samples were hydrolysed using 6M HCl at 110°C for 24 hours. Hydrolysed samples were then analysed using a Hitachi L-8800 amino acid analyser.

#### **5.4.3. Fourier Transform Infrared & Raman Spectroscopy**

A Perkin Elmer Spectrum Express was used to conduct the Fourier Transform Infrared Spectroscopy (FTIR) investigation. This instrument uses a germanium crystal within a testing platform, through which the IR beam is spread and passed into the sample. Embedded nest cell linings, prepared for TEM, were used in FTIR investigations. Samples were mounted such that the IR beam passed through transverse sections of the nest cell lining material. Before testing a background scan of the epoxy resin used for embedding was taken and subtracted from the experimental scans to ensure readings only represented the chemical makeup of the nest cell lining. Once a measurement was taken, embedded nest cell linings were cut to reveal a new transverse section of nest cell lining which was then analyzed.

As a complement to the FTIR investigation, *Colletes halophilus* nest cell linings were also investigated using Raman spectroscopy. Samples were sent to University College London for analysis. The external surface of the nest cell linings was examined using this technique.

#### **5.4.4. Time of Flight**

Before Time of Flight (TOF) measurements could be taken, nest cell lining samples were put into solution. Hexafluoro-2-Propanol (HFIP), a solvent often used to dissolve polyesters and peptides, was used. Nest cell linings were placed into HFIP at a concentration of approximately 2mg/mL and left for 48 hours at room temperature prior

to testing. After this time period some nest cell lining material remained undissolved, this material was filtered out before testing.

Time of flight experiments were completed at the University of Bristol's Mass Spectrometry Facility. For ESI-TOF, samples were injected using an Advion Nanomate nanospray source under a pressure of 0.3psi and using a spray voltage of 1.4kV. A positive ion source was used for ionization of the samples and ions were analysed using a Applied Biosystems QSTAR XL mass spectrometer.

For MALDI-TOF, nest cell linings in HFIP were further concentrated using a blow down valve. Once concentrated, samples were combined with solution that would later crystallize the form the assistance matrix material. Nest cell lining solution was combined with dithranol matrix solution (20mg/mL of dithranol in methanol) in a 1:1 ratio. Once mixed, the final solution was pipetted onto metal plates for testing. Samples were allowed to dry in an open atmosphere to ensure crystallization of the matrix. Once dry, the plate was loaded into an Applied Biosystems 4700 mass spectrometer for analysis. Samples were investigated for ion presence up to a mass of 50000amu.

## **5.5. Material Properties**

The thermal characteristics, as well as the mechanical properties of the nest cell lining samples, were explored using a variety of characterization techniques. The methods and materials employed for analysis are presented here.

### **5.5.1. Thermogravimetric Analysis**

Thermogravimetric Analysis (TGA) investigations were completed on a TGA4000 manufactured by Perkin-Elmer. Before testing nest cell lining samples were left in a desiccator overnight to remove any excess water from the samples. Once dried, approximately 7mg of *Colletes halophilus* nest cell lining was heated from ambient temperature to 600°C at a rate of 5°C/minute under nitrogen. Mass loss was recorded throughout the experiment resulting in a plot of temperature versus percent mass.



### 5.5.2. Differential Scanning Calorimetry

Phase changes of the nest cell lining material were investigated using Differential Scanning Calorimetry (DSC). Studies were completed on a DSC 2910 manufactured by TA instruments. Samples were weighed and loaded into aluminium pans for testing. The temperature profile for testing varied between runs. The heating rate varied between 10°C/min and 5°C/min, with lower rates being used to ensure accurate detection of phase transformations. The maximum temperature varied from 90°C to 400°C, with lower temperatures used for runs investigating cooling, and higher temperatures used to compare nest cell lining data to commercial materials. Additionally, one run was completed using a starting temperature of -60°C to investigate the glass transition temperature. All other runs started at approximately 20°C. A full list of runs with appropriate testing parameters can be seen in Table 5.

**Table 5: Operating parameters for DSC runs**

Run	Material	Mass (mg)	Start (°C)	End (°C)	Rate (°C/min)
1.	Nest cell lining	1.94	-60°C	120°C	10
2.	Nest cell lining	10.8	25	340	2
4.	Silk cocoon	7.63	25	400	5
5.	PLA	39.8	22	200	5

As well as using DSC studies to characterize nest cell lining samples a variety of control samples were also investigated. These samples included polylactic acid (PLA) and *Bombyx mori* silk cocoons. PLA was selected for comparison of the polymer nest cell lining with a commercial polyester derived from natural sources. *Bombyx mori* nest cell linings were selected to compare the nest cell lining with a common silk in the hope of further characterization of the silk present in the nest cell lining. Samples were pressed onto the same aluminium pans and runs were completed using similar heating profiles.

To corroborate the DSC results with visual information, a Mettler Toledo FP82H2 Hot Stage was used in conjunction with a Leica DME light microscope to observe phase

transformations identified during DSC. Nest cell lining samples were placed on glass microscope slides and heated at a rate of 5°C per minute under observation.

### 5.5.3. Mechanical Testing

Ten nest cell lining samples were prepared for mechanical testing using an Instron. Nest cell lining samples were cut into rectangular shapes which varied dimensionally depending on the morphology of the nest cell itself. Samples ranged in size from 4.73mm to 6.83mm in width and 3.31mm and 5.33 mm in length. All samples were assumed to have a thickness of approximately 20µm, the average material thickness as seen through SEM.

Once cut, the rectangular nest cell lining pieces were attached to pieces of card to ensure good contact with the Instron grips. Commercial epoxy was used for this attachment. A schematic of the prepared samples can be seen in Figure 16.

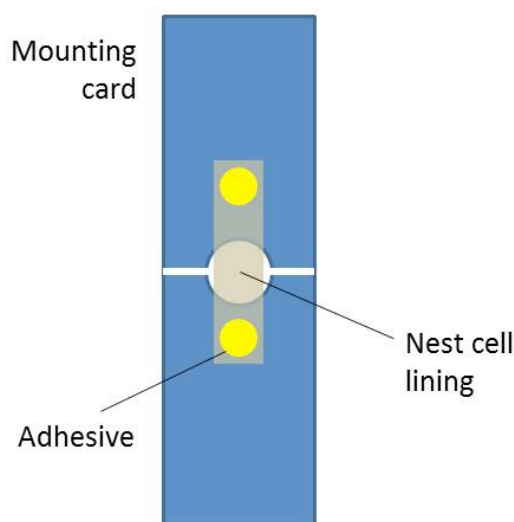


**Figure 16: Schematic of nest cell lining samples for Instron testing.**

Once mounted the samples were loaded into the Instron. An image of the finalized sample setup can be seen in Figure 17.

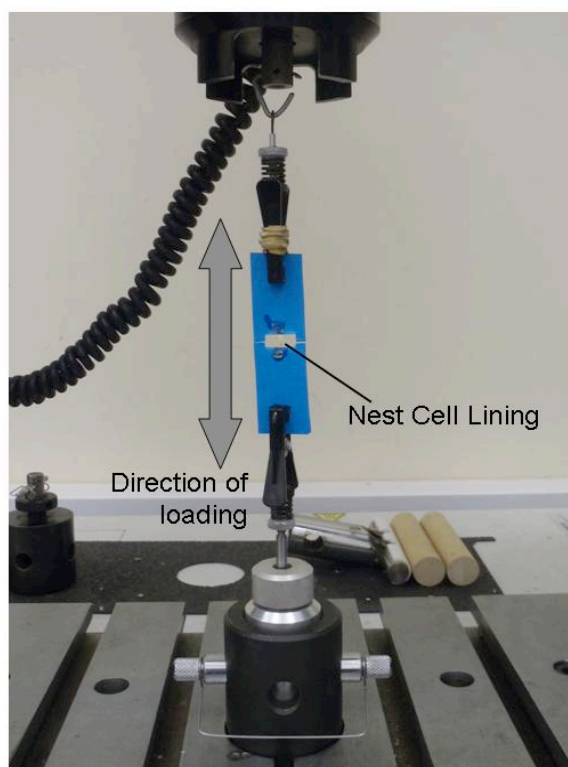


**Figure 17: Tensile testing setup for nest cell samples.**

A 10N load cell was used on an Instron 3365 for testing. The card was cut and an extension rate of 0.1mm/min was applied to the nest cell lining samples. Due to the delicacy and size of the nest cell lining samples, extension was measured by crosshead displacement. Samples were tested to failure.

## **5.6. Chapter Summary**

A wide variety of analytical techniques were employed for this investigation. The breadth of techniques, including those for chemical analysis, microscopy and material characterization, was used to achieve a comprehensive understanding of this material. The results from these investigations and how they relate to entomological knowledge will be presented in the following chapters.

## Chapter 6: Microstructure of *Colletes halophilus* Nest Cell Lining

### 6.1. Chapter Overview

The microstructure of the *Colletes halophilus* nest cell lining was investigated using SEM, TEM and confocal microscopy techniques. The images characterise the material's microstructure and allow the current understanding of how the nest cell linings are constructed in the natural environment to be re-evaluated.

### 6.2. Scanning Electron Microscopy

Initially SEM was used to investigate the structure and topography of the nest cell lining. Micrographs of the external and internal surfaces of the nest cell lining are presented in Figures 18 and 19 respectively.

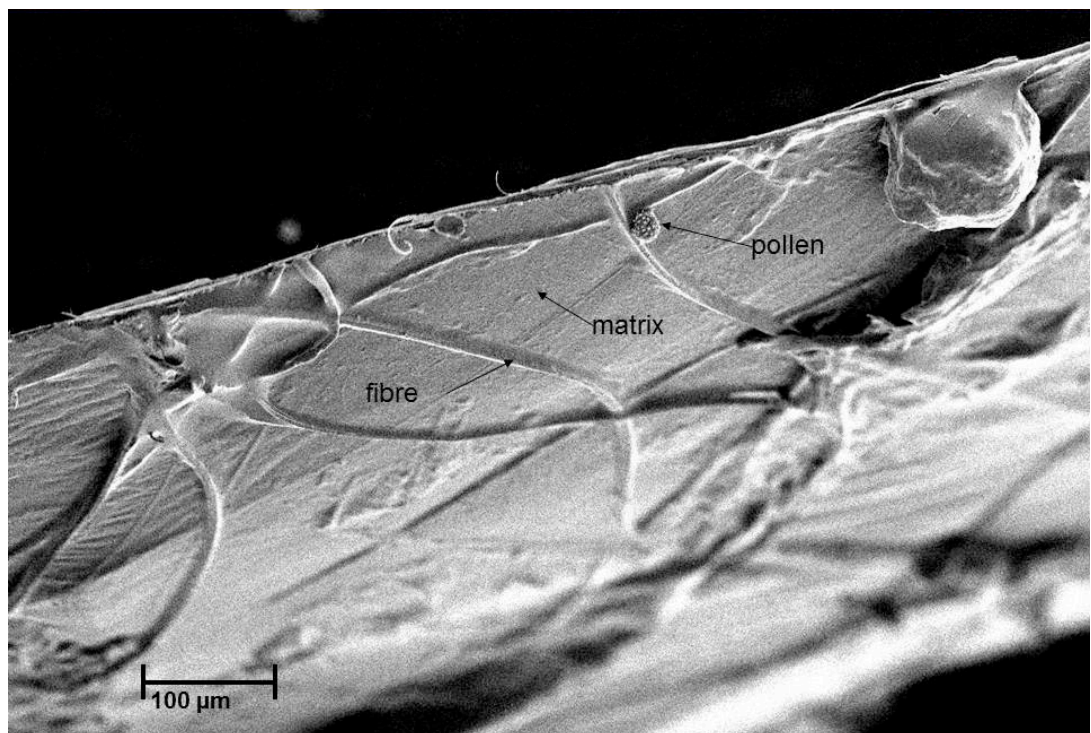
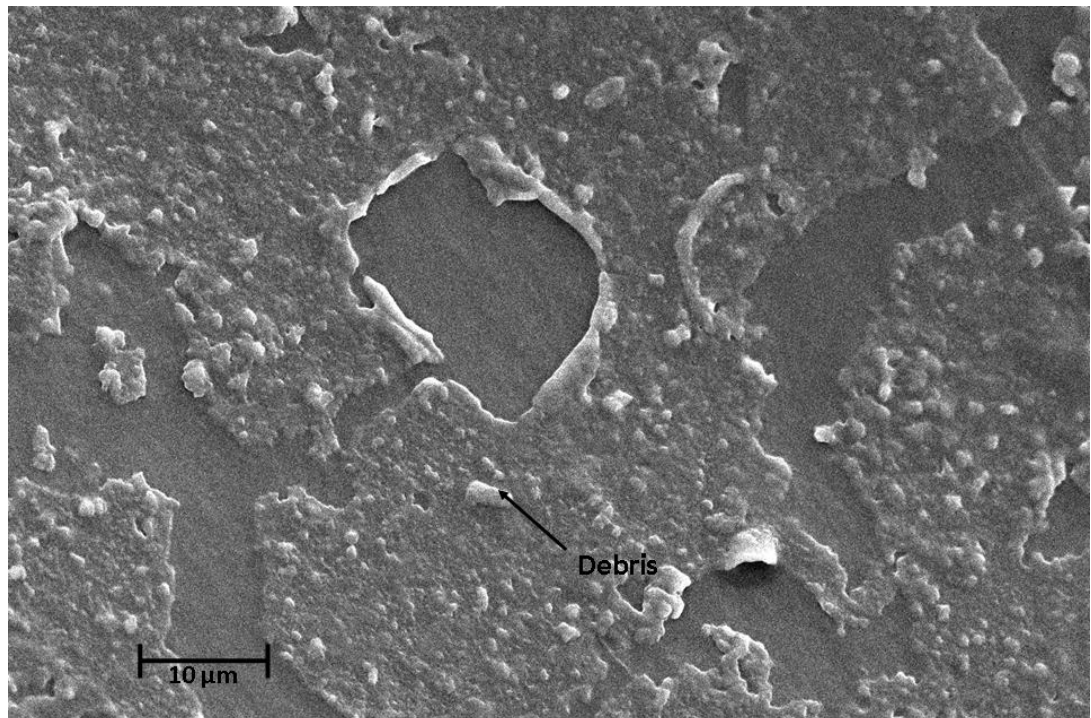


Figure 18: SEM image of external surface of nest cell lining



**Figure 19: SEM image of internal surface of nest cell lining**

These images confirm that the nest cell lining is a composite material composed of both fibres and matrix. From a comparison of Figures 18 and 19 it is clear that the fibres exist exclusively on the external surface of the nest cell lining. The distinct fibres visible in Figure 18 stand out in sharp contrast to the relatively smooth surface seen on the internal surface of the nest cell lining in Figure 19. To see any texture on the internal surface a much higher magnification is necessary as can be seen in Figure 19. The texture on the internal surface of the nest cell lining is attributed in part to environmental debris.

An SEM image of a transverse section, following tensile fracture, is seen in Figure 20.

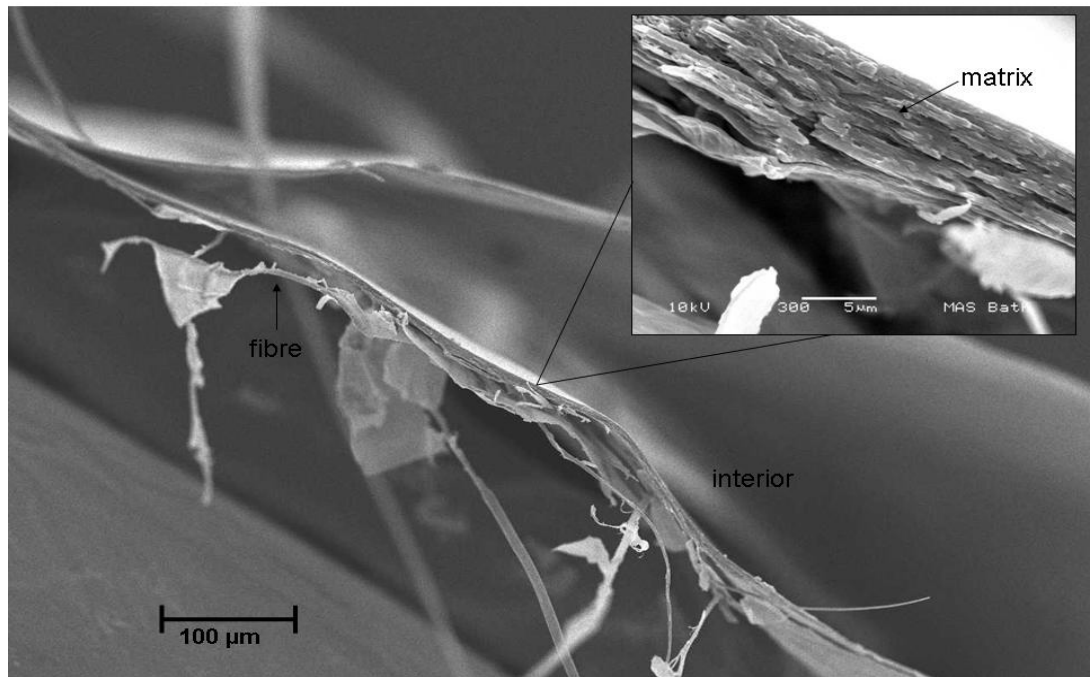


**Figure 20: SEM image showing detail of a transverse section of nest cell lining.**

Distinct fibres, revealed through tensile-fracture, can be seen in Figure 20 and range in size from 1 to 8µm in diameter. The bulk of the material can be classified as the matrix of this composite, also visible in Figure 20, which appears to be composed of a laminated structure. The individual layers are approximately 2µm in thickness, resulting in a bulk material that varies from approximately 10 to 20 µm in total thickness.

To confirm and better characterize the nest cell lining composite structure, further investigations were undertaken using various fracture techniques. One such investigation was the imaging of a sample embedded in epoxy resin. This sample, later used for TEM, was embedded and sectioned on an ultramicrotome allowing a detailed view of the transverse section of the nest cell lining. Micrographs of this transverse section can be seen in Figures 21 and 22.



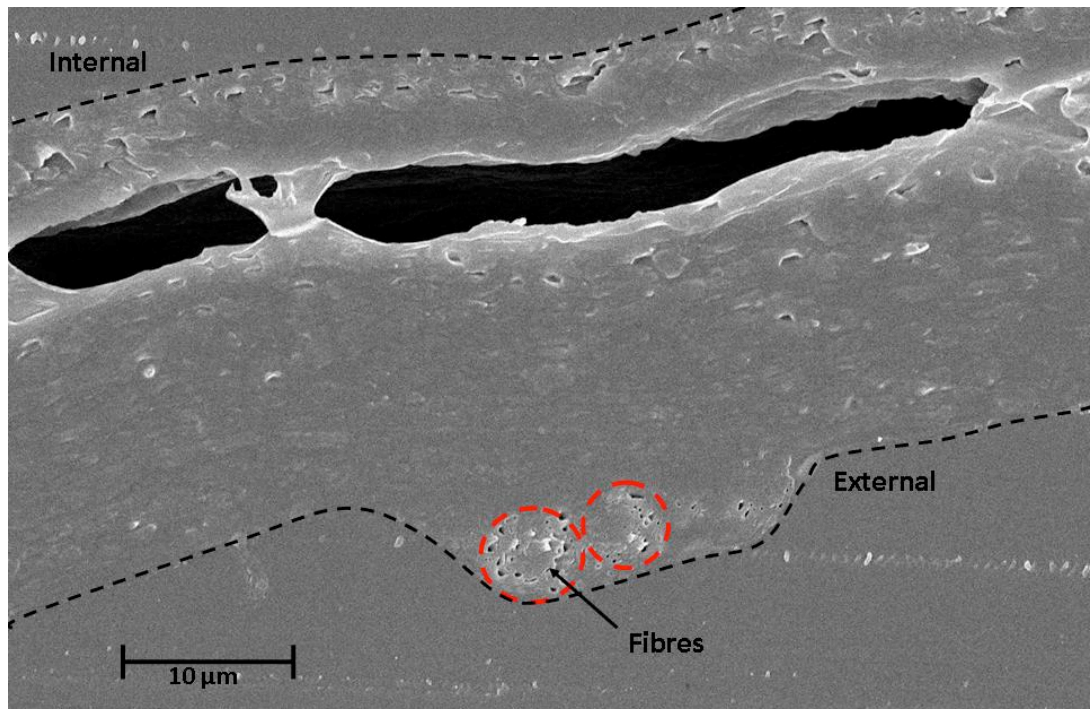


**Figure 21: SEM image of a transverse section of an embedded nest cell. The external and internal surfaces and fibre location are identified.**

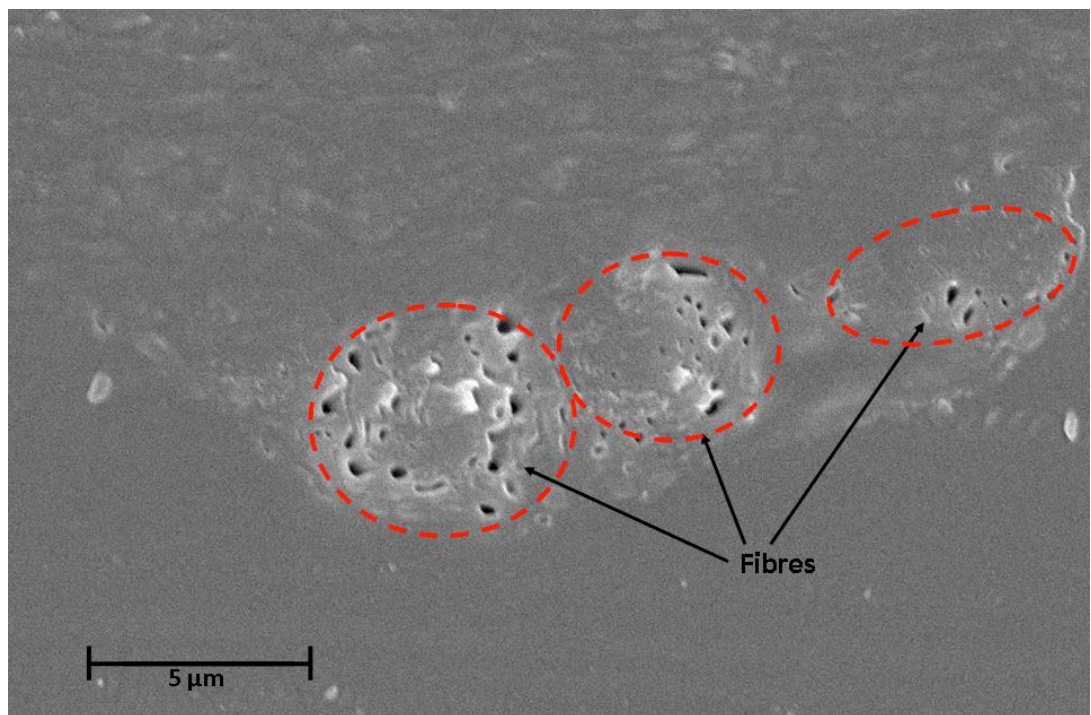


**Figure 22: SEM image of a transverse section of an embedded nest cell. Fibres are identified.**

In Figure 21 the embedded transverse section of the nest cell lining is visible with the edges of the material and fibre location highlighted. Fibres are visible on the external surface of the nest cell lining and, as seen in Figure 22, are notably porous in structure. The lamellar matrix is again visible in the transverse section, highlighted by the crack in Figure 21 which appears to propagate between lamellae in the centre of the material. This crack is likely to be the result of thermal stress on the material during the epoxy curing process. The crack has propagated in the plane of the nest cell lining and not through its thickness, suggesting that the interfacial bonding between layers is weaker than that within the material itself.

An additional study was carried-out to compare the main body of the nest cell lining and the nest cell cap. Both materials were freeze fractured or tensile fractured before being investigated using SEM. The results can be seen in Figures 23, 24 and 25.

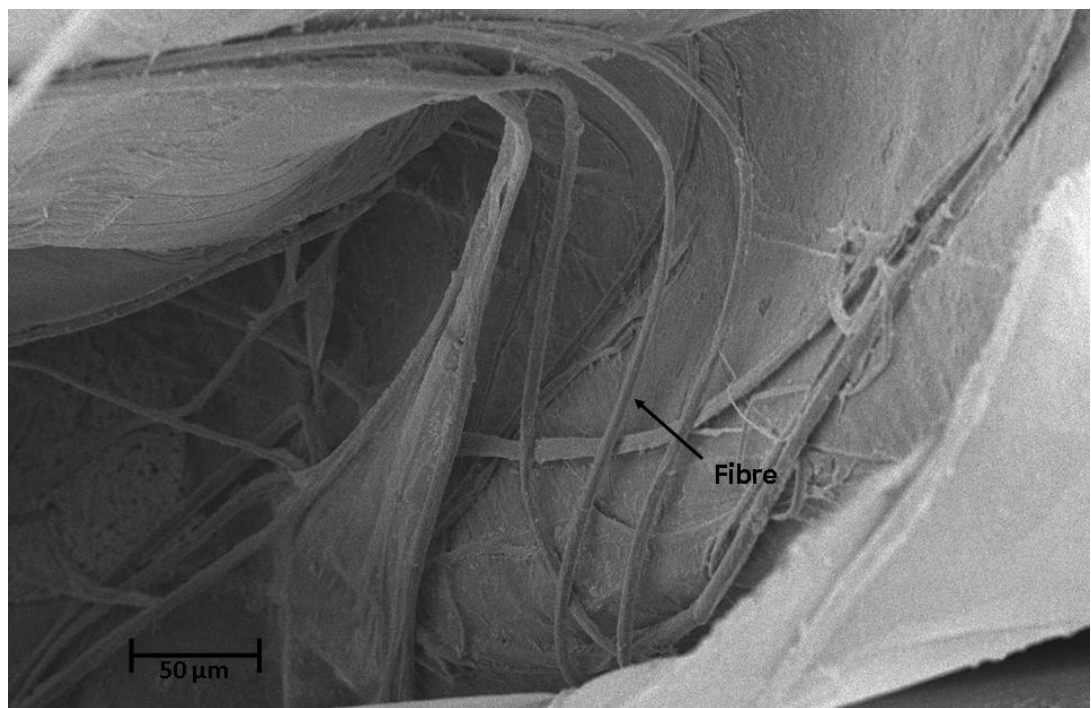


**Figure 23: SEM image of tensile fractured nest cell lining. Sample from nest cell cap.**



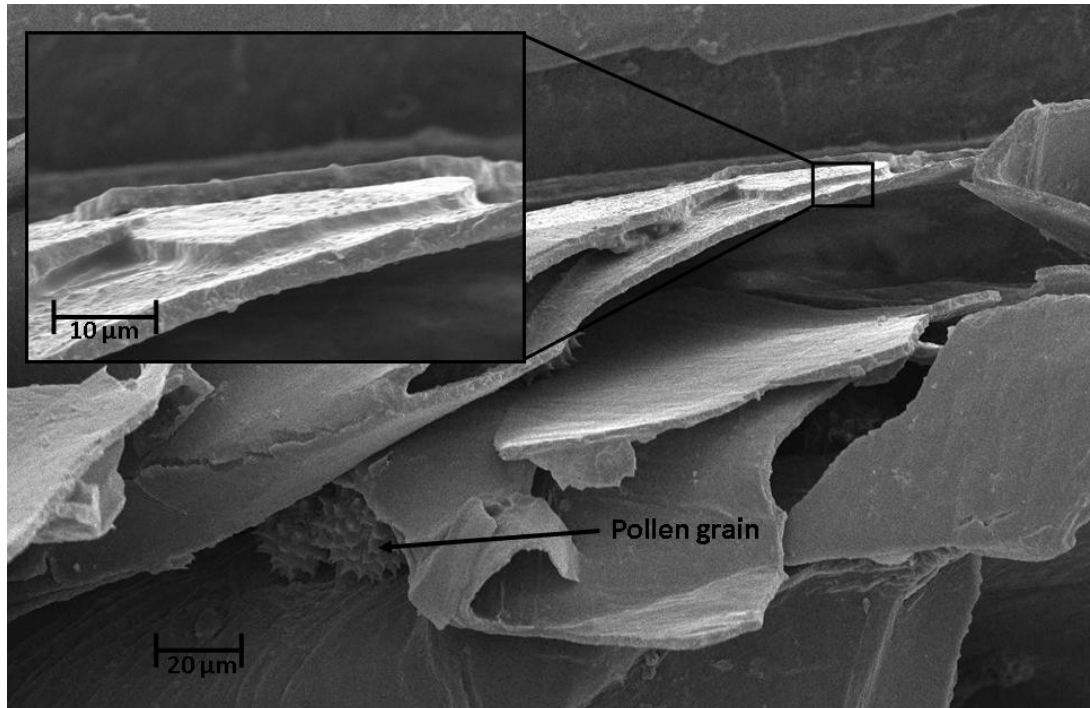


Figure 24: SEM image of freeze fractured nest cell lining. Sample from nest cell cap.

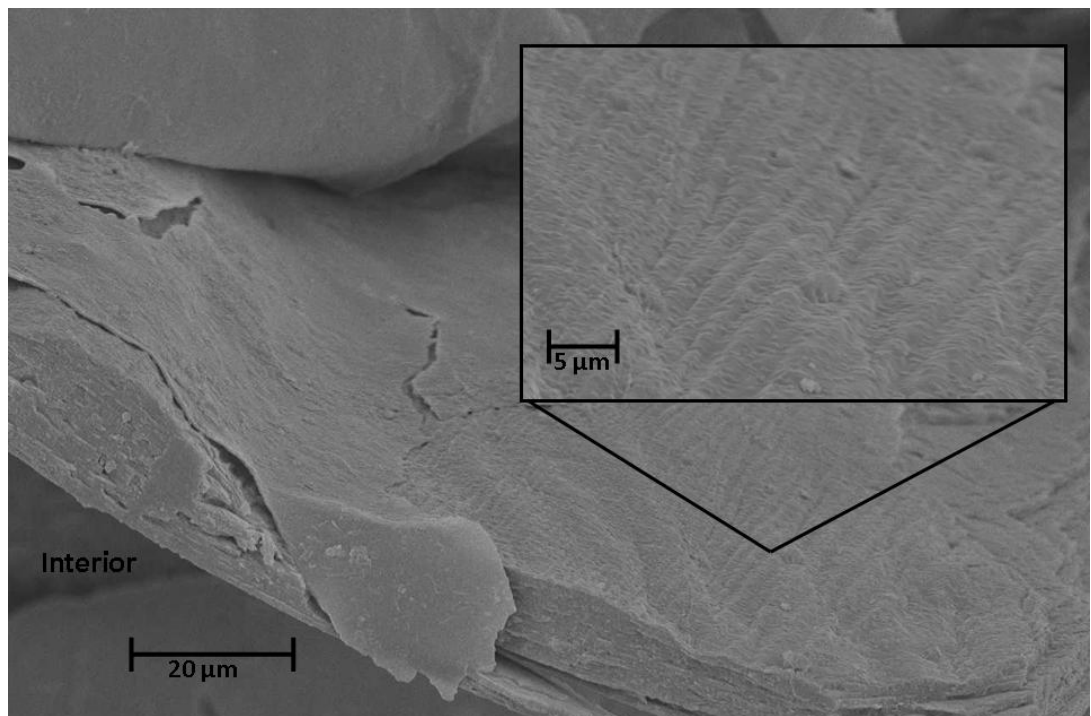
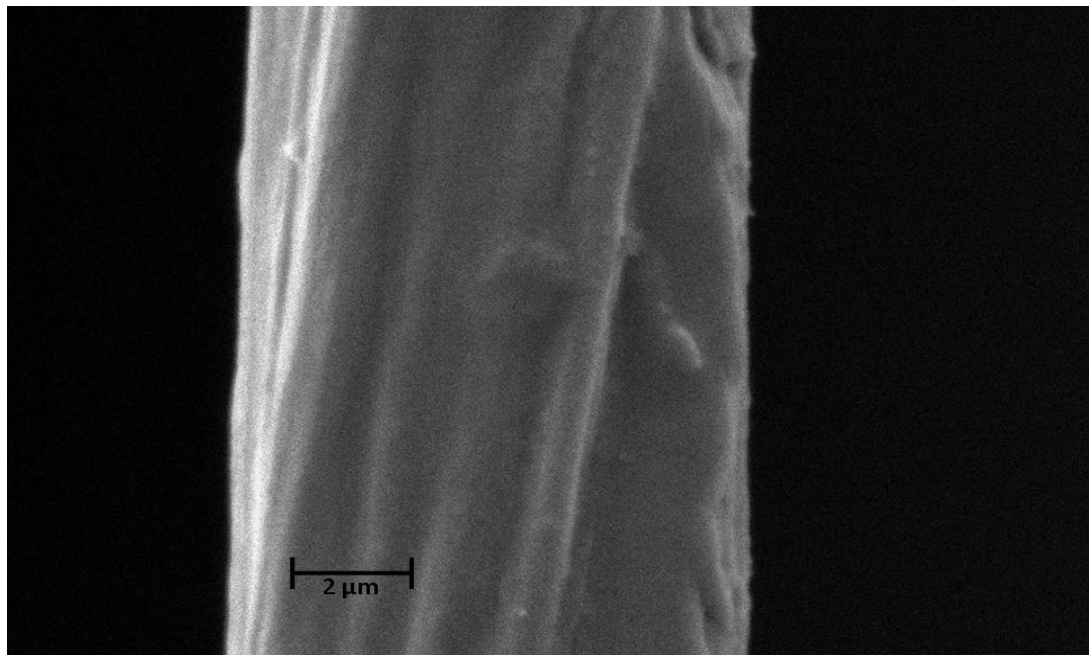


Figure 25: SEM image of freeze fractured nest cell lining. Sample from nest cell body.

Similar features, namely the presence of fibres and the lamellar-structured matrix, are seen in both samples. The abundance of fibres and presence of matrix are seen in Figure

23. However, the nest cell cap is significantly less ordered with large gaps and folds between layers of matrix material as seen in Figure 24 where distinct layers of material can be seen both attached (see inset) and highly folded with pollen trapped between layers. This level of disorder is not seen in the sample from the nest cell body in Figure 25. Instead the layers of material are mostly continuous, with the exception of the top layer which was dislodged during the freeze fracture process. Removal of this top layer however exposes a textured surface of regularly spaced ridges of material approximately  $2\mu\text{m}$  wide (see inset in Figure 25).

In order to better characterize the fibres a further study was undertaken. Fibres, which were partially exposed during heating of the nest cell lining material, were imaged using SEM. The results are presented in Figures 26 and 27.



**Figure 26: SEM image of large nest cell lining fibre, approximately  $8\mu\text{m}$  in diameter.**

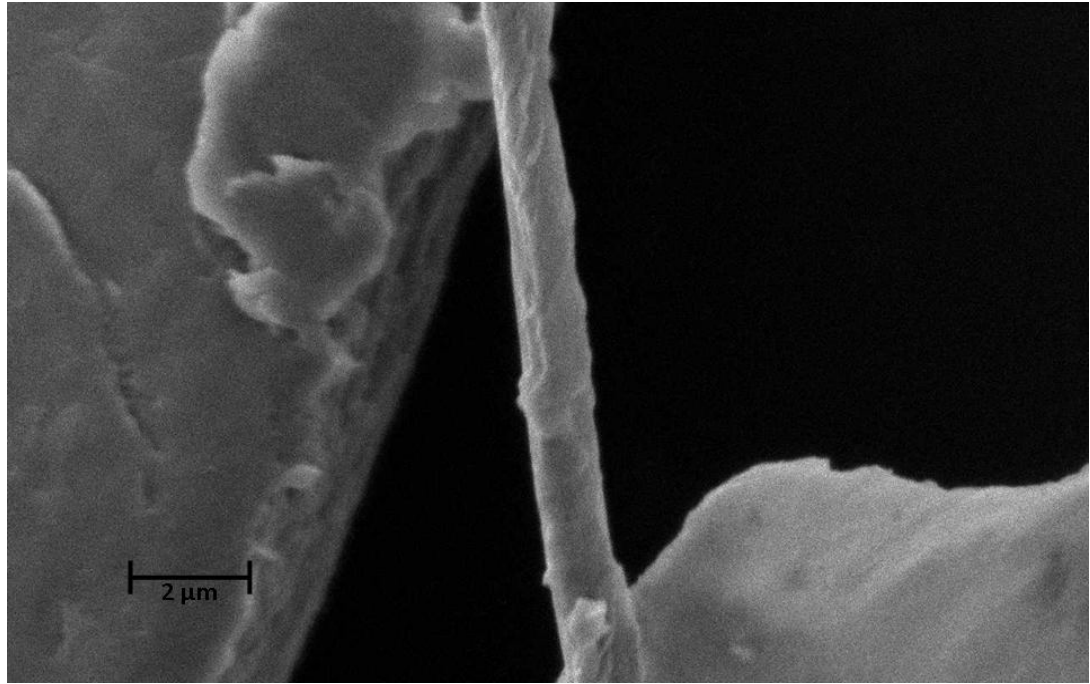


**Figure 27: SEM image of small nest cell lining fibre, approximately 1µm in diameter.**

From these SEM images the variation in diameter of the fibres is clearly visible, ranging from 8µm in Figure 26 down to 1µm in Figure 27. Also notable is the structure of the larger fibre. The ridges along its surface, Figure 26, suggest that it may comprise a bundle of smaller fibres. This striated topography visible on the larger diameter fibre in Figure 26 is not seen on the smaller diameter fibre in Figure 27.

### **Scanning Electron Microscopy Discussion**

From the SEM study several conclusions about the nest cell lining material can be drawn. The material appears to be a composite composed of fibres and a laminated matrix component. The fibres are located on the external surface of the nest cell lining and range in size from 1 to 8µm in diameter, with the larger fibres potentially comprising bundles of smaller fibres. The matrix appears lamellar in structure with a total thickness between 20 to 30 µm and layers of material approximately 1 to 2µm thick. Finally, although the cap of the nest cell is less ordered in structure and is thicker (roughly 50µm thick) than material taken from the body, both the cap and body of the nest cell lining have similar fibre and matrix features.

These results have several implications in relation to the current understanding of the construction of the nest cell lining. Firstly, the fact that the nest cell lining is a composite material indicates that *Colletes* bees are capable of producing two different material structures. This is the first microscopic evidence of fibre production within *Colletes*, in contrast to the previous work carried out on *Colletes succinctus*. There is a resemblance to other species within the subfamily Colletidae such as the silk producing species *Hyleaus cressoni* [10, 24, 25].

Though a composite, the nest cell lining is not a typical fibre-reinforced composite, which would have fibres roughly evenly dispersed within the matrix. As is visible in Figure 18 the fibres of the nest cell lining appear exclusively on the external surface. This fibre location indicates that the fibres must be laid down before the matrix material can be applied. The fibres must therefore be produced by adult *Colletes* bees and not by the larva as a cocoon spinning product as in the case of honey bees or as excrement as suggested by Torchio [21, 44, 60]. Additionally, being laid down first suggests that the fibres may play a role in the support or formation of the matrix material. The fibres appear in relatively low density with only approximately 2% of the surface area of the nest cell lining body being fibrous (see section 6.4) so it is unlikely that they are used to provide mechanical strength and stiffness as in a typical fibre-matrix composite. However, the fibres may still serve as a scaffold onto which the matrix can securely be built up, acting as a framework to which the matrix can adhere, in preference, to the surrounding dirt wall.

The existence of fibres gives more credence to the entomological observations of Torchio et al [21] over those of Batra [14]. While Batra noted no evidence of fibre production Torchio et al witnessed *Colletes kincaidii* extruding material, seemingly as a salivary secretion [21]. It is likely that this extruded material is that which has been identified as fibres in this study. However, while Torchio et al principally noted this extrusion for the construction of the nest cell cap, the fibres are prevalent across the nest cell lining material suggesting a more extensive use of this salivary excretion than previously thought.

With regards to the matrix material, the lamellar structure is consistent with the observations of both Batra [14] and Torchio et al [21]. If *Colletes halophilus* are

applying discrete layers of polymer material with their bilobed tongues a gradual build up of material would be expected, where additional layers of polymer liquid are applied to an already solidified material until the desired thickness is reached. The regular thickness of these layers suggests that the bees can apply a liquid layer approximately 1 to 2µm thick with each secretion. The texture on the matrix surface seen in Figure 25 could be the result of this application process. It has been observed that *Colletes* bees will lay down material by moving along the surface of the nest cell wall while dragging their bilobed tongue [21] which could create this type of regular topography. It is likely that this texture is not seen on the interior surface of the nest cell lining (Figure 19) due to the smoothing of the interior during provisioning.

The nest cell cap is thicker and more disordered than the nest cell lining (Figure 24), with a substantial number of fibres and gaps between the matrix layers. This is largely attributed to the multi-step process by which the nest cap is made. The nest cap is originally produced as an open flap consisting of a fibre framework on top of which a mixture of salivary and Dufour's gland secretions are applied [21]. This step is akin to the construction of the nest cell body. However, once the nest cell has been lined, provisioned and had an egg deposited within it, the nest cell cap must be closed and sealed. It has been observed in *Colletes kincaidii*, that in order to close the nest cell, the female begins by biting the nest cap which was made previously and pulling it towards closure. The female then alternates between this biting motion and smearing a secretion from her anus (likely from the Dufour's gland) onto the outer surface of the nest cap to seemingly soften the material. This process is repeated until the nest cap is closed and touching the surface of the provision. Once closed, additional abdominal secretions are applied to seemingly secure its position [21]. This continuous biting and smearing, as opposed to the licking addition of material, results in a structure that is more 3-dimensional in nature than the rest of the nest cell lining and less unified in appearance as a result.

Finally, the variation in fibre size is notable, ranging from 1 to 8µm in diameter (Figures 26 and 27). The topography of the larger fibres suggests that this may be a result of an underlying structure where larger fibres are in fact bundles of smaller fibres. This structural hierarchy is additionally supported by the seemingly porous structure of the

larger fibres when sectioned transversely (Figure 21). The pores may be attributed to gaps between smaller fibrils which make up the large fibre bundles.

### **6.3. Transmission Electron Microscopy**

A more detailed investigation of the nest cell lining was completed using TEM. First studies were completed using sectioned samples from nest cell linings embedded in LR white and exposed to osmium tetroxide. The results can be seen in Figures 28 and 29.

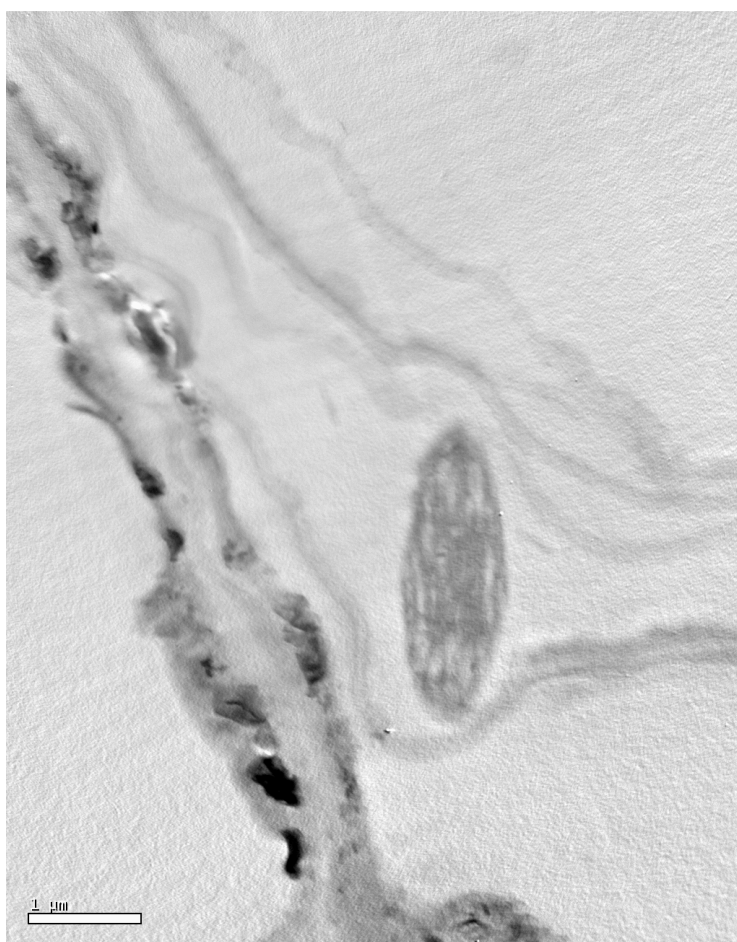


**Figure 28: TEM micrograph of a transverse section of nest cell lining exposed to osmium tetroxide. Fibre structure revealed.**



**Figure 29: TEM micrograph of a transverse section of nest cell lining exposed to osmium tetroxide. Layered structure revealed.**

Two principal structures are again visible in the nest cell lining, a fibre structure and a layered structure. The circular structure visible in Figure 28 appears to be a transverse section of the smaller fibres identified through SEM (Figures 21, 26 and 27). The image appears to be a glancing section, resulting in the ellipsoid shape, of a fibre roughly  $1\mu\text{m}$  in diameter. The fibre seen in Figure 28 is notably porous, a structure not seen in the smaller fibres though SEM. This may be attributed to the preparation process.

The second feature identified is a layered structure. Stained strips of material approximately  $0.3\mu\text{m}$  in width and oriented roughly parallel to each other are visible in Figure 29. The gaps between the stained layers are either unstained nest cell lining material or the LR White used for embedding.

For further analysis of the nest cell lining structure, a second study was completed using sectioned nest cell lining samples embedded in LR White and stained with ruthenium tetroxide, a more aggressive stain for hydrocarbon samples. Results can be seen in Figures 30 and 31.



**Figure 30: TEM micrograph of a transverse section of nest cell lining exposed to ruthenium tetroxide. Fibre revealed.**



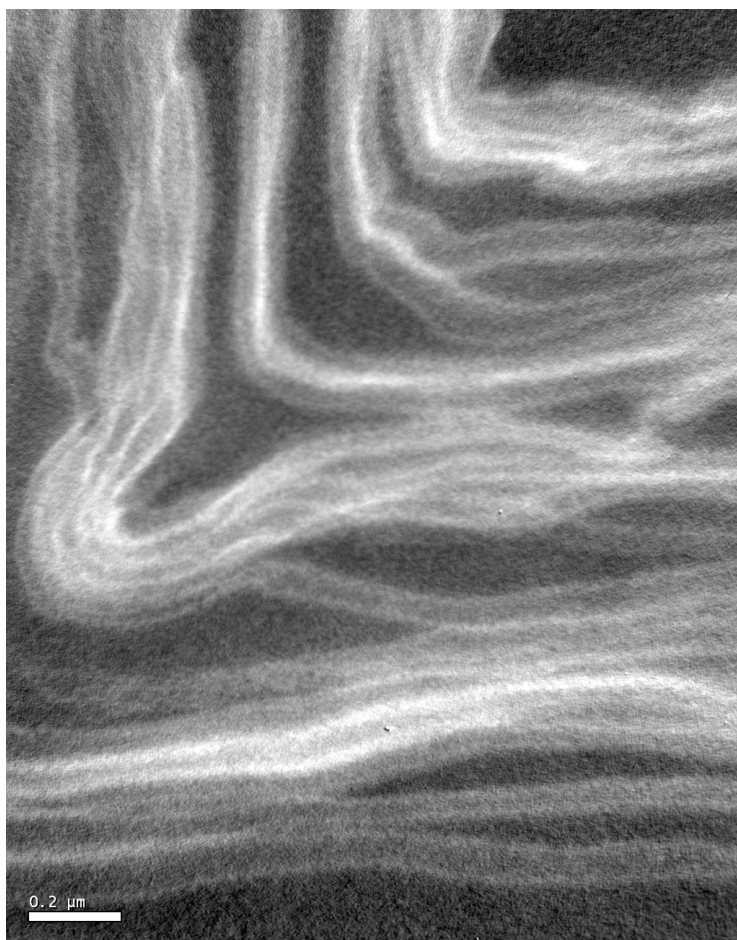


**Figure 31: TEM micrograph of a transverse section of nest cell lining exposed to ruthenium tetroxide. Layered structured revealed.**

Unlike with the osmium tetroxide stain, ruthenium tetroxide exposure successfully stains the LR White embedding medium, making it appear black and resulting in higher contrast in Figures 30 and 31. Though some morphological differences are noted, ruthenium tetroxide staining reveals similar features of the nest cell lining to those previously observed. Notably, a fibre structure and a layered structure are again visible in Figures 30 and 31.

An ellipsoid structure is visible in Figure 30 which can be attributed to the transverse section of a fibre with a diameter of approximately 1.5μm. No porous structure is noted in this fibre, but instead a somewhat spiral like pattern revealed through staining.

Additionally, a layered structure of approximately 1.7 $\mu$ m total thickness is seen in Figure 31. Individual layers are approximately 100nm thick and are again arranged approximately parallel to one another.

## **Transmission Electron Microscopy Discussion**

Investigations using TEM provide useful information with regards to the microstructure of the nest cell lining material. Although relating the TEM micrographs to those obtained through SEM is not entirely straightforward, the recurring presence of similar structures in TEM lends support to the observation of the *Colletes halophilus* nest cell lining as a composite material.

Although the two staining techniques employed for TEM (exposure to osmium tetroxide and ruthenium tetroxide) display similar morphological features, the micrographs appear quite different. This can be attributed to the varying degrees of aggression of the two stains. While osmium tetroxide is effective for staining polymers with unsaturations, ruthenium tetroxide is more aggressive and can stain aromatic and saturated polymers successfully – polymers such as PET [57, 58]. The low contrast in the images stained with osmium tetroxide (see Figures 28 and 29) suggests that the polymers in the nest cell lining are not heavily unsaturated. The high contrast seen in the samples stained with ruthenium tetroxide (see Figures 30 and 31) is expected for a hydrocarbon material.

Despite low contrast, structural features are still visible in the nest cell lining samples exposed to osmium tetroxide. What appears to be the transverse section of a fibre with a diameter of 1 $\mu$ m is visible in Figure 28. This is similar in morphology to the small fibres identified through SEM. The porous structure, though not noted in the small fibres seen in SEM, may be a product of the extrusion process which is likely used by *Colletes halophilus* for fibre synthesis. *Colletes* bees have been observed secreting material from their mouth parts which could affect the underlying microstructure of the fibres [21].

Additionally a layered structure is visible in the samples stained with osmium tetroxide (see Figure 39). Though layers of material are clearly visible, with a width of approximately  $0.3\mu\text{m}$  they are much narrower than those seen in SEM (1 to  $2\mu\text{m}$  thickness). Also the large gaps between the layers are unaccounted for in the SEM micrographs. It is possible that these gaps are LR White embedding material which appears between the nest cell lining sheets as a result of the nest cell lining not being flat within the cutting plane or rippling during sample preparation.

Components of the nest cell lining composite structure are also seen in the samples stained with ruthenium tetroxide. Though the internal structure of the fibre appears different to that revealed through osmium tetroxide staining (see Figure 30 versus 28), its ellipsoid shape suggests that it too is a smaller fibre with a diameter of approximately  $1.5\mu\text{m}$ . The differences in internal structure may be a result of the staining method. The pores noted in Figure 28 could be gaps between the layers of material which seem to coil around each other in Figure 30. The spiral like internal structure seen in Figure 30 may be a function of a spinning or extrusion process used to produce the fibres.

The layered structure of the nest cell lining is more clearly revealed by the ruthenium tetroxide staining method. The individual layers in Figure 31 are approximately 100nm in width and combine to form a structure with a total width of  $1.7\mu\text{m}$ . This corresponds to the thickness of a single layer of matrix material seen in SEM. The individual layers imaged through TEM thus correspond to a deeper level of organization where each lamella seen in SEM comprises multiple polymer layers.

The dimensions and staining of the 100nm layers seen in Figure 31, with a lighter exterior and darker interior, are suggestive of the organization of a copolymer within the sample. Each 100nm layer can be seen as a series of organized chains with different polymers components on the interior and exterior of the layer. Ruthenium tetroxide is a common staining method for copolymers since it affects the various polymer components differently, so variations in stain intensity in the nest cell lining sample would reflect such chemical differences [57].

Overall, although not all the features observed in the TEM micrographs can be reconciled with the features seen in SEM, they provide support for the composite

classification of the *Colletes halophilus* nest cell lining material and provide evidence of a more detailed organization of the individual material components.

#### **6.4. Confocal Microscopy**

Confocal microscopy was used to further characterize the nest cell lining microstructure. Samples, stained with Krypton™ Protein Stain were investigated. The results are presented in Figures 32 and 33.

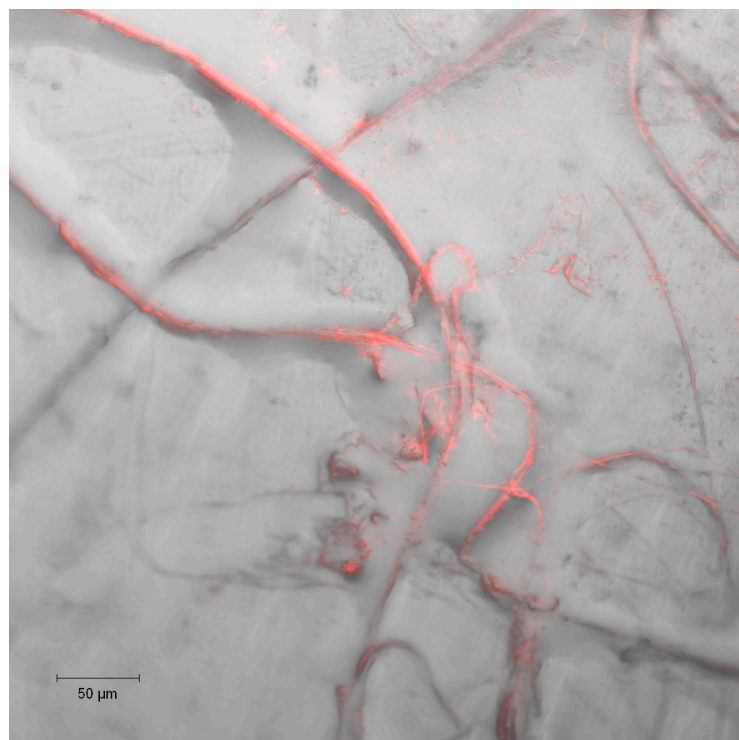


**Figure 32: Confocal image of stained nest cell lining with the black and white field image included.**

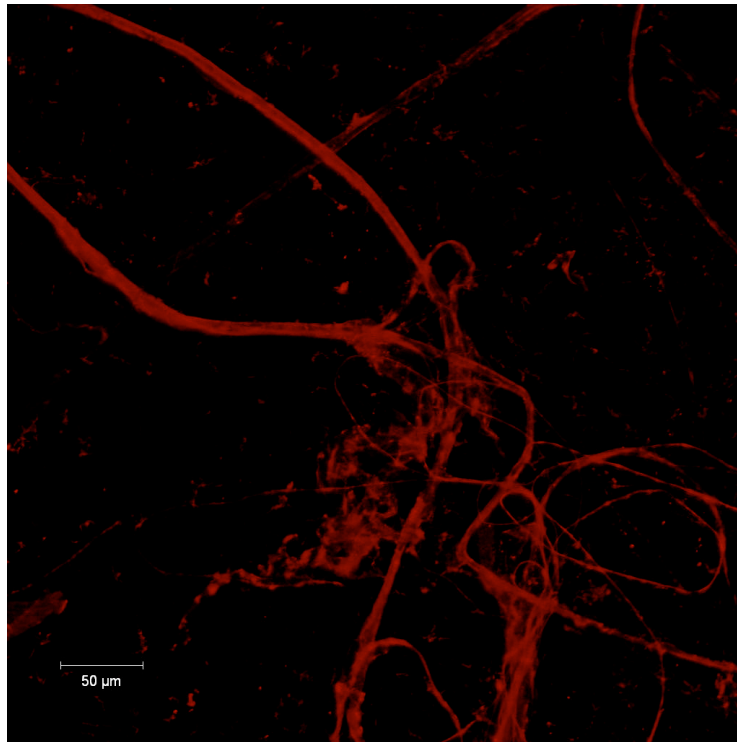


**Figure 33: Confocal image of stained nest cell lining, the black and white field image excluded.**

Before analysis of the nest cell lining samples, a control experiment was carried out on a sample known to be proteinaceous – a piece of commercial silk fibre. The sample was dyed and investigated using the same confocal microscopy method to be adopted and the silk fibres were seen to fluoresce at the emission spectrum of the Krypton™ Protein Stain, proving the validity of the protocol.

Figures 32 and 33 show the fibrous parts of the nest cell lining fluorescing with an emission spectrum above 580nm. This spectrum was selected to exclude the nest cell lining material's natural autofluorescence, which has a largely green (495-570nm) emission spectrum, and represents those components of the material affected by the Krypton™ Protein Stain itself. It is clear from Figure 32 that only the fibres of the nest cell lining were successfully stained. The matrix material, which is still visible in the black and white field image is unaffected by the process. This proves the fibres to be proteinaceous in composition.

To better visualize the stained components of the nest cell lining, the black and white field image was digitally removed leaving only those features affected by the Krypton™

Protein Stain. The result, seen in Figure 33, shows only the fibres and debris were successfully stained. The debris is likely pollen and *Colletes* excrement, both of which are proteinaceous in nature.

As well as aiding visualization of the proteinaceous fibres, Figure 33 was used to estimate the fibre area density. The surface area of components stained red was compared to the total surface area of the image using ImageJ software. The results showed fibres constituting approximately 2% of the nest cell lining surface area.

## Confocal Microscopy Discussion

Through confocal microscopy it is clear that the matrix and the fibres of the *Colletes halophilus* nest cell lining, indentified through SEM and discussed in section 6.2, are chemically distinct materials. The fibres are clearly proteinaceous and can be seen successfully stained in Figures 32 and 33. This implies that beyond being able to create two morphologically distinct materials, a fibre and a laminated matrix, *Colletes* bees are capable of creating two chemically distinct materials.

To do so, it is likely *Colletes halophilus* uses multiple glands in nest cell lining construction. The Dufour's gland has been shown to contain macrocyclic lactones and has been linked to the formation of linear polyesters [10, 22]. Since the matrix was unaffected by the protein staining it is likely that the bulk of the nest cell lining is the linear polyester and a product of the Dufour's gland secretions as previously thought. This supports the entomological observations of *Colletes* bees licking secretions from their abdomen onto the nest cell wall in a layered fashion [14, 21].

The source of the protein fibres however remains unknown. Their presence accounts for the elevated nitrogen content observed by Albans et al [10] in elemental analysis of nest cell linings, however the study by Albans et al [10] failed to identify a definitive protein source in the analysis of the Dufour's gland secretions. The Dufour's gland is additionally discredited as a source of protein by the investigation of Hefetz et al [22] which failed to report any nitrogen or protein content in the Dufour's gland. The *Colletes* bees have been observed extruding fibres from their mouths, so is possible the

protein source is from a salivary secretion [21]. The source and nature of this protein is discussed in further detail in section 7.3.

## **6.5. Chapter Summary**

Through the use of SEM, TEM and confocal microscopy techniques information regarding the structure and construction of the nest cell lining has been gained. In brief, it is evident that the *Colletes bees* are capable of creating a composite material with fibres on the external surface of a laminated matrix material which makes up the bulk of the nest cell lining. From the micrographs it can be deduced that adult *Colletes* females create their nest cell linings by first extruding proteinaceous fibres onto the dirt wall of their nest cell over which layers of cellophane-like material are applied resulting in a material approximately 20µm in total thickness. Once the nest cell lining is created it can then be provisioned and inhabited with an egg before being sealed with the thicker nest cell cap. The resulting structure is robust enough to remain intact in varying weather conditions until the following season when the brood emerge, roughly nine months later.

## Chapter 7: Chemical Composition of *Colletes halophilus* Nest Cell Lining

### 7.1. Chapter Overview

The chemical composition of the *Colletes halophilus* nest cell lining was investigated using x-ray diffraction, amino acid analysis, Fourier transform infrared spectroscopy and time of flight techniques. As well as presenting data on the chemistry of the nest cell lining, this information will be used to re-evaluate the current understanding of the nest cell lining composition which is currently thought to be composed of linear polyester chains.

### 7.2. X-Ray Diffraction

X-Ray Diffraction (XRD) was completed on powdered *Colletes halophilus* nest cell linings. A preliminary investigation to assess the crystallinity of the material was executed on cleaned nest cell linings. The results from this investigation can be seen in Figure 34.

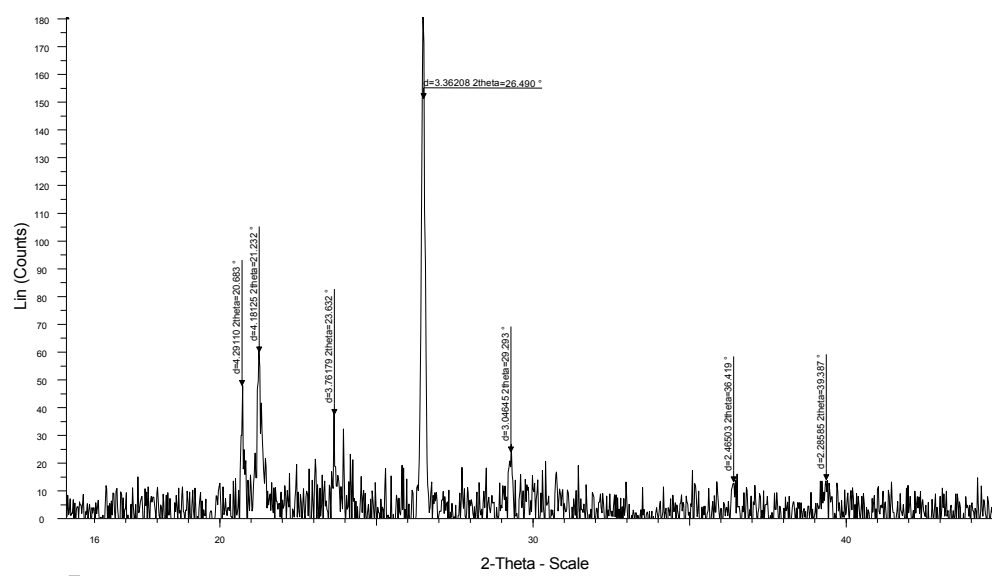


Figure 34: X-Ray diffraction pattern of powderised nest cell lining.



Several distinct peaks, indicative of the crystal structure of the nest cell lining material, are visible in Figure 34. As can be seen in the nest cell lining the peaks with the three highest intensities occur at  $26.49^\circ$  ( $3.36\text{\AA}$ ),  $21.23^\circ$  ( $4.18\text{\AA}$ ) and  $20.68^\circ$  ( $4.29\text{\AA}$ ) respectively. However, all three peaks identified are of very low intensity and difficult to isolate from the background noise of the diffraction pattern.

To better identify the peaks seen in Figure 34 a further study was conducted using a reduced sampling angle, decreased step size and longer sampling times. The more detailed diffraction patterns can be seen in Figures 35 and 36.

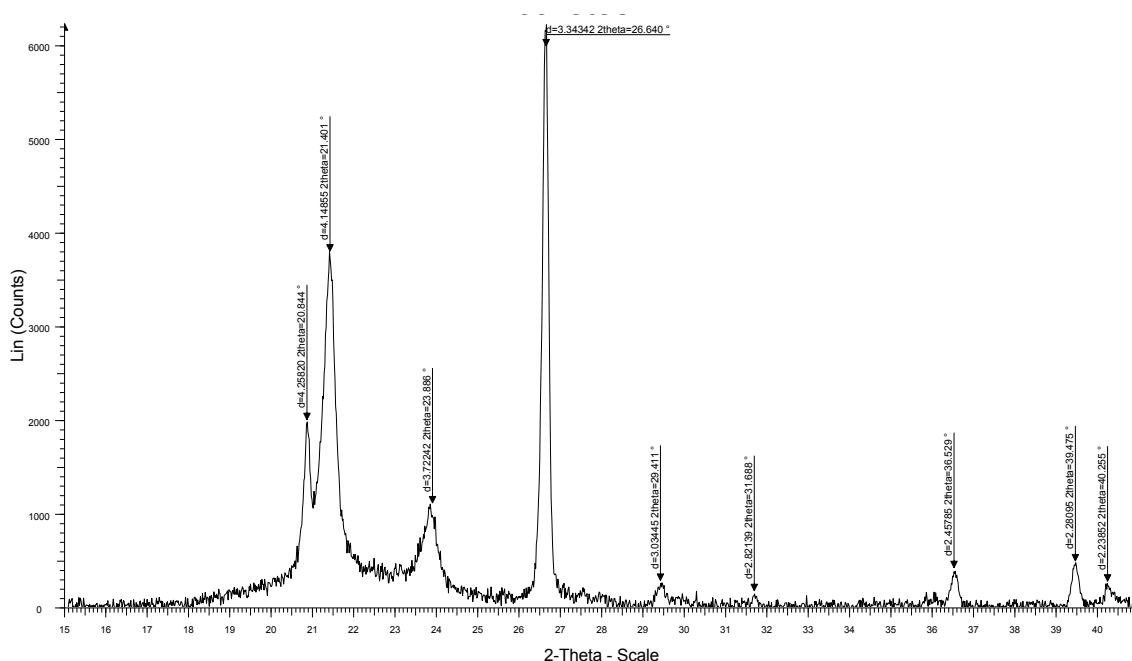
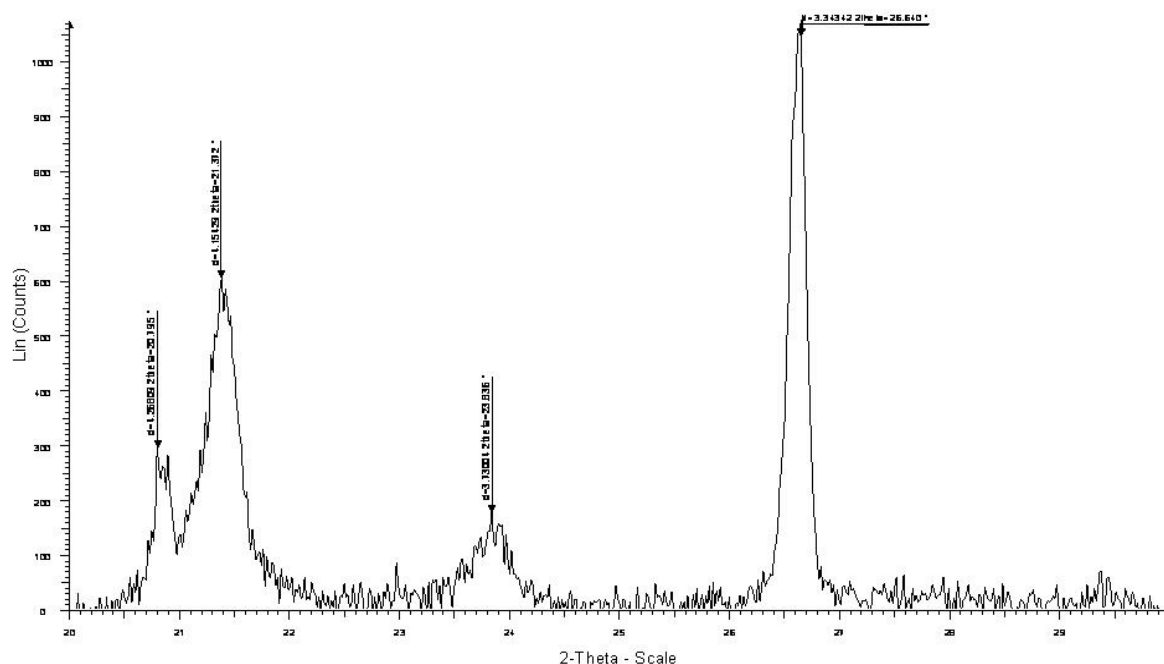


Figure 35: X-ray diffraction pattern of nest cell lining showing peaks between  $15^\circ$  and  $40^\circ$  2-Theta.



**Figure 36: X-ray diffraction pattern of nest cell lining showing peaks between 20° and 30° 2-Theta.**

In the slower scans the relevant peaks are broader and more easily distinguished from the background noise. A list of apparent peaks ordered from highest to lowest intensity is presented in Table 6.

**Table 6: Powder diffraction pattern for *Colletes halophilus* nest cell lining. Peaks ordered from highest to lowest intensity.**

Peak Number	d-Spacing (Å)	2-Theta Angle (°)
1.	3.34	3.36
2.	4.15	21.40
3.	4.26	20.84
4.	3.72	23.89
5.	2.28	39.48
6.	2.46	36.53
7.	3.03	29.41
8.	2.24	40.26
9.	2.82	31.69

From Table 6 it is clear that the peaks identified in the slower scans are very similar to those identified initially. The peaks intensities are seen to increase with increased sampling time. Since, the slower scans result in diffraction patterns with less noise and higher intensity (see Figures 35 and 36), the peak values reported in Table 6 were used for further analysis and comparison with the PDF2 database.

## **X-Ray Diffraction Discussion**

The results from XRD represent the first investigation of the crystallinity of the *Colletes* nest cell lining material. The XRD diffraction patterns visible in Figures 34, 35 and 36 show several distinct peaks, indicating some crystallinity within the sample. However, the results may not represent characteristics of the nest cell lining material itself, but rather debris on the surface of the nest cell lining which would have been powdered along with the nest cell lining.

It is likely that any crystallinity within the nest cell lining would go undetected in the XRD. It has been shown that there are at least two components to the nest cell lining, proteinaceous fibres and a polymer matrix, and either of these components could contain areas of crystallinity. However, since the *Colletes halophilus* nest cell linings are transparent it can be assumed that the polymer component is largely amorphous. This, combined with the fact that polymer crystal structures are more difficult to detect using XRD techniques, suggests that any regions of crystallinity within the polymer matrix would not be represented in the above diffraction patterns. Additionally the silk fibres, which should have regions of high crystallinity, are seen to represent a small fraction of the nest cell lining (approximately 2% of the external surface area) and would therefore be outside the detection range of the XRD.

To confirm this, the results from powder diffraction were compared to the PDF2 database produced by ICDD. It should be noted that the PDF2 database was designed for the analysis of inorganic materials, which the nest cell lining material is not. It is thus not the ideal database for completing this analysis, however it was used due to its availability at the time of this study. The results of this comparison showed similarities in the peaks identified in Figures 34, 35 and 36 and the diffraction patterns of a variety

of silica containing compounds. These apparent silicates in the nest cell lining sample are likely sand debris on the surface of the material, suggesting that the technique was not successful in characterizing the nest cell lining material itself as expected. A more effective use of XRD may be the analysis of intact silk fibres to determine their crystal structure if they can be effectively extracted from the polymer matrix material. This would alleviate the problem of their relative low density in the *Colletes halophilus* nest cell lining as a whole.

### 7.3. Amino Acid Analysis

AAA was completed at the University of California Davis Proteomics Core Facility on cleaned *Colletes halophilus* nest cell linings. The results of the AAA are presented in Table 7.

**Table 7: Amino acid content of *Colletes halophilus* nest cell linings.**

<b>Amino Acid</b>	<b><i>Colletes halophilus</i> (%)</b>
<b>Lysine</b>	2.63
<b>Histidine</b>	3.13
<b>Aginine</b>	0.58
<b>Aspartic Acid/Asparagine</b>	1.77
<b>Threonine</b>	0.82
<b>Serine</b>	16.41
<b>Glutamic Acid/Glutamine</b>	49.94
<b>Proline</b>	0.74
<b>Glycine</b>	3.34
<b>Alanine</b>	14.28
<b>Valine</b>	2.61
<b>Methionine</b>	0.06
<b>Isoleucine</b>	1.65
<b>Leucine</b>	1.12
<b>Tyrosine</b>	0.37
<b>Phenylalanine</b>	0.44

The majority of the amino acid content (80.63%) of *Colletes halophilus* nest cell linings comprises glutamic acid/glutamine (49.94%), serine (16.41%) and alanine (14.28%). Glutamic acid and glutamine content are reported together due to their inability to be distinguished during the amino acid analysis process employed.

## **Amino Acid Analysis Discussion**

From the amino acid content of the nest cell lining material it can be inferred that the proteinaceous component of the *Colletes halophilus* nest cell material is a silk. This is supported by the amino acid distribution, similarities between this material and other known insect silks and morphological data.

The evidence for silk is the particular residues present in the nest cell lining and the larger protein fibre structure. The nest cell lining contains significant quantities of the small amino acid residues, serine, alanine and to a lesser extent glycine. Of note, 34.03% of the proteinaceous component is comprised of small residues. Small amino acid residues allow for closer packing of the protein chains, a structure necessary for silk which has regions of high crystallinity [29]. Also notable is the high level of glutamic acid/glutamine (Glx) present in the *Colletes halophilus* nest cell linings. Glutamic acid and glutamine are very similar in structure and thus indistinguishable in most amino acid analysis methods. High levels of glutamic acid have been reported in other insect silks, including members of Hymenoptera such as the sawflies, though attributed to glutamine in the protein which has lost its amide group during hydrolysis [61]. In general, the chemical makeup of silks varies widely between species, for instance values for the residue alanine range from 4% to 56% across species [27]. However, the levels of glycine, alanine, serine and glutamic acid/glutamine detected are suggestive of silk [27, 37, 61].

Differences in amino acid composition can be noted between these results and those previously reported for *Colletes halophilus* [10]. In comparing this study to that of Albans et al [10], both sets of results show glutamic acid/glutamine and alanine among the most abundant amino acids, however glutamic acid is significantly more abundant in the previous study (71.8% versus 49.94%) and serine significantly less so (2.3% versus

16.41%) [10]. These discrepancies may be attributed to variations in testing method and contamination with proteinaceous debris such as excrement or pollen on the nest cell surface.

The validity of this amino acid study is supported by comparing the findings to those obtained for *Colletes inaequalis* (Table 4). These results were achieved using the same hydrolysis and AAA method so less variation due to testing method is expected. Results between the species are similar with glutamic acid/glutamine, serine and alanine being the most abundant amino acids. This suggests that the production of silk in *Colletes* bees is a characteristic of the genus rather than a particular species.

Beyond the chemical composition of the protein present in *Colletes halophilus* nest cell linings, the fact that the protein component of the nest cell lining is fibrous in structure supports the protein being silk (see 6.4). Silks, though they may vary chemically, all exist exclusively as fibres outside of the insect body. The fibres in the nest cell lining are indeed proteinaceous and are constructed from the liquid secretions of the *Colletes* bees, supporting their classification as a silk.

The presence of silk fibres has important implications for the current understanding of *Colletes* anatomy and nest construction. *Colletes* bees are capable of creating two distinct materials that are not only morphologically different but also chemically distinct. This finding indicates that the anatomy of female *Colletes* bees must contain separate glands for the production of these materials. The Dufour's gland has been shown to be the source of the polymer matrix material that comprises much of the nest cell lining. However the presence of amino acids or other nitrogen containing compounds within the Dufour's gland has never been confirmed [10, 22]. This suggests that the gland from which this silk is produced is anatomically elsewhere in the *Colletes* bees. Adult *Hylaeus* bees, known silk producers in the family Colletidae, produce silk from the salivary glands located in their thorax [24]. Though these glands are less developed in *Colletes* bees, it is possible they are the source of the silk fibres.

#### 7.4. Fourier Transform Infrared & Raman Spectroscopy

Fourier Transform Infrared Spectroscopy (FTIR) was used to identify the chemical bonds present within the *Colletes halophilus* nest cell lining. Transverse sections were taken from two different embedded nest cell linings for study. The results are presented in Figure 37.

From Figure 37 it is clear that major peaks are consistent between the transverse sections from different samples. A list of relevant peaks is presented in Table 8 where (a) and (b) were related to the same nest cell lining.

**Table 8: Peaks from FTIR spectra of *Colletes halophilus* nest cell linings.**

	Wavelength (cm <sup>-1</sup> )						
Spectra	Peak 1	Peak 2	Peak 3	Peak 4	Peak 5	Peak 6	Peak 7
(a)	2958	1733	1607	1509	1247	1154	828
(b)	2959	1731	1607	1509	1247	1154	828
(c)	2958	1727	1607	1509	1247	1073	745

Notably, all samples have three strong peaks in a cluster starting in the region of 2960cm<sup>-1</sup> and a sharp peak at approximately 1730cm<sup>-1</sup>. Weaker peaks are noted in all samples around 1600cm<sup>-1</sup>, 1500cm<sup>-1</sup> and 1247cm<sup>-1</sup>. Below 1500cm<sup>-1</sup>, the finger print region of the spectrum, variations are noted between IR spectra from different nest cell linings (see Figures 37(b) versus 35(c)). These variations are not noted in different transverse sections from within the same nest cell lining (see Figure 37(a) versus 37(b)).

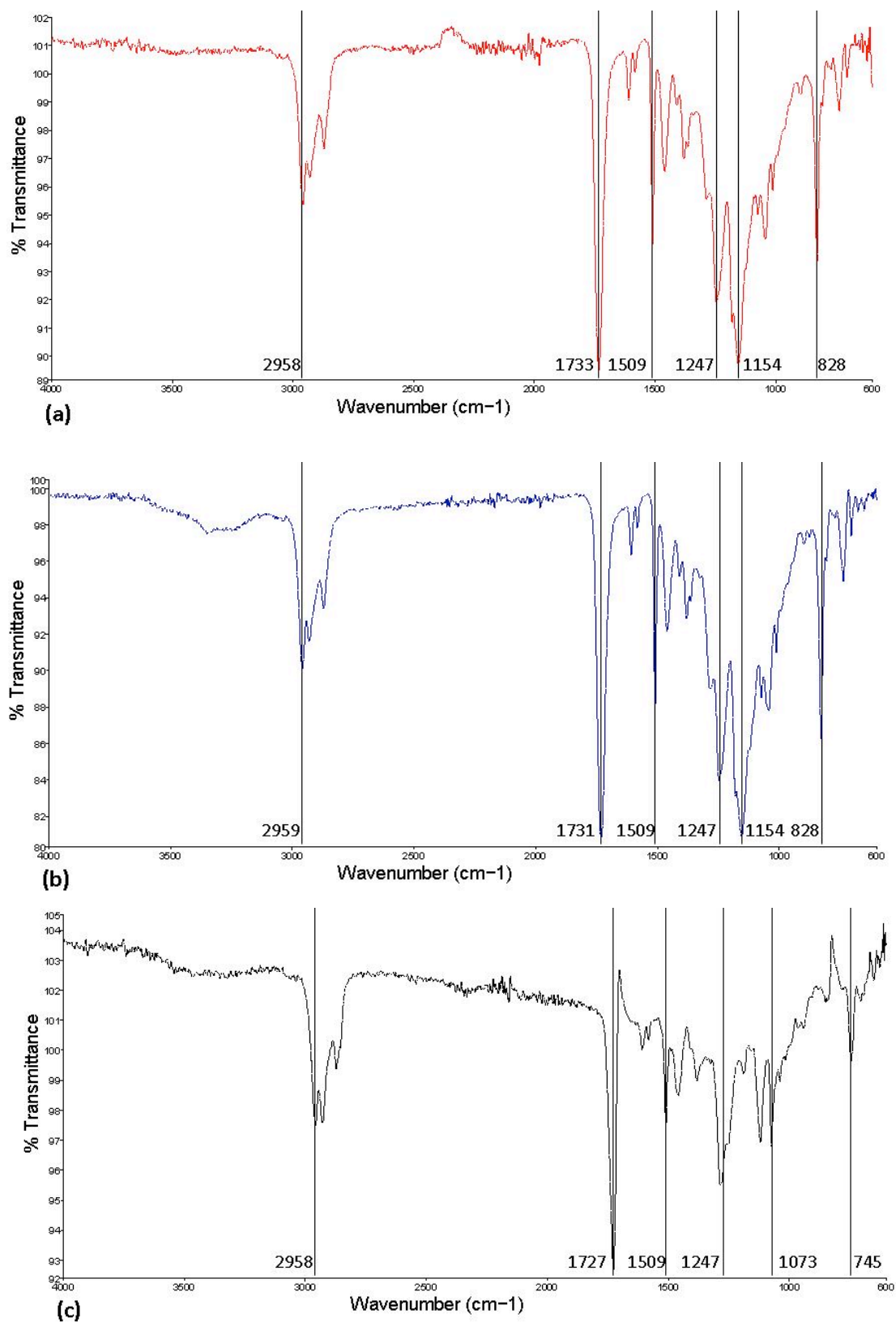
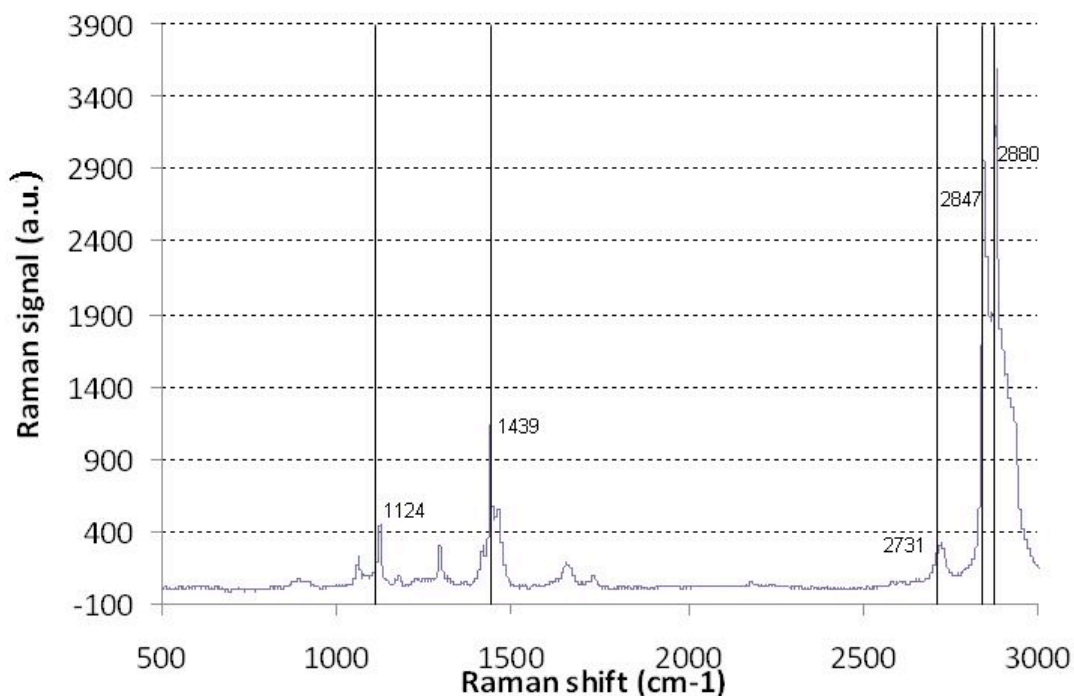


Figure 37: IR spectra of transverse sections through *Colletes halophilus* nest cell linings with significant peaks identified. Spectra (a) and (b) are from the same nest cell lining while (c) represents a different embedded sample.



To complement the FTIR results, Raman spectroscopy was also conducted. Results from this investigation can be seen in Figure 38.



**Figure 38: Raman spectrum for *Colletes halophilus* nest cell lining.**

Several distinct peaks are visible in the Raman spectrum related to characteristic molecular vibrations. In Figure 38 peaks are visible at  $1124\text{cm}^{-1}$ ,  $1439\text{cm}^{-1}$ ,  $2731\text{cm}^{-1}$ ,  $2847\text{cm}^{-1}$  and  $2880\text{cm}^{-1}$ .

### **Fourier Transform Infrared & Raman Spectroscopy Discussion**

From interpretation of the FTIR spectra several conclusions about the chemical composition of the *Colletes halophilus* nest cell lining can be drawn. Firstly, the three peaks starting around  $2960\text{cm}^{-1}$  correspond to the stretching vibrations of the carbon-hydrogen bonds found in hydrocarbon chains. Additionally there is a strong peak at  $1730\text{cm}^{-1}$  that can be attributed to the stretching frequency of a carbon-oxygen double bond [32].

The carbon-oxygen double bond can result in a sharp spectral peak from  $1850\text{cm}^{-1}$  in the case of acid anhydrides, down to  $1645\text{cm}^{-1}$  for some aldehydes [32]. The location of the peak is dependent upon the bonds surrounding the C-O double bond. At  $1730\text{cm}^{-1}$  the C-O double bond could be part of an ester, supporting the previous GC-MS findings suggesting that the nest cell lining is a polyester [22]. However, saturated esters generally have a peak at a slightly higher frequency, between  $1750\text{cm}^{-1}$  and  $1735\text{cm}^{-1}$ . The peak at a lower frequency suggests that the ester could be conjugated with an aryl ring or be  $\alpha,\beta$ -unsaturated (conjugated with an alkene). If the ester was  $\alpha,\beta$ -unsaturated the spectra should show a sharp peak between  $1640\text{cm}^{-1}$  and  $1590\text{cm}^{-1}$ , of which there is no evidence. There is however some evidence of an aryl ester with peaks around  $1600\text{cm}^{-1}$  and  $1500\text{cm}^{-1}$ , the stretching frequencies of aromatic rings [32]. This suggests a complexity to the polymer chain not previously identified.

From the peaks discussed the nest cell lining appears to be composed of polyester, potentially an aryl polyester. However, a portion of the *Colletes* lining has already been identified as silk (see 5.4.2). There is little evidence of the amide I, amide II and amide III bonds which would be indicative of protein in Figure 37. The peak at  $1247\text{cm}^{-1}$  could represent the amide III bond, but its presence without evidence of amide I (sharp peak between  $1680\text{cm}^{-1}$  and  $1630\text{cm}^{-1}$ ) and amide II (sharp peak between  $1570\text{cm}^{-1}$  and  $1515\text{cm}^{-1}$ ) bonding does not strongly support silk presence [30, 31]. This lack of evidence for silk can largely be attributed to the small proportion of silk which would be present in a transverse section of the nest cell lining. The fibres occur only on the external surface of the nest cell lining in low densities so the vast majority of the material detected would be that of the matrix material. It can thus be inferred that the results from FTIR largely represent the matrix material and not the fibres.

There are additional peaks in the region below  $1500\text{cm}^{-1}$ , the fingerprint region, which represent the various bending frequencies of the bonds within the nest cell lining. This region is coined the “fingerprint region” due to its material specificity. The bending frequencies are numerous and vary widely depending on the overall material chemical structure, making peaks below  $1500\text{cm}^{-1}$  of little diagnostic use. However, these peaks are useful in comparing spectra to determine if samples are chemically identical. In the transverse sections taken from the same *Colletes halophilus* nest cell lining (see Figures 37(a) and 37(b)) the fingerprint regions, though not identical, are very similar

suggesting that chemical composition is consistent within a nest cell lining. This consistency does not extend to different nest cell linings. Though the main peaks remain consistent there is variation in the fingerprint region between the spectra of different nest cell linings (see Figures 37(b) and 37(c)) suggesting some chemical difference between the linings. This may be attributed to variations in diet or environmental conditions when the two distinct nest cell linings were constructed.

Finally, fewer peaks are visible in Raman spectroscopy (Figure 38) compared to the FTIR findings. The three peaks indicative of carbon-hydrogen bonding can be seen but additional peaks are more difficult to match. No ester peak is visible in the Raman results, though it is not uncommon for peaks in FTIR not to be apparent in Raman. Two peaks at around  $1500\text{cm}^{-1}$  and  $1600\text{cm}^{-1}$  could be suggestive of a benzene ring, though they are not characteristically sharp [32]. The results from Raman spectroscopy do not provide additional chemical bonding information to that which was seen in FTIR, suggesting that none of the chemical bonds of the nest cell lining samples are symmetric. Also, while FTIR scans were completed on transverse sections of material those, those for Raman were completed on the nest cell lining surface and are thus less likely to represent the chemical structure of the bulk of the nest cell lining material.

## **7.5. Time of Flight**

ESI-TOF and MALDI-TOF were used to analyze the chemical makeup and size of the molecule present within the nest cell lining material. Both techniques were used to characterize different components of the nest cell lining – ESI-TOF provided more accurate information on lower molecular weight molecules while MALDI-TOF, though less accurate, had a higher detection range. The results from ESI-TOF are presented in Figure 39.

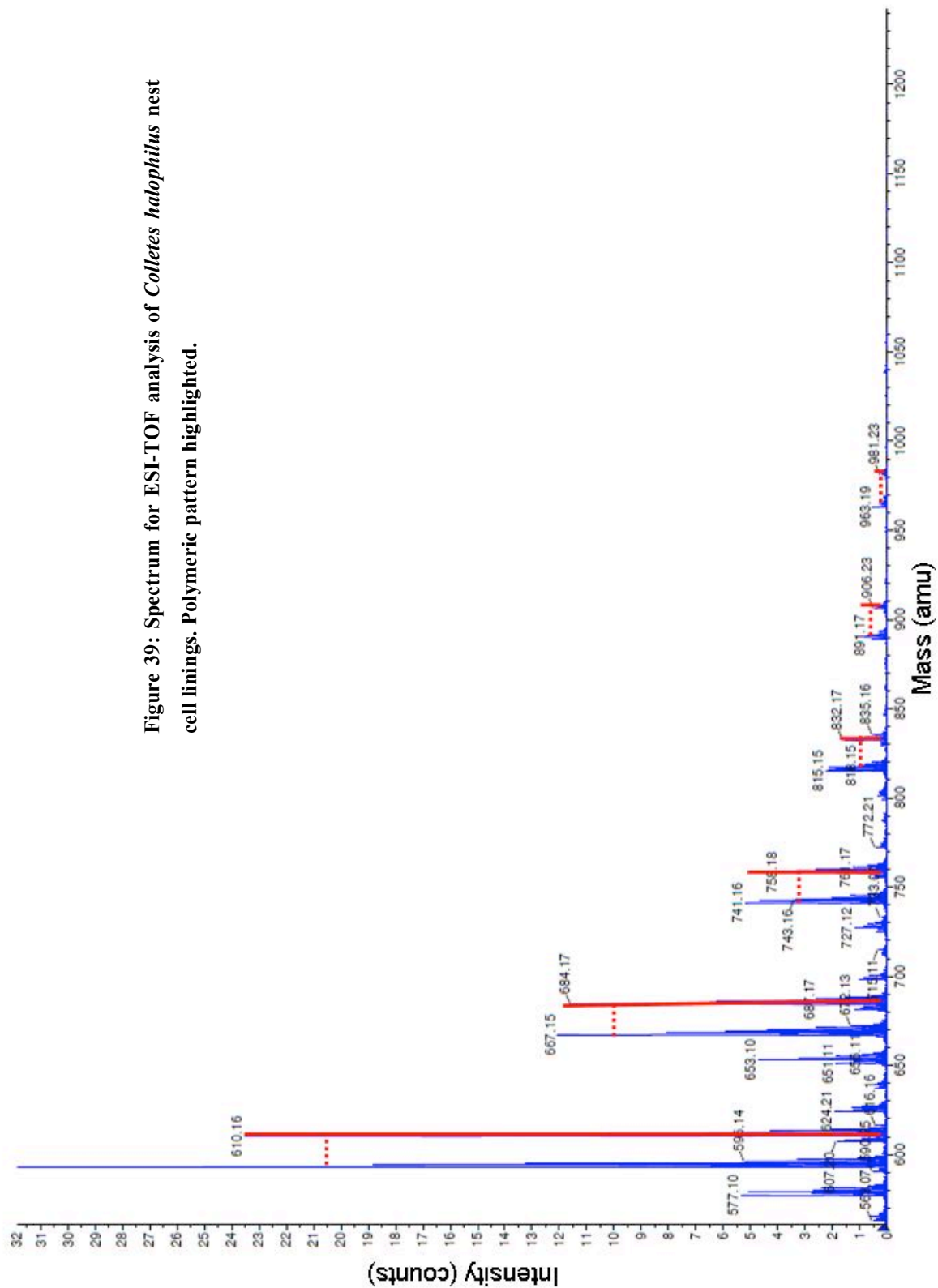


Figure 39 shows the molecules of the nest cell lining with molecular weights between 500 and 1200amu (where amu is the atomic mass unit). These results show a polymeric pattern, with regularly spaced peaks with decreasing magnitude at higher molecular weights. In Figure 39, two of these patterns (one of which is highlighted in red), offset by 17amu (highlighted with dashed line), can be seen. Within both polymer patterns (595.14amu, 667.15amu, 741.16amu, 815.15amu, 891.17amu, 963.19amu and 610.16amu, 684.17amu, 758.18amu, 832.16amu, 905.23amu, 981.23amu respectively) the spacing between peaks is approximately 74amu.

MALDI-TOF was used to characterize those components with higher molecular weight within the nest cell lining. The results from this investigation can be seen in Figure 40 which shows the molecules of the nest cell lining with molecular weights between 600 and 3000amu. A high number of low molecular weight molecules (below 1000amu) were detected using MALDI-TOF resulting in the detectors being overwhelmed. In spite of this, several larger molecules were detected. The peaks above 1100amu show a polymeric pattern with a spacing of approximately 282amu with the last detectable peak at a molecular weight of 2322.5amu.

## **Time of Flight Discussion**

Analysis of TOF results reveals information on the molecules which constitute the *Colletes halophilus* nest cell lining as well information of the construction of said molecules. However, it is important to note that the results from ESI-TOF and MALDI-TOF do not represent all the constituents of the nest cell lining material. It should be noted that HFIP did not effectively dissolve the entirety of the nest cell lining – fluffy white particulate material remained in the solution at the time of testing – so the components which did not dissolve are not reflected in the TOF results. Additionally there were problems with both the complexity of the nest cell lining and effective ionization of its constituent molecules. The nest cell lining was seen to contain a high number of small molecular weight molecules. These smaller molecules overwhelmed the sensors in MALDI-TOF and inhibited the effective detection of higher molecular weight components. With regard to ionization, HFIP is not a solvent commonly used

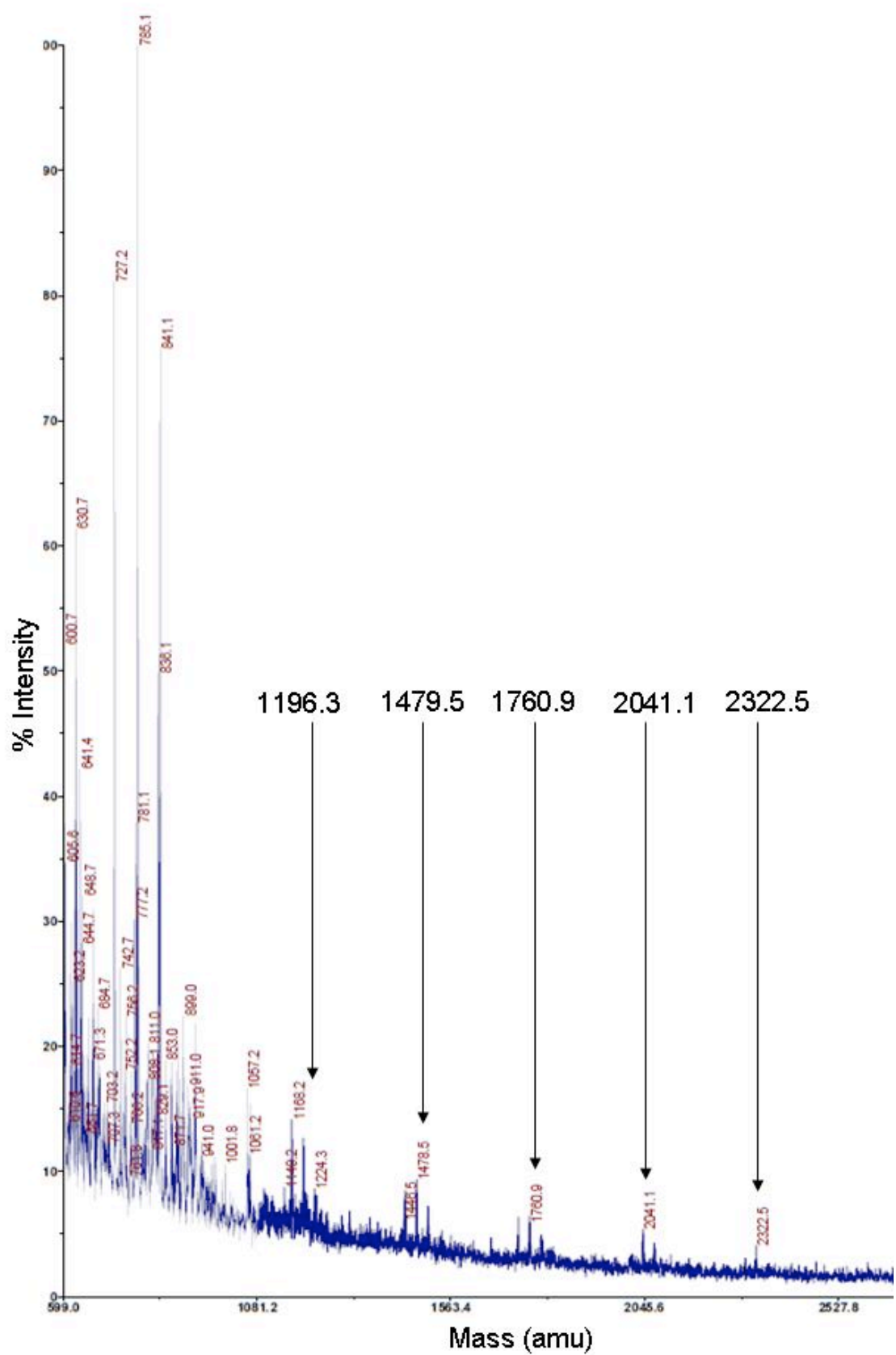


Figure 40: Spectrum for MALDI-TOF analysis of *Colletes halophilus* nest cell linings.

with MALDI-TOF and ESI- TOF techniques so the ionization of the nest cell lining within solution was less predictable.

Despite these problems, some reliable molecular information can be gained from the TOF results. With regard to the ESI-TOF results, the two most notable trends are the offset of 17amu between the polymeric patterns and the peak spacing of 74amu within each set. The 17amu may be attributed to a hydroxyl group. The 74amu peak spacing may suggest the presence of a polymer chain consisting of smaller ester molecules, such as methyl or ethyl esters, which would represent a polyester molecule composed of significantly smaller monomers than the lactones found in the Dufour's gland of *Colletes* bees [22, 32]. Alternatively, the 74amu peak spacing may be suggestive of the loss of an aryl ring from a polymer chain. An ion formed from the loss of an aryl ring would have a mass of 77amu. Although the spacing between major peaks is 74amu, the peaks are clustered such that a spacing of 77amu is visible in the results. The presence of an aryl ring in the polymer chain is further supported by the FTIR results which indicate that the ester group within the nest cell lining material is conjugated with an aryl ring. In either case, whether composed of small esters or aromatic groups, the results from ESI-TOF suggest the presence of a polymer within the *Colletes halophilus* nest cell lining which had previously not been considered.

Further molecular information is gained through analysis of the MALDI-TOF results. The presence of higher molecular weight polymer is seen with an inter-peak spacing of 282amu. This spacing corresponds to the molecular weight of one 18-Carbon macrocyclic lactone, a molecule known to be present in the Dufour's gland and which was thought to be a main constituent of the nest cell lining [22]. This suggests that at least one polymer component of the nest cell lining is formed by the ring-opening polymerization of these macrocyclic lactones. The final apparent peak around 2500amu implies that this polyester is roughly 10 monomer units in length. However due to the problems discussed with ionization and detection it is possible that the molecule is larger but these larger fragments are not visible. It should also be noted that the polymeric masses noted are not evenly divisible by 282amu, suggesting that the polyester chain identified may not be constituted of simply 18-C macrocyclic lactones.

In comparing ESI-TOF and MALDI-TOF, polymeric patterns are noted in both sets of results however their inter-peak spacings are not equal, suggesting that multiple polymers or a copolymer structure may be present within the *Colletes halophilus* nest cell lining. This presents a complexity to the nest cell lining material not previously considered. Beyond the distinctly polymeric components, many low molecular weight components were detected using these techniques. In addition to macrocyclic lactones, smaller esters and hydrocarbons have been identified as constituents within the Dufour's gland [10, 22]. It is likely that these smaller molecules seen in TOF originate from wax esters and hydrocarbons which are incorporated into the nest cell lining along with the more organized polymers.

Finally, no distinct evidence of silk peptides is visible in the TOF results. It is possible that the silk component of the nest cell lining did not successfully dissolve in HFIP. Additionally, if the silk did dissolve, its molecular weight would most likely have been beyond the detection range, with many silk proteins being larger than 10,000amu in size. Small peptide fragments would be visible which could have easily been among the many lower molecular weight peaks detected.

## **7.6. Chapter Summary**

Through XRD, AAA, FTIR and TOF analysis a deeper insight into the chemistry of the *Colletes halophilus* nest cell lining material as well as how this chemical information relates to the material microstructure has been gained. From these results it can be deduced that the adult *Colletes* females are capable of producing silk fibres as well as a largely amorphous polymeric matrix material which together constitute the nest cell lining material. The polymeric matrix is chemically more complex than previously thought. Though a component of the matrix appears to be the linear polyester made of 18-Carbon macrocyclic lactones previously detected in the Dufour's gland, it is not the only compound present. There is evidence of aryl conjugation within the polyester chain which suggests the presence of a copolymer system within the nest cell lining. Additionally, large quantities of smaller molecules, most likely wax esters and small hydrocarbons, have been detected as part of the nest cell lining material. Together, these components – the silk fibres, the polyester chains and the smaller organic molecules –



constitute the *Colletes halophilus* nest cell lining material. This illustrates a material complexity not previously identified.

## Chapter 8: Material Properties of *Colletes halophilus* Nest Cell Lining

### 8.1. Chapter Overview

With an understanding of the structure and chemical make up of the *Colletes halophilus* nest cell lining, work was completed to characterize the materials properties of the nest cell lining. TGA, DSC, and mechanical testing techniques were used to both relate chemical information to material performance and assess the potential of the nest cell lining material for engineering applications.

### 8.2. Thermogravimetric Analysis

TGA was used to record the decomposition rate of the *Colletes halophilus* nest cell lining material. The results from this investigation can be seen in Figure 41.

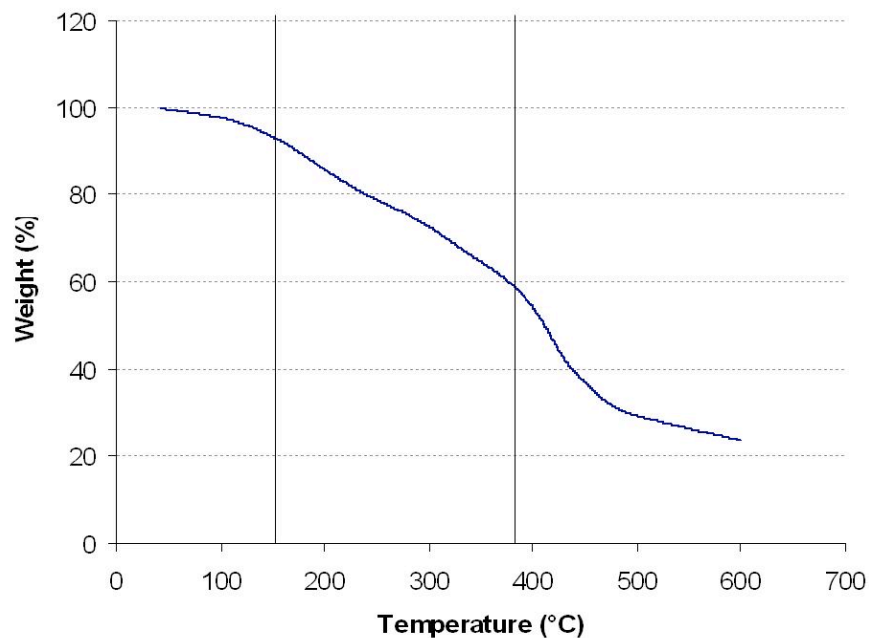


Figure 41: Decomposition of *Colletes* nest cell lining achieved through TGA. Varying decomposition stages distinguished.

From Figure 41, three regions of decomposition are visible. The first loss of mass is of approximately 10wt% and is seen between 50°C and 160°C. The second decomposition is visible from 160°C to 380°C with a resulting mass loss of approximately 30wt%. The final decomposition step occurs above 380°C with a resulting mass loss of approximately 35%.

## Thermogravimetric Analysis Discussion

TGA results provide information both on the thermal stability and the chemical make up of the nest cell lining material. From Figure 41 three distinct decomposition stages are visible. These stages of mass loss can be attributed to three distinct components in the nest cell lining. The first decomposition stage, between 50°C and 160°C can be attributed to water loss within the sample. Despite being desiccated prior to testing, samples were seen to readily absorb water when exposed to the atmosphere, so some rehydration and corresponding water loss are expected upon heating.

The second decomposition step, with a mass loss of approximately 30wt% between 160°C and 380°C, can largely be attributed to the decomposition of smaller molecules, such as waxes and esters, and silk within the sample. Studies have shown various silks, including that of *Antheraea pernyi* (wild silkworm) and dragline silk from *Nephila clavipes* (spider), to be viable up to temperatures of 220°C, after which they experience thermal degradation [34, 35]. However, if one were to assume all of the nitrogen content noted in combustion analysis is protein, the expected weight percent of silk would be between 12wt% and 23wt% — this is considered a high estimate since debris including pollen and excrement are likely contributors to detected nitrogen content as well — significantly less than the detected 30wt% loss. Though 30wt% is beyond the expected mass percentage of silk in the nest cell lining it is likely other components are decomposing in this temperature range as well. Beeswax as well as other wax esters and hydrocarbon waxes have reported decomposition temperatures ranging from approximately 100-200°C [52, 55]. If these smaller molecules are present in the nest cell lining (as suggested by TOF results presented in 7.4.), they too would decompose in this temperature range, accounting for the larger than expected mass lost.

The final decomposition step, from 380°C and onward, accounts for approximately 35% of the material loss. This decomposition step can most likely be attributed to the decomposition of the polyester material. This is supported by a main constituent of the material being identified as polyester as well as this temperature range being appropriate for the decomposition of a polyester. Polyesters such as PLA and PET have decomposition ranges of approximately 330°C to 400°C and 380°C to 500°C respectively [47, 62]. Since it is believed that the polyester component of the nest cell lining contains an aryl conjugated ester, similar to the PET backbone, it is not surprising the final decomposition range of the nest cell lining is closer to that of PET. Finally, what is notable from the TGA results is the impressive thermal stability of the nest cell lining, which demonstrates a gradual degradation in mass of the nest cell lining to temperatures above 500°C.

### **8.3. Differential Scanning Calorimetry**

DSC was used to record the various phase transformations within the nest cell lining material. However, before *Colletes halophilus* nest cell linings were investigated, several control samples were run. These experiments, performed using PLA and *Bombyx mori* silk cocoons, aimed to identify key phase transformations in materials related to the nest cell lining. These results were used as validation for the DSC technique and for comparison with the phase transformations observed within the nest cell lining material. The results of this investigation can be seen in Figures 42 and 43.

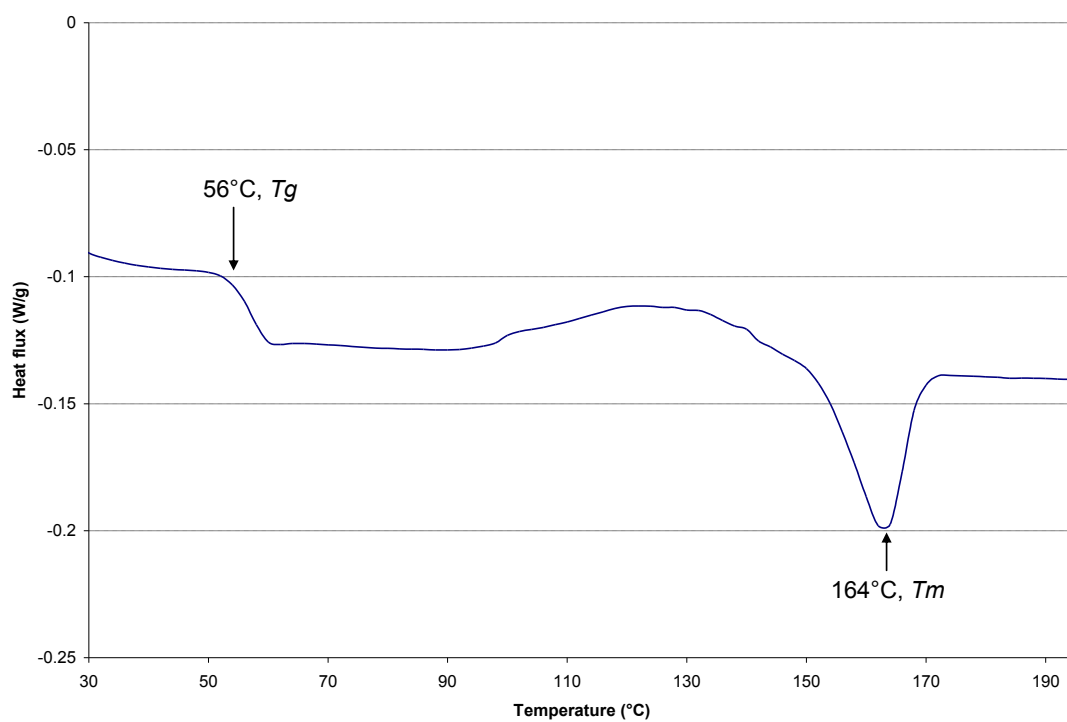


**Figure 42: DSC spectrum for a PLA sample with heating rate of 5°C /min. Glass transition temperature ( $T_g$ ) and melting temperature ( $T_m$ ) identified.**

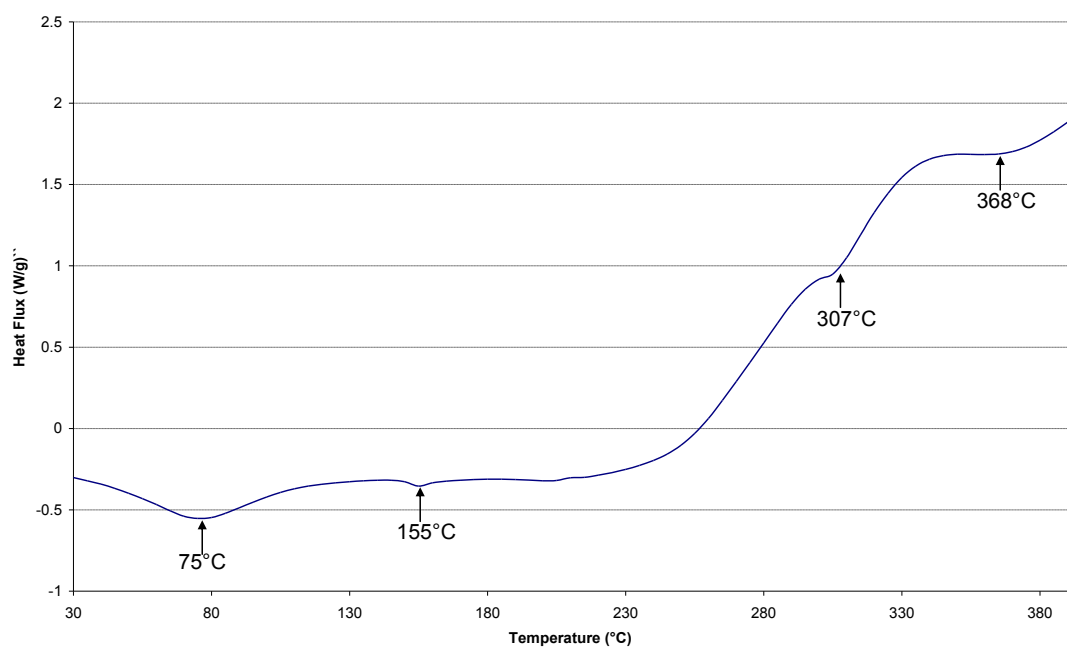
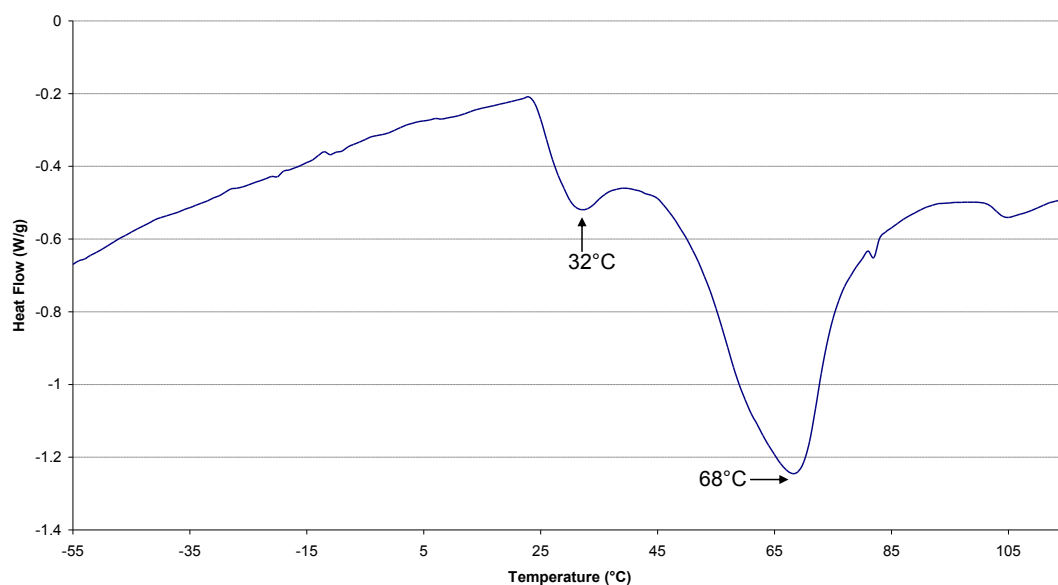


**Figure 43: DSC spectrum for a *Bombyx mori* silk cocoon with heating rate of 5°C/min. Endothermic peaks identified.**

From Figures 42 and 43 several distinct phase transformations within the materials can be seen. In the case of PLA, a bio-thermoplastic polyester, a distinct glass transition temperature ( $T_g$ ) and melting temperature ( $T_m$ ) are visible. The  $T_g$  is marked by the downward step in the graph at approximately 56°C. The  $T_m$  is marked by the endothermic peak with its minimum at 164°C. These values correspond with the literature values for PLA materials [63].

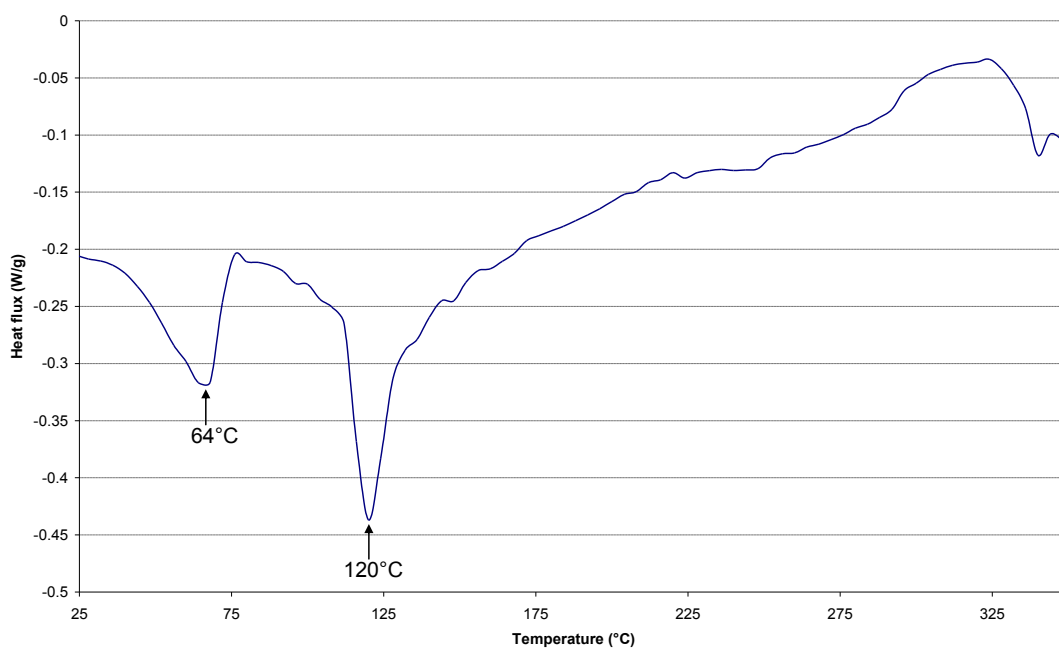
With regards to the *Bombyx mori* cocoon, the peaks are less distinct. A steep rise in the baseline of the graph can be seen at temperatures above 230°C, which is a result of material decomposition. Despite this baseline shift, weak endothermic peaks can be seen with minima at 75°C, 307°C and 368°C. These peaks correspond to moisture loss, degradation of amorphous  $\beta$ -sheets, and degradation of crystalline  $\beta$ -sheets respectively [34]. A weaker endothermic peak is seen with a minimum at 155°C. This may correspond to the  $T_g$  of *Bombyx mori* silk, though it lacks the traditional endothermic step indicative of such a phase transformation [36].

Figure 44 shows the DSC results of a nest cell lining heated from -55°C to 110°C. This run was carried out over a wider temperature range, -55°C to 110°C, in an attempt to identify the  $T_g$  of the nest cell lining material. However, no graphical feature akin to that seen for the  $T_g$  of PLA in Figure 42 is visible in Figure 41. Despite the lack of shift in the trace which would be indicative of a  $T_g$ , large endothermic peaks with distinct minima at 32°C and 68°C are visible.



**Figure 44: DSC spectrum for a *Colletes halophilus* nest cell lining with a heating rate of 10°C/min.**

To explore these endothermic reactions as well as the phase transformations at higher temperatures another investigation of *Colletes halophilus* nest cell linings was performed. The sample was heated at the slower rate of 2°C/min and to a maximum temperature of 330°C. These results can be seen in Figure 45.



**Figure 45: DSC spectrum for a *Colletes halophilus* nest cell lining with a heating rate of 2°C/min.**

From Figure 45 it is seen that at a slower heating rate the endothermic peak noted in Figure 44 appears to be one wider peak with a minimum at 64°C. The minimum appears at 64°C instead of 68°C due to slower heating rate, and is a more accurate reflection of the phase transformation temperature. An additional sharp endothermic peak is noted with a minimum at 120°C. Both of these peaks had corresponding exothermic peaks upon cooling of the nest cell lining. Above approximately 150°C the baseline of the graph is seen to increase most likely due to decomposition within the material.

## Differential Scanning Calorimetry Discussion

DSC results provide information on the chemical makeup of the nest cell lining material as well as its properties and potential performance as an engineering material. Firstly, the melting of several components within the nest cell lining is revealed through DSC. In Figures 44 and 45 several endothermic peaks are visible; these peaks mark the  $T_m$  of various components within the nest cell lining. The lower and broader peak, with an onset at 25°C and a minimum at 64°C, can be attributed to the melting a various small wax esters and hydrocarbons with in the nest cell lining material. Beeswax from social bees shows a similar melting profile, with a progressive softening and melting ending around 75°C, and is composed principally of small ester molecules [54].

An additional endothermic peak is seen at 120°C. The material with which this peak corresponds is less certain. However, despite being within 40°C of the  $T_m$  of PLA it does not correlate with the  $T_m$  of the polyester material that has been identified as forming the bulk of the nest cell lining. Using a hot stage microscope the nest cell linings were observed during heating and the bulk of the material, though discoloured at higher temperatures, remained a solid throughout heating. An image of the nest cell lining material after heating to 200°C can be seen in Figure 46.



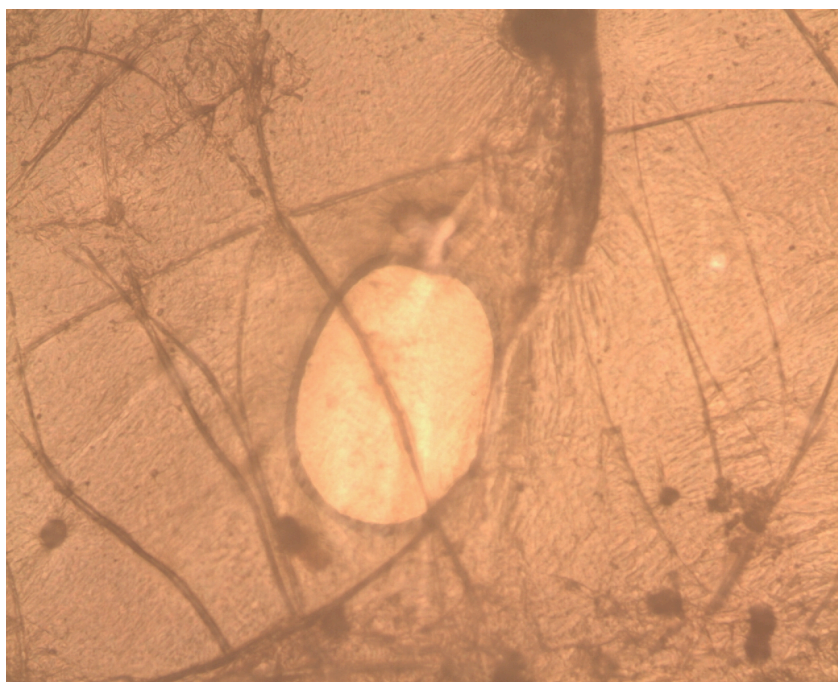


**Figure 46:** *Colletes halophilus* nest cell lining heated to 200°C on a hot stage microscope at 200X.

The brownish material in Figure 46 is the nest cell lining material. It is clear from this micrograph that although affected by the heat treatment the bulk of the material remains solid. The peak at 120°C may correspond to water loss or perhaps to a different component of the nest cell lining, perhaps small ester containing molecules, which have been thought to exist within the material [22]. The presence of these small molecules is further supported by the ESI-TOF results and knowledge of the Dufour's gland. A multitude of smaller molecules were seen to be present in the nest cell lining material indicating that the nest cell lining is not simply long polyester and protein chains. Additionally, as well as macrocyclic lactones the Dufour's gland contains a variety of other hydrocarbons and smaller esters so the presence of wax-like materials is not unexpected [10, 22].

Although two endothermic peaks were identified within the DSC results of the nest cell lining, a clear downward step indicating a  $T_g$  is not seen. This is most likely the result of the baseline noise and endothermic reactions. DSC is not the preferred method for identifying the  $T_g$  of a material because DSC identifies all phase transformations and thermal events, and  $T_g$  often overlaps with other phase transformations which mask it.

A preferable method for finding the  $T_g$  of the nest cell lining material would be Dynamic Mechanical Thermal Analysis (DMTA), however the samples were too delicate for examination using this method. It is additionally possible that the nest cell lining polymers do not go through a glass transition. Such would be the case if the bulk of the material was a fully cross-linked thermoset, though additional testing would be needed to confirm this.

Additionally, the two endothermic peaks identified in the heating of the nest cell lining material do not correspond to the melting of the main polyester material. This suggests that the polyester is a thermoset material and has a  $T_m$  which is above its decomposition temperature – meaning that once solidified the polymer cannot be melted or resolidified. Thermoset materials, such as epoxy resins, are generally heavily crosslinked, resulting in improved strength and high operating temperatures. Both of these traits are positive when considering applications of the nest cell lining material in engineering. However, thermoset materials have the negative characteristic of not being recyclable. This is a negative with consideration to the environmental benefit of the nest cell lining material, though the *Colletes* nest cell linings have been seen to decompose so recycling may be less of a concern [28].

Finally, as well as the wax and polyester components, the nest cell lining has been shown to contain silk fibres. However, in comparing the DSC results of the *Colletes halophilus* nest cell lining (Figure 45) to those of the *Bombyx mori* silk cocoon (Figure 43) the peaks relating to the decomposition of silk structures are not seen. This can be attributed to the relatively small quantity of silk within the nest cell lining samples. The endotherms at 307°C and 368°C, which correspond to the thermal degradation of  $\beta$ -sheets, are low in magnitude in the silk cocoon sample [35]. Thus it is not surprising they are not distinguishable in a sample that is not entirely composed of silk.

#### **8.4. Mechanical Testing**

An Instron testing machine was used to investigate the mechanical properties of the nest cell lining material using a tensile load. Preliminary results from this investigation are presented in Figure 47.

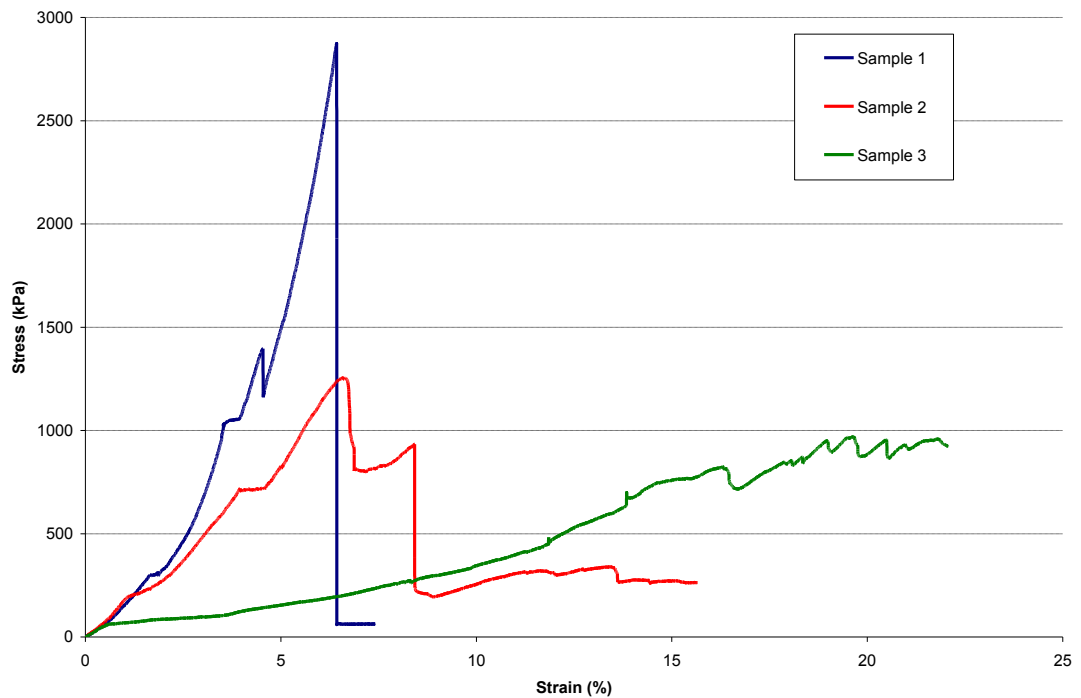


**Figure 47: Tensile stress versus strain in three different *Colletes halophilus* nest cell linings.**

Figure 47 shows the results of tensile testing for three of the nest cell lining samples with an assumed thickness of 20 $\mu$ m. Of the ten samples produced, only these three did not fracture before testing – however all samples showed evidence of minor cracking before testing as a result of the preparation method. From Figure 47 it is clear that the mechanical properties of the nest cell lining material as well as the testing method employed were not consistent. To illustrate this, values for fracture stress and initial tangent modulus for the three samples are presented in Table 9.

**Table 9: Selected results from tensile testing of *Colletes halophilus* nest cell linings.**

Sample	Fracture Stress (MPa)	Tangent Modulus (GPa)
1	2.873	0.025
2	1.255	0.017
3	0.98	0.003

The variation in nest cell lining properties can be seen in Table 9. Within the three samples, values for failure stress range from approximately 1MPa to 3MPa and values for elastic modulus range from approximately 0.003GPa to 0.025GPa. The sample

failure mode varied, with samples 1 and 2 failing from a linear crack moving across the width of the sample, while sample 3 showed multiple failures resulting in the shredding of the material. Overall the material was found to be too delicate for examination using this testing method. Due to the inconsistency of the testing method and limited amount of nest cell lining material available, further mechanical testing was not conducted.

## **Mechanical Testing Discussion**

Mechanical testing of the nest cell linings was not particularly successful, so few reliable conclusions can be drawn from the results in relation to the performance of the nest cell lining material. The problems in testing can largely be attributed to the delicacy of the material coupled with the multi-step process required to prepare samples for tensile testing. These problems resulted in variable results from testing and high material loss (only 30% of materials prepared were sufficiently intact to be used in testing).

The results from the three tests successfully completed show a high degree of variability, with material properties such as fracture stress ranging from approximately 1MPa to 3MPa. Although some variability in results would be expected from a natural material due to changes in material composition or fibre orientation, this large variation can be largely attributed to varying degrees of damage to the nest cell linings prior to testing. As part of the preparation for mechanical testing, nest cell linings were first cut into rectangular shaped pieces using a scalpel blade. The nest cell linings are naturally curved in shape and opening and cutting the cells into a more planar shape often resulted in the formation of small cracks on the edges of the material. Additionally, samples were often further damaged when loaded into the grips on the Instron itself.

Beyond the values for stress, the strain values reported are also not particularly reliable. Due to the fragility of the nest cell lining an extensometer could not be attached to the samples so crosshead displacement was used to calculate displacement instead. This is a less accurate form of measurement as it does not account for any stretching of the grips, mounting or initial unbending of the material.

In order to resolve this variability in testing a large data set would be required. This would necessitate the creation of many more nest cell lining samples and thus access to large amounts of nest cell lining material. Additionally, even if large amounts of material were acquired, there would remain an inherent variability in the nest cell lining performance as a result of material age and condition during collection. Due to the limited quantities of *Colletes halophilus* nest cell lining available for this study, additional testing was deemed too wasteful with regards to material.

Despite the problems with mechanical testing, some initial conclusions can be drawn from the results. Firstly, the material appears to stiffen with increased loading. This is noted by the increased modulus for all three samples under increasing strain, and can likely be attributed to the alignment of polymer chains in the nest cell lining material during the test. Additionally, the nest cell lining samples tested show some evidence of yield and plastic deformation before failure. This toughness of the material is further supported by analysis of the fracture surface of the nest cell lining (Figure 20) which shows fibres pulled from the bulk of the nest cell lining material during tensile testing. Further analysis of the fracture surface (Figure 20) suggests a ductile failure of the material. However variation in the mechanical testing results prevents definitive conclusions being drawn on the relative ductility or toughness of the material.

Despite problems in the testing method resulting in damage to the *Colletes halophilus* nest cell linings prior to testing, initial results suggest that nest cell lining material has comparable mechanical properties to common engineering plastics. The tensile strength of the nest cell lining samples (average of 1.7MPa for the three samples) is much lower than that of related polyesters – 55MPa in the case of PET and ranging from 400MPa to 1420MPa for varieties of silk [29, 44]. The current measured tensile strength of the nest cell lining is more comparable to low density polyethylene, which can exhibit tensile strengths as low as 7MPa [49]. This is to be expected considering the damage to the samples during preparation for testing and lack of fibre orientation. It is possible that with selective fibre orientation and better sample preparation the nest cell lining samples would perform more like other engineering plastics.

The Young's modulus of the *Colletes halophilus* nest cell linings is also significantly lower than that of common polyesters. While commercial polyesters have Young's

moduli ranging from 1.0GPa to 4.0GPa, the maximum initial tangent modulus for the nest cell lining material was 0.025GPa – more like the Young's modulus of elastomeric polymers than that of engineering plastics [49]. Once again, improved sample preparation may result in improved stiffness of the nest cell lining material. Additionally, the % strain measurements, which were calculated using crosshead displacement on the Instron, likely overestimate the extension of the nest cell lining material since they do not account for any unbending of the sample, lengthening in the grips or stretching of the adhesive.

Overall the Instron testing protocol was not appropriate for the nest cell lining material given its delicacy and the amount of material available for testing. In the future a less destructive method, such as nanoindentation testing, would be more desirable for investigating the mechanical properties of the *Colletes halophilus* nest cell lining material.

## **8.5. Chapter Summary**

Through TGA, DSC and mechanical testing information regarding the chemistry and performance of the *Colletes halophilus* nest cell linings was gained. In brief, work from TGA and DSC support the chemical model of the nest cell lining as a composite material composed of silk, polyester and a variety of smaller hydrocarbon and wax ester molecules. Additionally, the techniques discussed in this chapter provide information on the thermal and mechanical performance of the material. The nest cell lining material appears to be thermally stable until approximately 260°C. Though some components of the nest cell lining are capable of melting and recrystallizing, most likely the wax ester and hydrocarbon components, the majority of the nest cell lining (including the silk and polyester components) does not have this property. This suggests that the polyester component of the nest cell lining is a thermoset and most likely heavily cross-linked. Finally, though polymeric behaviour such as chain alignment is noted in the mechanical testing results, the method employed was not reliable for use with the delicate nest cell linings. However, improved experimental methods may prove the *Colletes halophilus* nest cell lining material comparable to modern engineering plastics with regards to mechanical performance.

## Chapter 9: Final Discussion and Conclusions

### 9.1. Chapter Overview

In this chapter the aims of this thesis are reviewed. Additionally, a discussion of the success in achieving these aims is presented. The goals for this project, as set forth in Chapter 1, were the following:

1. Resolve discrepancies in chemical data by creating a complete picture of nest cell lining chemistry.
2. Resolve discrepancies in observed nest cell construction.
3. Explore the microstructure of the nest cell lining and how this relates to chemical composition.
4. Characterize material properties of nest cell lining material to assess the potential of the material in engineering applications and the potential environmental benefit.

Through the application of the variety of techniques presented in this thesis, significant achievements have been made in each of these research areas, providing a clearer understanding of the *Colletes halophilus* nest cell lining material. Some of these results have been presented at an international conference and published in a peer-reviewed scientific journal (Appendix B). Additional results have been submitted for publication in the Journal of Material Science (Appendix C).

### 9.2. Resolution of Discrepancies in Chemical Composition

At the time of this study there was an incomplete understanding of the chemical composition of the *Colletes* nest cell lining. It was shown to be a polyester material formed from the polymerization of lactones within the Dufour's gland through GC-MS. However the polymerization mechanism for the formation of the nest cell lining was

unknown and the detection of elevated nitrogen content through combustion analysis of the materials was not resolved with this model of chemical composition [10, 22].

Through the application of a variety of chemical analysis techniques including AAA, FT-IR, and TOF, a more complete understanding of the chemical composition of the *Colletes halophilus* nest cell linings has been achieved (results presented in Chapter 6). Although TOF results indicate that a component of the nest cell lining appears to be a linear polyester synthesized through the ring opening polymerization of 18-Carbon macrocyclic lactones as previously reported [22], the composition of the nest cell lining is significantly more complicated than that of a pure polyester.

With regards to the polyester components, there is apparent variation in the chains present with some being the linear chains described and others composed of aryl conjugated ester groups. These polymer chains are not seen to be of high molecular weight (highest molecular weight detected at roughly 2500amu), but smaller molecules, including wax esters and small hydrocarbons, are most likely part of the *Colletes halophilus* nest cell lining as well.

Beyond those polymer components which can largely be attributed to secretions from the Dufour's gland, an appreciable amount of protein was detected in the *Colletes* nest cell linings. This protein content, which accounts for the elevated nitrogen previously detected in the material, appears to be a silk within the sample. Together, these components, the silk, the polyester chains, the smaller esters and hydrocarbons, resolve the discrepancy noted between combustion analysis and GC-MS results as well as presenting a more complex chemistry of the *Colletes halophilus* nest cell lining. This is a major advance in the current understanding of the chemical composition of the *Colletes halophilus* nest cell lining.

### **9.3. Resolution of Discrepancies in Nest Cell Construction**

At the time of this study the understanding of nest cell construction by *Colletes* bees was based on observations made by entomologists both in the field and in laboratories. These observations, though providing detailed information on the behaviour of *Colletes*



bees, presented conflicting accounts of nest cell construction. The method of production of fibres was debated between studies as well as the method by which Dufour's gland secretions are applied to the nest cell wall. Disagreement existed as to whether they are ingested and mixed with salivary secretions in the crop before application or if they are licked on to the nest cell wall in alternating applications with salivary secretions [14, 21]. In this study the nest cell lining material itself was examined to provide information concerning the construction of the nest cell lining by adult *Colletes* females.

Using various microscopy techniques including SEM, TEM and confocal microscopy (results presented in Chapter 5) various morphological features were identified. Notably, the presence of fibres on the external surface of the nest cell lining was confirmed and a laminated matrix material identified. The existence and location of these features inform the understanding of the nest cell lining construction. From these micrographs it can be inferred that adult *Colletes* females begin nest cell lining construction by extruding a network of fibres which form a scaffold in the shape of the nest cell lining body and cap. Matrix material, composed of Dufour's gland secretions mixed with salivary secretions, is then layered onto the scaffold surface. Whether these materials are mixed in the crop of the *Colletes* bees or on the surface of the nest cell lining remains unclear, though the more detailed observations of Torchio et al [21] suggest the latter. Over time the matrix material is built up to a thickness of approximately 20µm, after which it can be provisioned by the adult females and eventually sealed with the application of more matrix material to the nest cell lining cap. These findings give a more definitive understanding of the sophistication of nest cell construction.

#### **9.4. Relation of Chemical Composition to Microstructure**

To have a complete understanding of the *Colletes halophilus* nest cell lining material it is necessary to understand the microstructure of the material in connection with its chemical composition. While previously the material was described as a cellophane-like sheeting material composed of a linear polyester, this study has revealed a more detailed and more complex nest cell lining material.

The *Colletes halophilus* nest cell lining material is a composite material composed of silk fibres and a copolymer matrix. The adult *Colletes* females are capable of producing both of these morphologically and chemically distinct components. The silk fibres have varying diameters suggesting that *Colletes halophilus* has control over the size and morphology in the extrusion process. The polymer matrix is a laminated structure composed of various polyester and wax like molecules which can largely be traced to the Dufour's gland for their chemical origin, though no aromatic molecules have been noted in the Dufour's gland but appear to be present in the nest cell lining. The laminated structure of the matrix material is apparent down to the nanometre scale, with layers of material 100nm thick being visible constituents of the nest cell lining, suggesting a potentially layered organization of copolymer chains. These results indicate a greater degree of complexity to the nest cell lining material than hitherto appreciated.

## **9.5. Potential of Nest Cell Lining Material**

In addition to the microstructure and chemical composition of the *Colletes halophilus* nest cell lining, the physical properties of the material was assessed. A main motivation for this study was the potential environmental benefit of developing a polymer material similar to the silk-reinforced polyester nest cell lining lining – a material which is both biologically derived and biodegradable. However, the utility of such a material depends upon the physical properties of the nest cell lining and how they compare to other engineering plastics.

Mechanical and thermal properties of the *Colletes halophilus* nest cell linings were studied using TGA, DSC and mechanical testing techniques (results presented in Chapter 7). Although some difficulties were experienced with these techniques, a model of the nest cell lining material as a silk fibre and amorphous thermoset composite with a thermal stability of approximately 200°C was suggested. Since the material can biodegrade, the environmental negatives of the material being a thermoset and thus unrecyclable are less detrimental. Little information can be gained from mechanical testing due to problems with the method employed, however initial results suggest that with material optimization and fibre alignment the nest cell lining material has the

potential to perform comparably to other commonly used polymeric materials. The use of thermo-chemical analysis has resulted in more detailed insight into the physical structure and properties of the nest cell lining.

## **9.6. Comparing *Colletes halophilus* to *Colletes inaequalis***

The work investigating the *Colletes* nest cell linings in depth began with the American species *Colletes inaequalis*. Although results from that investigation (results presented in Chapter 3) are significantly less complete, they suggest that the material is more complex than was previously thought. Preliminary studies of the *Colletes inaequalis* nest cell lining suggested that the material was a composite material and that some component within that material was proteinaceous. These initial results correspond with the more complete findings of this study for the nest cell linings of *Colletes halophilus*. This suggests that the results presented here, though specific to the *Colletes halophilus* species, may represent the material characteristics of the nest cell linings of the *Colletes* genus as a whole.

## Chapter 10: Future Directions

### 10.1. Chapter Overview

Though much has been achieved in terms of advancing the knowledge of the *Colletes* nest cell linings, much further work needs to be carried out to achieve a more complete understanding. The potential for future work to further achieve the goals identified for this thesis are presented below.

### 10.2 Resolution of Discrepancies in Chemical Composition

Although the understanding of the chemical composition of the *Colletes halophilus* nest cell lining material has been deepened through this study, many questions with regards the synthesis and structure of the chemical components identified remain. Notably, the catalyst for polymerization of the nest cell lining as well as much detail of the silk and polyester components remain unknown. To resolve these questions further analysis of the *Colletes* anatomy and further separation of nest cell lining components are necessary. Additionally, a more robust analysis examining the nest cell linings of *Colletes* bees from varying environments may reveal variation in chemical composition between individual insects.

The construction of the linear polyester chains can be attributed to the ring opening polymerization of lactones within the Dufour's gland. However, the contents of the Dufour's gland do not polymerize in open atmosphere suggesting the presence of a catalyst to promote polymerization. To identify this catalyst the other glands of the *Colletes* bee should be explored more thoroughly. Although the contents of the Dufour's gland have been well documented, components of the salivary and mandibular glands are less so. Since the *Colletes* bees have been seen to combine the Dufour's gland secretions with secretions from their mouth parts before the material begins to harden, the necessary enzyme or material for polymerization is likely to exist in one of the other glands of the *Colletes*. These glands should thus be explored more thoroughly

using chemical analysis techniques such as GC-MS, the original technique used to characterize the Dufour's gland contents.

Additionally, although various components of the nest cell lining have been identified many of the details of these components remain unknown, so there is potential for a deeper understanding of the *Colletes halophilus* nest cell lining. Details yet to be explored include detailed molecular structure, the crystallinity and levels of cross-linking within the polymer components as well as the crystal structure of the silk fibres. To better characterize these features separation of the various molecular components is necessary. If the nest cell lining samples can be successfully transferred into solution the various molecular components can be separated using a chromatography technique such as thin-layer chromatography. Once separated, individual components can be investigated in more detail without the complexity of being part of a mixture – this would allow the use of advanced techniques such as nuclear magnetic resonance for more complete understanding of the particular molecules present.

Finally, if the silk fibres could be isolated from the other polymers they could be further analyzed. Using techniques such as XRD on the isolated fibres could provide information on the crystal structure of the silk itself. This would allow for a more effective comparison between the silk produced by adult *Colletes* females and other insect silks.

### **10.3. Resolution of Discrepancies in Nest Cell Construction**

Although a better understanding of the microstructure and construction of the nest cell lining has been achieved through this study, questions around the formation and motivations behind the structures identified remain. In particular, the method by which the Dufour's gland secretions and the salivary secretions are applied to the nest cell wall is not entirely clear. Additionally, although the presence of fibres has been confirmed the biological motivation for the fibres remains unclear.

To achieve a better understanding of the method of matrix application new entomological studies should be conducted. The last study observing *Colletes* bees

constructing their nest cell linings was completed in 1988 [21]. Video technologies have improved significantly in the past 20 years which would allow for a more detailed recording and visualization of the nest cell construction. The detail of a modern recording could allow for a more accurate interpretation of the sequence events in nest cell lining formation, whether secretions are swallowed or simply licked onto the nest wall surface, as well as providing more information on the anatomical features used for fibre formation.

Beyond the method of nest cell construction, this study has raised questions with regards to why the nest cell lining is created in the form in which it exists. The fibres are notably sparse along the external surface of the *Colletes* nest cell lining, suggesting that they are not needed for mechanical strength or stiffness. It is possible that they play a role in the polymerization of the matrix, serve as a scaffolding onto which the matrix can effectively adhere or act as scaffold to keep dirt debris out of the nest cell area, however this remains unclear. Further study of the mechanical properties of the fibres as well as the polymerization mechanism of the matrix material may help to resolve this.

#### **10.4 Relation of Chemical Composition to Microstructure**

Although there have been many investigations concerned with the chemistry and microstructure of the *Colletes halophilus* nest cell linings, there is potential for a deeper understanding of how the chemical composition of the nest cell lining affects the material microstructure, particularly at a molecular level.

In this study TEM has been used to visualize nest cell lining structures at the nanometre scale with some success. However there is potential to use TEM to identify the various polymer crystals and microstructures in more detail at a molecular level. Several polymer components have been identified as constituents of the matrix of the nest cell lining and with the appropriate ruthenium tetroxide staining they should be distinguishable. Additional knowledge of the chemical composition of these various polymers (obtained through the techniques discussed in section 8.2.1.) coupled with more effective TEM imaging could reveal information regarding the crystallization and

microstructure of the material. This information would influence the understanding of both the polymerization of the material as well as its performance.

### **10.5. Potential of Nest Cell Lining Material**

Although initial results do not identify problems with using a material like the *Colletes halophilus* nest cell lining for other applications, much work still needs to be carried out to assess its potential use. Most importantly, reliable testing of the mechanical properties of the nest cell lining is necessary.

Many problems were encountered using an Instron testing machine for mechanical testing of the delicate nest cell linings. Results were unreliable and the method to prepare samples for testing often compromised material integrity prior to experimentation. To avoid these problems and ensure more accurate results, a more sensitive testing method is required. Nanoindentation would be an appropriate technique for measuring the mechanical properties, such as Young's modulus, of the nest cell lining material.

Another property which was not measured successfully in this study was glass transition temperature. The transition was not successfully noted in DSC and the nest cell lining samples were too small and delicate for use with DMTA. The use of micro-thermal analysis, though still being developed as a technique, could allow for the identification of the glass transition temperature of individual components within the nest cell lining. Finally, as the aim of this project is to create a material inspired by the nest cell lining material an important task in the future will be to apply the understanding of the chemistry and microstructure of the nest cell lining and to the construction of synthetic samples. Although more work is necessary to understand the polymerization of the material before this is possible, once created, synthetic samples could be produced in sizes more suitable to macro scale testing methods such as DMTA and mechanical testing.

## References

1. O'Toole, C. and Raw, A., *Bees of the world*. 1999, Blandford Press: London.
2. Michener, C.D., *Evolution of the nests of bees*. American Zoologist, 1964. **4**(2): p. 227-239.
3. Almeida, E.A.B., *Colletidae nesting biology (Hymenoptera : Apoidea)*. Apidologie, 2008. **39**(1): p. 16-29.
4. Cane, J., *Chemical evolution and chemosystematics of the Dufour's gland secretions of the lactone-producing bees (Hymenoptera: Colletidae, Halictidae, and Oxaeidae)*. Evolution, 1983. **37**(4): p. 657-674.
5. Lanham, U.N., *Evolutionary origin of bees (Hymenoptera: Apoidea)*. Journal of the New York Entomological Society, 1980. **88**(3): p. 199-209.
6. Michener, C.D., *The bees of the world*. 2007, The John Hopkins University Press: Baltimore.
7. Danforth, B.N., Sipes, S., Fang, J. and Brady, S.G., *The history of early bee diversification based on five genes plus morphology*. Proceedings of the National Academy of Sciences of the United States of America, 2006. **103**(41): p. 15118-15123.
8. Kirby, W., *Monographia apum angliae*. 1802, J. Raw: Ipswich.
9. McGinley, R.J., *Glossal morphology of the Colletidae and recognition of the Stenotritidae at the family level (Hymenoptera: Apoidea)*. Journal of the Kansas Entomological Society, 1980. **53**(3): p. 539-552.
10. Albans, K., Aplin, R., Brehcist, J., Moore, J. and O'Toole, C., *Dufour's gland and its role in secretion of nest cell lining in bees of the genus Colletes (Hymenoptera: Colletidae)*. Journal of Chemical Ecology, 1980. **6**(3): p. 549-564.
11. Almeida, E.A.B. and Danforth, B.N., *Phylogeny of colletid bees (Hymenoptera: Colletidae) inferred from four nuclear genes*. Molecular Phylogenetics and Evolution, 2009. **50**(2): p. 290-309.
12. Brady, S. and Danforth, B., *Recent intron gain in elongation factor-1 of colletid bees (Hymenoptera: Colletidae)*. Molecular biology and evolution, 2004. **21**(4): p. 691.



13. Michener, C.D., *The social behaviour of bees*. 1974, Harvard University Press: Cambridge.
14. Batra, S., *Ecology, behavior, pheromones, parasites and management of the sympatric vernal bees Colletes inaequalis, C. thoracicus and C. validus*. Journal of the Kansas Entomological Society, 1980 **53**(3): p. 509-538.
15. Bergström, G. and Tengö, J., *Linalool in mandibular gland secretion of Colletes bees (Hymenoptera: Apoidea)*. Journal of Chemical Ecology, 1978. **4**(4): p. 437-449.
16. Cane, J.H., Gerdin, S. and Wife, G., *Mandibular gland secretions of solitary bees (Hymenoptera: Apoidea): Potential for nest cell disinfection*. Journal of the Kansas Entomological Society, 1983. **56**(2): p. 199-204.
17. Espelie, K., Cane, J. and Himmelsbach, D., *Nest cell lining of the solitary bee Hylaeus bisinuatus (Hymenoptera: Colletidae)*. Cellular and Molecular Life Sciences, 1992. **48**(4): p. 414-416.
18. Dufour, L., *Observations sur les métamorphoses du Cerceris bupresticida et sur l'industrie et l'instinct entomologique de cet Hyménoptère*. Annales des Sciences Naturelles, 1841. **2**: p. 353-370.
19. de Lello, E., *Adnexal glands of the sting apparatus of bees: Anatomy and histology, I (Hymenoptera: Colletidae and Andrenidae)*. Journal of the Kansas Entomological Society, 1971. **44**(1): p. 5-13.
20. Kuhlmann, M., Else, G., Dawson, A. and Quicke, D., *Molecular, biogeographical and phenological evidence for the existence of three western European sibling species in the Colletes succinctus group (Hymenoptera: Apidae)*. Organisms Diversity & Evolution, 2007. **7**(2): p. 155-165.
21. Torchio, P., Trostle, G. and Burdick, D., *The nesting biology of Colletes kincaidii Cockerell (Hymenoptera: Colletidae) and development of its immature forms*. Annals of the Entomological Society of America, 1988. **81**(4): p. 605-625.
22. Hefetz, A., Fales, H.M. and Batra, S.W.T., *Natural polyesters: Dufour's gland macrocyclic lactones from brood cell laminesters in Colletes bees*. Science, 1979. **204**(4391): p. 415-417.
23. May, D.G.K., *An investigation of the chemical nature and origin of the waxy lining of the brood cells of a sweat bee, Augochlora pura (Hymenoptera,*

- Halictidae*). Journal of the Kansas Entomological Society, 1974. **47**(4): p. 504-516.
24. Batra, S., *Some properties of the nest-building secretions of Nomia, Anthophora, Hylaeus and other bees*. Journal of the Kansas Entomological Society, 1972. **45**(2): p. 208-218.
  25. Packer, L., *Taxonomic and behavioural notes on Patagonian Xeromelissinae with the description of a new species (Hymenoptera: Colletidae)*. Journal of the Kansas Entomological Society, 2004. **77**(4): p. 805-820.
  26. Jakobi, V.P.D.H., *Über die Löslichkeit des Brutzellenwachses von Wildbienen*. Zeitschrift für Bienenforschung, 1963. **7**(3): p. 72-76.
  27. Sutherland, T.D., Young, J.H., Weisman, S., Hayashi, C.Y. and Merritt, D.J., *Insect silk: one name, many materials*. Annual Review of Entomology, 2010. **55**: p. 171-88.
  28. Clark, P., *Urban jungle: The changing natural world at our doorstep* in *The Washington Post*. 2011: Washington D.C.
  29. Wainwright, S.A., Biggs, W.D., Currey, J.D. and Gosline, J.M., *Mechanical design in organisms*. Second ed. 1982, Princeton University Press: Princeton.
  30. Shao, J., Zheng, J., Liu, J. and Carr, C.M., *Fourier transform Raman and Fourier transform infrared spectroscopy studies of silk fibroin*. Journal of Applied Polymer Science, 2005. **96**(6): p. 1999-2004.
  31. Asakura, T., Kuzuhara, A., Tabeta, R. and Saito, H., *Conformational characterization of Bombyx mori silk fibroin in the solid state by high-frequency carbon-13 cross polarization-magic angle spinning NMR, x-ray diffraction, and infrared spectroscopy*. Macromolecules, 1985. **18**(10): p. 1841-1845.
  32. Williams, D.H. and Fleming, I., *Spectroscopic methods in organic chemistry, sixth edition*. 2008, McGraw-Hill Higher Education: Maidenhead.
  33. Chen, X., Knight, D.P., Shao, Z. and Vollrath, F., *Regenerated Bombyx silk solutions studied with rheometry and FTIR*. Polymer, 2001. **42**(25): p. 09969-09974.
  34. Kweon, H. and Park, Y.H., *Dissolution and characterization of regenerated Antheraea pernyi silk fibroin*. Journal of Applied Polymer Science, 2001. **82**(3): p. 750-758.
  35. Cunniff, P.M., Fossey, S.A., Auerbach, M.A., Song, J.W., Kaplan, D.L., Adams, W.W., Eby, R.K., Mahoney, D. and Vezie, D.L., *Mechanical and thermal*

- properties of dragline silk from the spider Nephila clavipes*. Polymers for Advanced Technologies, 1994. **5**(8): p. 401-410.
36. Magoshi, J. and Nakamura, S., *Studies on physical properties and structure of silk. Glass transition and crystallization of silk fibroin*. Journal of Applied Polymer Science, 1975. **19**(4): p. 1013-1015.
  37. Craig, C.L., *Evolution of arthropod silks*. Annual Review of Entomology, 1997. **42**: p. 231-267.
  38. Hsueh, T.Y. and Tang, P.S., *Physiology of the silkworm. I. Growth and respiration of Bombyx mori during its entire life-cycle*. Physiological Zoology, 1944. **17**(1): p. 71-78.
  39. Agnarsson, I., Dhinojwala, A., Sahni, V. and Blackledge, T.A., *Spider silk as a novel high performance biomimetic muscle driven by humidity*. Journal of Experimental Biology, 2009. **212**(13): p. 1989-1993.
  40. Lombardi, S.J. and Kaplan, D.L., *The amino acid composition of major ampullate gland silk (dragline) of Nephila clavipes (Araneae, Tetragnathidae)*. Journal of Arachnology, 1990. **18**(3): p. 297-306.
  41. Lewis, R., *Unraveling the weave of spider silk*. BioScience, 1996. **46**(9): p. 636-638.
  42. Kameda, T. and Tamada, Y., *Variable-temperature <sup>13</sup>C solid-state NMR study of the molecular structure of honeybee wax and silk*. International Journal of Biological Macromolecules, 2009. **44**(1): p. 64-69.
  43. Sutherland, T.D., Campbell, P.M., Weisman, S., Trueman, H.E., Sriskantha, A., Wanjura, W.J. and Haritos, V.S., *A highly divergent gene cluster in honey bees encodes a novel silk family*. Genome Res, 2006. **16**(11): p. 1414-21.
  44. Weisman, S., Haritos, V.S., Church, J.S., Huson, M.G., Mudie, S.T., Rodgers, A.J., Dumsday, G.J. and Sutherland, T.D., *Honeybee silk: recombinant protein production, assembly and fiber spinning*. Biomaterials, 2010. **31**(9): p. 2695-700.
  45. Hefetz, A., Blum, M.S., Eickwort, G.C. and Wheeler, J.W., *Chemistry of the Dufour's gland secretion of halictine bees*. Comparative Biochemistry and Physiology -- Part B: Biochemistry and Molecular Biology, 1978. **61**(1): p. 129-132.
  46. McCrum, N.G., Buckley, C.P. and Bucknall, C.B., *Principles of Polymer Engineering*. 1997, Oxford University Press: Oxford.

47. Wang, N., Yu, J. and Ma, X., *Preparation and characterization of thermoplastic starch/PLA blends by one-step reactive extrusion*. Polymer International, 2007. **56**(11): p. 1440-1447.
48. Saha, B. and Ghoshal, A.K., *Thermal degradation kinetics of poly(ethylene terephthalate) from waste soft drinks bottles*. Chemical Engineering Journal, 2005. **111**(1): p. 39-43.
49. Ashby, M.F., *Materials Selection in Mechanical Design*. Third edition ed. 2005, Butterworth-Heinemann: Oxford.
50. Wang, J.G. and Bakken, L.R., *Screening of soil bacteria for poly- $\beta$ -hydroxybutyric acid production and its role in the survival of starvation*. Microbial Ecology, 1998. **35**(1): p. 94-101.
51. Somerville, C.R., *Production of industrial materials in transgenic plants*. Philosophical Transactions: Biological Sciences, 1993. **342**(1301): p. 251-257.
52. Hagemann, J. and Rothfus, J., *Oxidative stability of wax esters by thermogravimetric analysis*. Journal of the American Oil Chemists' Society, 1979. **56**(6): p. 629-631.
53. Patel, S., Nelson, D.R. and Gibbs, A.G., *Chemical and physical analyses of wax ester properties*. Journal of Insect Science, 2001. **1**(4): p. 1-7.
54. Buchwald, R., Breed, M.D. and Greenberg, A.R., *The thermal properties of beeswaxes: unexpected findings*. Journal of Experimental Biology, 2008. **211**: p. 121-127.
55. Namdar, D., Neumann, R., Goren, Y. and Weiner, S., *The contents of unusual cone-shaped vessels (cornets) from the Chalcolithic of the southern Levant*. Journal of Archaeological Science, 2009. **36**(3): p. 629-636.
56. Seligman, A.M., Wasserkrug, H.L. and Hanker, J.S., *A new staining method (OTO) for enhancing contrast of lipid-containing membranes and droplets in osmium tetroxide-fixed tissue with osmiophilic thiocarbonylhydrazide (TCH)*. The Journal of Cell Biology, 1966. **30**(2): p. 424-432.
57. Brown, G.M. and Butler, J.H., *New method for the characterization of domain morphology of polymer blends using ruthenium tetroxide staining and low voltage scanning electron microscopy (LVSEM)*. Polymer, 1997. **38**(15): p. 3937-3945.
58. Haubruge, H.G., Jonas, A.M. and Legras, R., *Staining of poly(ethylene terephthalate) by ruthenium tetroxide*. Polymer, 2003. **44**(11): p. 3229-3234.

59. Thermo Fischer Scientific, I., *Instructions: Krypton Protein Stain*. 2010.
60. Torchio, P.F., *The nesting biology of Hylaeus bisinuatus forster and development of its immature forms (Hymenoptera: Colletidae)*. Journal of the Kansas Entomological Society, 1984. **57**(2): p. 276-297.
61. Rudall, K. and Lucas, F., *Extracellular fibrous proteins: The silks*. Comprehensive Biochemistry, 1968. **26**: p. 475-558.
62. Liu, W., Tian, X., Cui, P., Li, Y., Zheng, K. and Yang, Y., *Preparation and characterization of PET/silica nanocomposites*. Journal of Applied Polymer Science, 2004. **91**(2): p. 1229-1232.
63. Chen, C.-C., Chueh, J.-Y., Tseng, H., Huang, H.-M. and Lee, S.-Y., *Preparation and characterization of biodegradable PLA polymeric blends*. Biomaterials, 2003. **24**(7): p. 1167-1173.

## Personal Bibliography

1. Belisle, R., Turner, I.G. and Ansell, M.P., *Evidence of biocomposite structure in Colletes halophilus nest material*. Journal of Materials Science, 2011. **46**(18): p. 6154-6157.
2. Belisle, R., Taylor, S., Turner, I., Chachra, D., Ansell, M., Morse, C. and Christianson, R., *Investigation of Colletes nest cell linings*. Presented at Materials Research Society Spring Meeting. San Francisco, CA. April, 2011.
3. Belisle, R. *Bees in Bath*. Presented at US-UK Fulbright End-cap Forum. Edinburgh, UK. July, 2011.
4. Belisle, R. *Investigation of Colletes halophilus nest cell linings*. Presented at Meeting of the Minds Conference. Bath, UK. June, 2011.
5. Belisle, R., Turner, I.G. and Ansell, M.P., *Evidence of copolymer structure in Colletes halophilus nest cell lining through chemical analysis*. Submitted for publication in Journal of Materials Science, 2011.